Experimental evolution of bacterial resistance to copper

A thesis presented in partial fulfillment of the requirements for the degree of
Master of Science
in
Biological Science

at Massey University, Auckland,
New Zealand

Xinyue Li

2020

Abstract

Hospital-acquired infections (HAIs) are a serious health concern worldwide. Currently in New Zealand, around one in ten patients admitted to hospitals will acquire an infection while receiving treatments for other diseases in hospitals. One of emerging strategies to reduce the risk of HAIs is to apply metallic copper on the commonly touched items, providing sustained protection against microbial contamination. This is owing to the fact that bacterial pathogens are rapidly killed on copper surfaces through a process termed contact killing. However, the mechanisms of contact killing still remains elusive.

Research in our laboratory aims to elucidate the mechanism of copper-mediated contact killing and investigate the probable overlapping antimicrobial resistances to copper and antibiotics. Based on a previous experimental evolution, we found several different responses potentially conferring copper resistance: increased tolerance to copper ions, decreased pyoverdine production and elevated mutation rate. Also, consistent to our expectation, evolved copper-resistant strains showed altered levels of resistance to antibiotics such as tobramycin.

Next, two unique approaches of experimental evolution were used to assess the potential of bacteria to develop resistance to ionic copper, involving colony-to-colony transfer and broth-to-broth transfer. Specifically, *P. fluorescens* SBW25 and *P. aeruginosa* MPAO1 were subjected to passage of sub-lethal concentrations of copper ions on LB agar and in LB broth. After several transfers, the evolved strains exhibited an increase of minimal inhibitory concentration of copper ions.

Taken together, data presented in this thesis implicates potential evolutionary mechanisms of bacterial resistance to metallic copper, and further suggest the probable evolution of overlapping bacterial resistances to copper and antibiotics. Primary data were obtained for the experimental evolution of bacterial pathogen in the presence of toxic copper ions.

Acknowledgements

First and foremost, I would like to express my deep and sincere gratitude to my research supervisor, Associate Professor Xue-Xian Zhang, for giving me the opportunity to do research and providing invaluable guidance throughout this research. His dynamism, vision, sincerity and motivation have deeply inspired me. He has taught me the methodology to carry out the research and to present the research works as clearly as possible. It was a great privilege and honor to work and study under his guidance. I am extremely grateful for what he has offered me.

I would like to say thanks to Dr. Kiran, Naren, Wenjuan Kang for helping me with each small question and for their constant encouragement and all the fun when we were working in the lab together. I am extending my thanks to every academic staffs and fellow students in Evolutionary Genetics and Microbial Ecology Laboratory.

Also, I would like to take this opportunity to thank Sha Liu and Feng Xu for their previous work on experimental evolution of SBW25 to develop resistance to metallic copper, which forms the basis of this master work.

Finally, I am extremely grateful to my parents and friends for their love and caring for encouraging me in all of my pursuits and educating and preparing me for my future.

List of Abbreviations

Amp	ampicillin
bp	base pairs
Cb	carbenicillin
CF	cystic fibrosis
CFU	colony forming unit
DNA	deoxyribonucleic acid
dNTP	deoxyribo nucleotide tri-phosphate
EPA	the United States Environmental Protection Agency
EPS	exopolysaccharides or extracellular polysaccharides
g	gram
Gem	gentamicin
h	hour
HAIs	hospital-acquired infections
ICU	intensive care units
KB	king's B
Km	kanamycin
kV	kilovolt
LB	luria-bertani
LPS	lipopolysaccharide
MIC	minimal inhibitory concentration
min	minutes
ml	milliliter
mM	millimolar

MRSA	methicillin-resistant *Staphylococcus aureus*
Nal	nalidixic acid
Nm	neomycin
OD	optical density
PBPs	penicillin-binding proteins
PCR	polymerase chain reaction
Pen	penicillin
ROS	reactive oxygen species
s	seconds
Str	streptomycin
Tet	tetracycline
Tob	tobramycin
TBE	tris-borate-ethylenediamine tetraacetic acid
UV	ultraviolet
VBNC	viable but nonculturable condition
WHO	world health organization
WT	wild type
^{o}C	degrees Celsius
µg	microgram
µl	microliter
µm	micrometer
µM	micromolar

Table of Contents

List of Figures

List of Tables

CHAPTER ONE: INTRODUCTION

1.1 Hospital-acquired infections

Due to the increased use of medical devices, hospital-acquired infections (HAIs), also referred to as healthcare-associated infections, have become a global complication that are yet to be solved. In the United States hospitals, the Centers for Disease Control (CDC) estimates that HAIs are the cause of 1.7 million infections and more than ninety thousand associated deaths per annum (Al-Tawfiq et al., 2014). In other developed countries, it is estimated that around 10% patients acquire HAIs during their hospital admission, with significantly higher risks in surgical intensive care units (ICU) and in neonates (World Health Organization., 2011). According to the statistics published by the World Health Organization (WHO), the prevalence rate of HAIs in New Zealand is around 12%. HAIs are a serious risk to not only hospitalised patients but also healthcare workers and other visitors through dermal contact.

In addition to significant mortality and morbidities, HAIs account for substantial costs to patients and healthcare system as HAIs prolong the length of hospital stay of patients and their recovery time. HAIs pose a greater risk to vulnerable individuals, such as premature babies, elderly patients and people with immunodeficiencies resulting from certain chronic diseases. As estimated by Graves et al. (2003), the annual cost to HAIs in New Zealand is around $136.61 million in total, including both medical and surgical admissions.

Over a half of these infections can be prevented at an early stage and, consequently, HAIs prevention has been a top priority in healthcare institutions. Normally, to mitigate the acquisition of HAIs, two approaches are implemented: (1) vertical approaches targeting specific pathogens, such as active surveillance testing and decolonisation; and (2) horizontal broad-based approaches, including maintenance of the hospital environment cleaning, disinfection and hand hygiene and minimisation of the overuse of invasive medical devices (Septimus et al., 2014). However, the compliance rate of hand hygiene is only about 40%, and hand hygiene alone cannot fully counter HAI acquisition (Pittet et al., 2000).

Currently, contact surfaces in hospitals, such as doorknobs, faucets and bed rails, are made of materials deficient in antibacterial activity, such as stainless steel, chrome and

plastics. However, the study by Sharpe et al. (2011) has shown that microbes can persist on these dry inanimate surfaces for several months even after deep cleaning and be transmitted through contact between patients, visitors and staff. Thus, an emerging HAIs prevention strategy is applying inherently antimicrobial properties to commonly touched surfaces within the clinical setting and one of such examples is metallic copper and its alloys. Copper can rapidly eliminate a wide range of pathogenic bacteria through the 'contact killing' process, thus providing protection between routine cleaning and decontamination and further decreasing HAIs.

1.2 Application of copper bactericidal properties in HAIs prevention

1.2.1 The antimicrobial efficacy of copper

Copper with its atonic number 29 is an essential trace element for living organisms. Copper has been used by human civilisations for thousands of years owing to its excellent strength, malleability and thermal conductivities. The medical application of copper, either alone or in copper complexes, can be dated back to between 2600 and 2200 B.C and was first recorded in an Egyptian medical text, the Smith Papyrus, in which it was mentioned that copper was used to sterilise chest wounds and disinfect drinking water. In more recent eras, the antimicrobial property of copper was supported by the evidence that copper miners appeared to be immune to the cholera that broke out in Paris in the 19th century and arthritis in Finland (Dollwet, 1985). Additionally, copper and copper compounds were used to heal postoperative wounds and treat other infections, ranging from tuberculosis to skin problems, throughout human history (Dollwet, 1985; Borkow, 2014).

In New Zealand, the $1 and $2 coins in current circulation are made of an aluminium-bronze alloy mainly composite of copper. In addition to performance advantages such as corrosion resistance, durability and recyclability, copper is selected as coinage material as it is more sanitary than other metals. A research conducted in 2016 showed that the American penny consisting of a copper-plated zinc core exhibited a significant reduction in microbial infections associated with human hands as compared to the modern New Zealand 10 and 50 cent coins containing steel and nickel (Vriesekoop et al., 2016).

In 2008, after being supported by extensive antimicrobial efficacy testing, copper was officially approved as the first and only antibacterial metallic agent by the American Environmental Protection Agency (EPA) due to its inherent ability to eliminate several

disease-causing pathogens within hours, even including the hospital multiple-drug-resistant nosocomial pathogens methicillin-resistant *Staphylococcus aureus* (MRSA) and vancomycin-resistant *Enterococci* (VRE) (Salgado et al., 2013).

1.2.2 The potential of copper-containing antimicrobial materials in reducing the risk of HAIs

As copper surfaces can kill harmful bacteria, there is now great hope that copper, with its self-sanitising properties, can aid in reducing the nosocomial infections acquired in hospitals and therefore cross-contamination as a supplement to existing hand hygiene and disinfection regimens. To implement its use in the healthcare sector, copper can be mixed with other metals to optimise the final properties of the resulting alloy.

An initial laboratory study performed at the University of Southampton, UK, indicated that the copper-base coating on the surface of hospital facilities is effective against the following pathogens: *Enterobacter aerogenes*, *Escherichia coli* O157:H7, MRSA, *Pseudomonas aeruginosa*, *Staphylococcus aureus* and VRE. The study showed that more than 99.9% of those bacterial strains were killed within two hours under typical indoor conditions. As an example, as shown in Figure 1.1 (adapted from https://www.copperalloystewardship.com/), copper provided a defence against MRSA at room temperature and humidity, while two silver-containing materials from two different manufacturers showed no antimicrobial efficacy under the same condition; moreover, stainless steel, which was included as the negative control, proved no different.

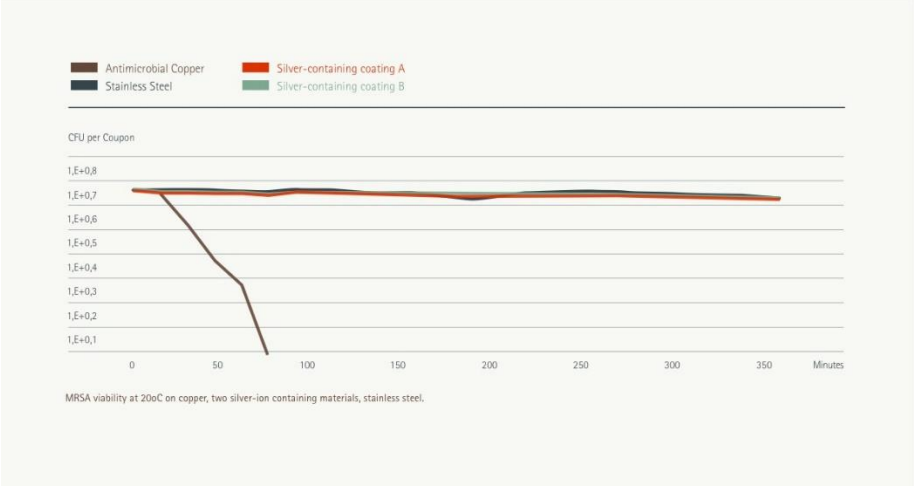

Figure 1.1. A comparison of antibacterial activity between copper and three other materials. This figure was adapted from the EPA Registration Copper Stewardship Site (https://www.copperalloystewardship.com/), showing the trend of colony forming units

(CFU) of MRSA per coupon over a period of 350 minutes. (copper, brown line; sliver-containing coating A, red line; silver-containing coating B, green line; stainless steel, blue line).

Based on the inherent antimicrobial ability of copper and copper alloys in the laboratory, a number of clinical trials have been conducted or are now ongoing around the world; they aim to evaluate the efficacy of copper alloys in sustaining hospital cleaning levels and reducing the incidence of HAIs. Figure 1.2 shows countries in which clinical trials have been undertaken; they include the United Kingdom, United States, South Africa, Japan and Ireland (Figure 1.2 is adapted from https://www.copperalloystewardship.com/). However, similar clinical trials have not been performed in New Zealand.

Figure 1.2. Worldwide hospital trials assessing the antimicrobial efficiency of copper alloys. This figure is adapted from the EPA Registration Copper Stewardship Site (https://www.copperalloystewardship.com/)

Overall, the data so far consistently indicate that compared to the control materials such as glass, plastics and stainless steel, the introduction of copper-containing surfaces can decrease infection risk by around a quarter on a continuous basis (Pineda et al., 2017). The first ten-week clinical trial conducted at Selly Oak Hospital in Birmingham, UK, showed that bacterial contamination on copper-containing toilet seats, tap handles and door push plates was 90% to 100% lesser than when using other standard materials. More importantly, no methicillin sensitive *Staphylococcus aureus* (MSSA), VRE and *E. coli* were isolated from the copper surfaces (Casey et al., 2010). More recently, a large clinical trial took place in the Unites States in the ICUs over a period of 43 months. The result showed that the introduction of copper alloys resulted in a significant reduction (around 80%) of microbial burden when compared to the control surfaces containing no copper (Schmidt et al., 2012).

Taken together, all these trials supported the efficacy of copper-based composite coating in reducing HAIs within hospital facilities and providing a safer environment for both patients and healthcare workers.

1.3 The mechanism of metallic copper-induced cell death

1.3.1 The current understanding of copper-mediated contact killing

Elucidating the mechanisms of copper-mediated contact killing can strengthen our comprehension about the use of copper surfaces in healthcare settings and their further development. However, the chemical interactions of the bacterial-metal contact are quite complex, and consequently, the mechanisms underlying bacterial inactivation on copper surfaces are yet to be fully understood.

At the current state of knowledge, it appears that copper-mediated contact killing initiates with dissolving of copper ions released from copper surfaces. Then, bacterial cells suffer a nonenzymatic oxidative damage of membrane phospholipids, leading to the leakage of specific nutrients. Following the damage of the outer and inner bacterial cell membrane, the released copper ions can penetrate the bacterial cell, thus facilitating the access of copper ions into cellular components. The increased amount of intracellular copper ions, in turn, causes irreversible oxidative stress and the production of hydroxyl radicals demonstrated by a redox cycling between the different forms of copper ions (Vincent et al., 2017).

Overall, although current evidence clearly indicates that the ROS damage induced by copper ions dissolved from metallic copper is the major cause of cell death during the contact killing process, the contact killing mediated by copper and its alloys is a combined effect and there are other mechanisms where the metal-bacterial contact damages the cell envelope. However, the exact sequential events of copper contact killing of cellular substances and their relative importance remain elusive and may in fact be different, depending on the type of microorganism (Warnes et al., 2012).

1.3.2 The toxicity of copper ion

Copper is a nutrient element essentially required for most prokaryotic and eukaryotic

organisms. The ionic form of copper is crucial for cell metabolism as it is required as a cofactor for many cellular enzymes such as cytochrome oxidase, superoxide dismutase and lysyl oxidase and electron transport proteins owing to its redox-active capacity to alternate between cuprous Cu^{+} (the reduction state) and cupric Cu^{2+} (the oxidation state). However, copper ion is toxic to bacterial cells when in surplus (Grass et al., 2010). Inside the bacterial cytoplasm, highly reactive hydroxyl radicals (ROS) are generated through the following Fenton-type reaction combined with the Haber-Weiss cycle (Liochev & Fridovich, 2002):

$$Cu^{+} + H_2O_2 = Cu^{2+} + 2OH^{-}$$

Copper ions can also cause the depletion of sulfhydryls, such as in cysteines or glutathiones, in a cycle between the following two reactions:

$$2Cu^{2+} + 2RSH = 2Cu^{+} + RSSR + 2H^{+}$$
$$2Cu^{+} + 2H^{+} + O_2 = 2Cu^{2+} + H_2O_2$$

Then, the hydrogen peroxide can participate in the abovementioned Fenton-type reaction and the Haber-Weiss cycle, amplifying the generation of toxic free hydroxyl radicals. Under aerobic conditions, those copper-induced extremely reactive hydroxyl radicals can efficiently induce pathology by inhibiting cellular respiration, causing irreversible oxidative damage of cellular molecules, such as lipids, proteins and deoxyribonucleic acid (DNA) (Espirito Santo et al., 2008). Cellular ROS stress and membrane lipid peroxidation induced by ionic copper have been observed in *Escherichia coli* and *Salmonella* cells when exposed to metallic copper alloys (Mathews et al., 2015). However, bacterial cells have evolved multiple mechanisms to maintain a low concentration of intracellular H_2O_2, thus preventing the damage caused by ROS. On the other hand, an alternative route of copper ion toxicity has been shown to cause non-Fenton damage in *E. coli* (Vincent et al., 2018). With the presence of copper ions, iron-sulfur cluster enzymes are inactivated as a result of the displacement of iron atoms from iron-sulfur clusters and a copper binding to the corresponding sulfur atom, resulting in the damage of several catabolic and biosynthetic pathways (Macomber & Imlay, 2009). Therefore, the toxicity of ionic copper is ascribable to the capacity of generating ROS by redox cycling between the different copper species such as Cu(0), Cu(I) and Cu(II) and interfering with the iron-sulfur clusters.

However, copper is considered safe for regular contacts as a common metal with a long history of domestic use, as is evidenced by the recorded low possibility of adverse reactions (O'gorman & Humphreys, 2012). Previous research indicated that the concentration of free ionic copper released from the surface of metallic copper is only around 0.3 μM during 24h at 25 ^{o}C, which is not sufficient to kill pathogenic bacteria (Espirito Santo et al., 2008). In another research, Mathews et al. (2013) placed a synthetic inert polymer between copper coupons and *Enterococcus hirae* cells in order to prevent the direct contact between bacterial cells without affecting the transmission of the released copper ions. Surprisingly, the result showed that a rapid killing of bacteria was strongly attenuated: cell survival was reduced only by 1 log even after 3.5 h whereas more than 106 bacteria cells were completely killed on uncoated copper coupons within 30 min. Thus, this study highlighted the importance of direct bacteria-copper surface contact in cellular damage.

Figure 1.3. SEM image of the honeycomb-like structures of *E. hirae* cells. *E. hirae* cells were wet plated on a CA contact array and the sample was processed for electron microscopy after air drying. (A) Image at low magnification; (B) image at high magnification (Mathews, et al., 2013).

Taken together, the information available suggests that the toxicity of copper ions can only partially explain the contact killing mediated by metallic copper. There are other mechanisms attributable to the observed rapid killing of bacterial cells upon contact with metallic copper in addition to the free radical-induced oxidative damage.

1.3.3 The copper ions burst releasing hypothesis

The current model of contact killing, as shown in Figure 1.4, was proposed by Grass et al. (2011). This model highlights the contribution of toxic copper ions to bacterial cell death, but the source of high accumulation of copper ions is still tentative.

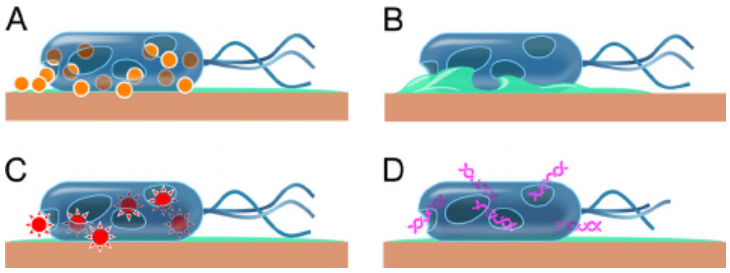

Figure 1.4. Current model of the tentative events in contact killing. (A) Copper dissolves from the copper surface and causes cell damage. (B) The cell membrane ruptures because of copper and other stress phenomena, leading to the loss of membrane potential and cytoplasmic content. (C) Copper ions induce the generation of reactive oxygen species, which cause further cell damage. (D) Genomic and plasmid DNA becomes degraded (Grass et al., 2011).

All bacterial strains harbour several copper chelating factors and copper efflux systems that mainly serve to pump excess copper ions outside of cells and detoxify the copper ions from the cytoplasm or periplasm. However, these systems can only delay rather than prevent bacterial cell death upon contact with metallic copper, contradicting ion release from metallic copper surface as the lethal agent (Espírito Santo et al., 2008). Thus, it is reasonable to assume that when exposed to metallic copper, bacterial cells continuously absorb and accumulate large amounts of intracellular copper ions until the copper efflux systems are outpaced, thereby resulting in cell death.

In general, bacterial cells produce various forms of extracellular components such as extracellular polymeric substances (EPS), lipopolysaccharide (LPS), capsule, pili and flagella, which contain nitrogen, sulphate or phosphate in their structure, providing bacteria from environmental stresses (Kleanthous & Armitage, 2015). These cell surface components normally contain nitrogen, sulphate or phosphate in their structure and potentially react with copper ions, thus producing more and more toxic copper ions. The EPS and polysaccharides isolated from EPS have been reported previously to be capable of binding heavy metals, in particular Cu (Mittelman & Geesey, 1985; Chen et al., 2011). These strongly indicate that the contact between metallic copper and bacterial surface components seems to be sufficient to trigger a release of copper ions from the surface.

The recent work by Liu and Zhang (2016) showed that EPS and LPS stimulated the rates of copper-mediated contact killing, in agreement with the copper ions burst releasing

hypothesis that bacterial cells are predominantly killed by a burst release of toxic copper ions (Cu^{+}/Cu^{2+}) resulting from chemical interactions between bacterial cell surface components and copper surfaces (Figure 1.5). The copper ions burst releasing hypothesis clearly explains the accumulation of copper ions and highlights the critical role of copper ions in copper contact killing.

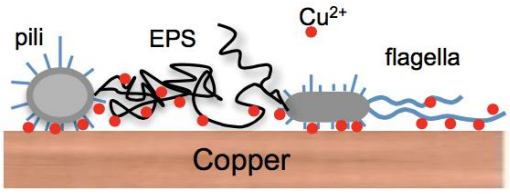

Figure 1.5. The copper ion burst releasing (CIBR) model of contact killing. Cell surface components, such as exopolysaccharides (EPS), lipopolysaccharide (LPS), pili and flagella, can react with copper ions and are critical in copper-mediated contact killing (Liu & Zhang, 2016).

1.4 The potential of bacteria to develop overlapping resistance to copper and antibiotics

1.4.1 The mechanism and medical use of antibiotics

Antibiotics refer to the antibacterial substances that act by inhibiting the growth of bacteria and directly killing bacteria or through a combination of both mechanisms. Since the discovery of the antibiotic penicillin by Sir Alexander Fleming in 1928, antibiotic medications have been widely used in hospitals to treat or prevent bacterial infections (Ventola, 2015). In this study, we chose nine types of antibiotics covering major classes and measured their minimal inhibitory concentration of evolved strains. Several of them are on the World Health Organization's List of Essential Medicines, which contains the most effective medicines in the health system.

The aminoglycosides are one of the oldest classes of antimicrobial agents derived from Streptomyces or *Micromonospora* spp and include kanamycin, tobramycin, neomycin, gentamicin and streptomycin. After the aminoglycosides enter the bacterial cells through the outer cell membrane, the aminoglycosides exert their antibacterial activity by binding to the aminoacyl site of 16S ribosomal RNA (rRNA) within the 30S ribosomal subunit (Farouk et al., 2015). Aminoglycosides exhibit antimicrobial activity against a wide

spectrum of different microorganisms and were frequently prescribed to treat complicated urinary tract infections in clinical practice. Additionally, despite being presented with the significant problem of advancing antimicrobial resistance, aminoglycosides are still widely used in everyday practice in combination with other antibiotic agents in spite of its potential for renal toxicity and ototoxicity (Spelman et al., 1989).

Beta-lactam antibiotics, such as ampicillin and carbenicillin, are the most frequently used antibiotics worldwide and constitute the basis of antimicrobial treatment of infections caused by susceptible organisms. Most beta-lactam antibiotics prevent bacterial growth by inhibiting the synthesis of a peptidoglycan layer of bacterial cell walls (Fisher et al., 2008). Until 2003, β-lactam compounds accounted for more than half of the commercially available antibiotics for medical use (Elander, 2003).

Tetracycline displays a low toxicity and broad spectrum against both gram-negative and gram-positive bacteria. Tetracycline inhibits protein synthesis by preventing the attachment of aminoacyl-tRNA to the 30S subunit of ribosomal acceptor (A) site, thus causing bacterial cell death (Chopra & Roberts, 2001). As it can be taken orally and is inexpensive, due to its the absence of reported adverse side effects, tetracycline was extensively used in the United States during the 1950s and was particularly prescribed for outpatient therapy (Speer et al., 1992). Although, nowadays, the emergence of tetracycline-resistant strains limits the use of tetracycline, tetracycline is still used to treat gastritis and the peptic ulcer disease associated with *Helicobacter pylori* (Chopra & Roberts, 2001).

Nalidixic acid belonging to the fluoroquinolones antibiotics possesses a broad spectrum of antimicrobial activity. Following a simple diffusion across the bacterial cell membrane, nalidixic acid acts in a bactericidal manner by binding to the DNA gyrase and DNA topoisomerase IV essential for mediating the topological state of DNA (Zhanel et al., 2002). However, the medical use of nalidixic acid is limited to the oral treatment of urinary tract infections (Blondeau, 1999).

1.4.2 The antibiotic resistance crisis

Antibiotics are considered among the major breakthroughs in modern medicine for making a significant contribution to health care-associated bacterial infections. However, according to the World Health Organization, the emergence and dissemination of antibiotic resistance and multi-drug resistance subsequent to antibiotic use are recognised as a major global

threat to public health and may become the leading cause of death by 2050 (O'Neill et al., 2016). For example, MRSA is the cause of deaths of nearly 20,000 people and more than 300,000 hospitalisations in the United States annually (Martens & Demain, 2017). Antibiotic resistance is also considered a huge economic burden to health care and society at large. Although there is an absence of data on the economic burden of antibiotic resistance in New Zealand, it is estimated that antibiotic resistance costs the U.S. health care system $20 billion (Nguyen et al., 2019). Following globalisation, antibiotic resistance may become more serious.

Bacteria can intrinsically be resistant to certain classes of antibiotics. The molecular basis of the intrinsic resistance of Gram-negative bacteria to Gram-positive antibiotics is the presence of the Gram-negative outer membrane impermeable to many antibiotics such as vancomycin and active efflux pumps serving to reduce the intracellular concentration of antibiotics (Cox & Wright, 2013).

In addition to the intrinsic resistance of bacterial pathogens, bacteria can evolve inheritable resistance to antibiotics through direct acquisition of new antibiotic-resistant genes via mobile genetic elements or the modification of existing genes under an environmental selection caused by antibiotics or other antimicrobials. Genetic mechanisms underlying an evolved antibiotic resistance include modification of the intracellular target through genetic mutation or post-translational modification to decrease the binding capacity of antibiotics, over-expression of efflux systems and decreased expression of antibiotic uptake system, mutations regarding biofilm formation and drug inactivation by enzymes such as β-lactamase (Tegos et al., 2012). For instance, the MRSA phenotype results from the mutation of penicillin-binding proteins (PBPs) with low-affinity to β-lactam antibiotics, encoded by the horizontally acquired *mecA* genes on its chromosomal DNA, that take over the functions of the resident staphylococcal PBPs and hence confers resistance to conventional β-lactam antibiotics (Rossolini et al.,2014).

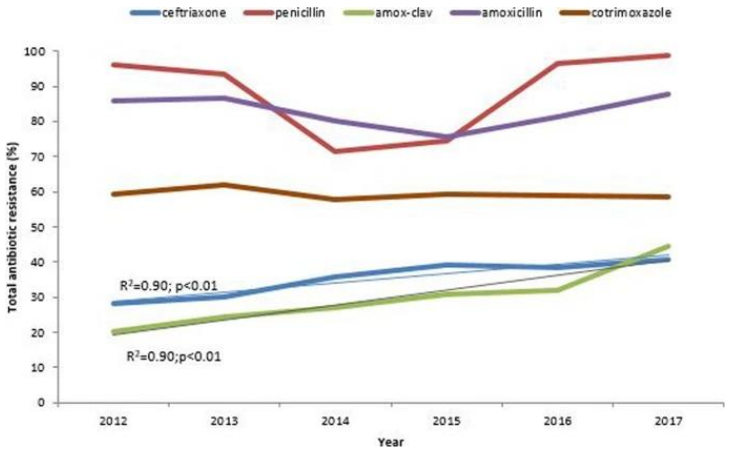

Figure 1.6. Trends of total antimicrobial resistance by common antibiotics. A retrospective record review of data was collected from the microbiology department at a private laboratory between January 2012 and December 2017. (Mhondoro et al., 2019).

1.4.3 The mechanism of co-selection of heavy metals and antibiotics

While inappropriate prescription and the large-scale production of antibiotics in medicine and agriculture clearly stimulates the proliferation of antibiotic resistance, heavy metals have also been suggested to play an important role. The anthropogenic application of antibacterial metal (ion) in the environment coupled with their persistence allows for long-term impacts and interactions with microbial communities and the subsequent selection for metal resistance and indirect co-selection for antibiotic resistance, facilitating intra- and interspecies spread. The structural and functional characteristics of antibiotic resistance share common strategies with those with heavy metal resistance. When a mutation confers to resistance to both metals and antibiotics (cross-resistance) or when metal resistance- and antibiotic resistance-genes are genetically linked to mobile genetic elements (co-resistance), metals can co-select for resistance to clinically relevant antibiotics (Baker-Austin et al., 2006).

There is a concern often voiced about the emergence of pathogens resistant to metallic copper as a result of the increased and constant use of antimicrobial copper alloys in the healthcare setting, similar to the spread of antibiotic-resistant microbes after the introduction of antibiotics. In a worst-case scenario, the impacts of metallic copper on the current medical use of common antibiotics might become an issue, as copper functions as a long-lasting selective agent. Copper and copper-containing compounds have been extensively used in agriculture and aquaculture for centuries as bactericides and fungicides. Previous research has shown that copper amendment in soil environments selects for

various antibiotic resistance in the copper resistant bacteria (Berg et al., 2005; Seiler & Berendonk, 2012). In terms of molecular mechanisms, taking *E. coli* as an example, it has been revealed that copper defence was metabolically associated with antibiotic resistance through a conserved multiple antibiotic resistance regulator (MarR) family of transcription factors (Hao et al., 2014).

Therefore, it is highly possible that bacteria resistant to copper may exhibit reduced susceptibility to antibiotics and antiseptics due to the increased use of metallic copper surfaces in healthcare settings. However, this has rarely been experimented. Until now, there has been only one research testing the antibiotic resistance of bacteria surviving on copper coins (Espirito Santo et al., 2010). Although the result indicated that coin bacteria were no more antibiotic resistant than their type strains, it cannot be concluded that copper resistance is not linked to antibiotic resistance as these bacteria were also sensitive to copper surfaces.

1.5 The mechanism of copper homeostasis in bacteria

The majority of bacteria require trace quantities of copper for basic cellular function such as oxidative phosphorylation and photosynthesis, whereas copper ions are highly toxic to bacterial cells when in excess. It is therefore critical for micro-organisms to evolve into a network of well-regulated copper homeostasis systems in order to balance the cellular requirement for copper with the adversary effects of overexposure to copper ions. So far, the mechanisms of copper homeostasis generally include efficient extracellular uptake of copper ions, intracellular copper-specific transport, relative impermeability of the outer and inner bacterial membranes to copper ions, metallothionein-like copper-scavenging proteins in the periplasm and active export of copper from cells in the extracellular environment through copper-ATPase export pumps (Zhang & Rainey, 2008; Grass et al., 2011).

For example, the non-pathogenic SBW25, which is the model organism of *Pseudomonas fluorescens*, is a plasmid-free plant growth-promoting bacterium that was originally isolated from the phyllosphere of field-grown sugar beet (Bailey et al., 1995). Due to its plant growth promoting properties and potential as a biocontrol agent, SBW25 has been extensively studied and the genome of SBW25 has been sequenced. As it can evolve rapidly when exposed to the appropriate selection pressure to generate a large repertoire of mutants, SBW25 is extensively used in many experimental evolution studies (Rainey & Travisano, 1998; Trippe et al., 2013). In SBW25, two copper-specific transporter systems (Cop and

Cue) are integrally responsible for copper homeostasis and the expression of both is regulated by concentration of copper ions in the medium (Figure 1.7). In environment replete with copper, the Cue systems involving CueA and CueZ are up-expressed to transport excess copper ions outside the bacterial cells under control of the MerR-type CueR regulator, thereby maintaining intracellular copper levels at subtoxic levels and minimising deleterious effects. Under low copper concentrations, the Cop system involving CopCD is activated under the control of CopRS to facilitate the cellular copper uptake, ensuring sufficient supply of copper ions to essential cuproenzymes (Zhang & Rainey, 2008).

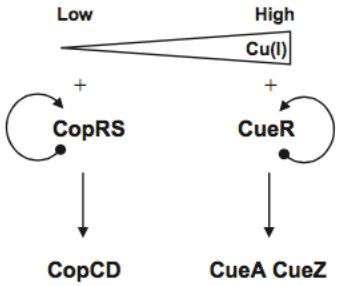

Figure 1.7. A proposed model of copper homeostasis in *P. fluorescens* SBW25. Expression of the gene *copCD* is controlled by CopRS. The system is activated at low levels of copper and repressed by high concentration of copper. Together the Cue system serves to pump excess copper ions out of the bacterial cell. Expression of *cueA* and *cueZ* is controlled by CueR. Both CopRS and CueR are subject to self-regulation (Zhang & Rainey, 2008).

P. aeruginosa, which belongs to the same genus as the *P. fluorescens*, is a gram-negative rod-shaped bacterium mainly thriving in moist environments, such as water and soil (Bodey et al., 1983). *P. aeruginosa* is of medical importance as it has recently emerged as an opportunistic nosocomial respiratory pathogen responsible for a wide range of HAIs in most long-term care facilities during the past two decades. Of high clinical relevance is the ability of *P. aeruginosa* to establish itself within the lungs of those with cystic fibrosis (CF, a genetic disorder caused by a mutation in *cftr* gene). PAO1 is the archetypal strain of *P. aeruginosa* and has undergone complete genome sequencing (Wright et al., 2019).

In *P. aeruginosa* PAO1, the major components of copper homeostasis can be described in the form of three systems: CueR-controlled genes that maintain cytoplasmic Cu^{+} levels, mainly involving a plasma membrane CopA1 and a CusCAB transport system; genes

under control of the Cu^{2+}-sensing two-component CopR/S system regulating Cu^{+} periplasmic distribution; along with genes probably involved in copper influx strongly down-regulated in the presence of external Cu^{2+} (Figure 1.8. Quintana et al., 2017).

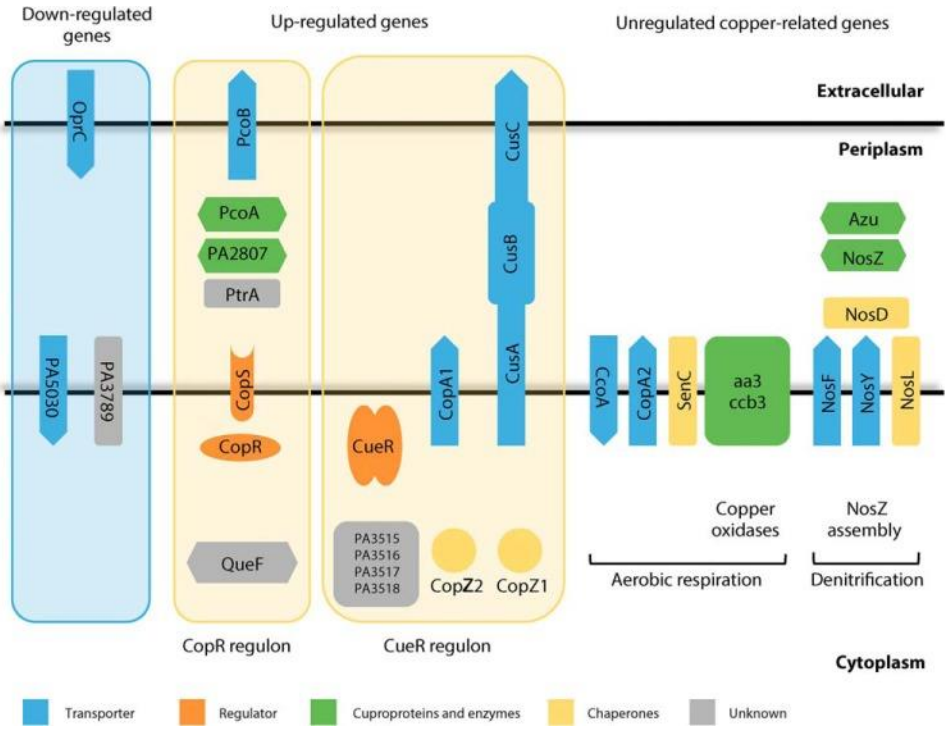

Figure 1.8. A proposed model of copper homeostasis in *P. aeruginosa* PAO1. The model depicts key components of *P. aeruginosa* copper ion distribution mechanisms. The candidates for Cu^{+} influx transporters (green, down-regulated genes), the CopR and CueR regulon (red, up-regulated genes), and the proteins responsible for metallation of cuproproteins (non-induced) are shown. Blue, transmembrane transporters; orange, transcriptional regulators; green, cuproproteins; yellow, chaperones; gray, proteins of unknown role. Hexagonal shapes highlight redox activity (Quintana et al., 2017).

In this study, we used an evolutionary experiment based on the selection of random mutants accumulated in the MPAO1 and SBW25 population either spontaneously or upon mutagenesis to explore the potential of bacteria to develop resistance to ionic copper and better understand the biological response of bacterial cells to copper exposure.

1.6 Specific objectives of this study

The primary goal of this project is to assess the risk of introducing copper alloys in hospital environment. More specifically, we tested a hypothesis that bacterial pathogens can

develop resistance to metallic copper and ionic copper, which is overlapped with resistance to antibiotics. To test this hypothesis, we conducted evolution experiments on metallic copper and to copper ions.

Specific aims of this project are listed as below.

1. Experimental evolution of bacterial resistance to metallic copper.

- A non-pathogenic strain of *P. fluorescens* SBW25 was subjected to a daily passage of sub-lethal conditions on the surface of brass (Cu 63.5%) and pure copper. Rates of copper contact killing will be determined every 10 days for a period of 320 days in total. The accumulated mutations were determined by re-sequencing the genomes of the evolved strains.

  Of note, this experimental task was performed by previous researchers in Zhang's lab.

- **Phenotypic characterization of functional traits associated with the evolution of copper resistance.** The evolved *P. fluorescens* strains were subjected to phenotypic analysis of mutation rate (a), their ability of pyoverdine production (b), minimum inhibitory concentrations of copper ions (c).

- **Investigation of the probable overlapping antimicrobial resistance to metallic copper and antibiotics and antiseptics** This work was performed by comparing bacterial resistance to various classes of antibiotics with a non-pathogenic model strain of P*seudomonas fluorescens* SBW25 and evolved strains subjected to long-term copper contact killing, also involving a panel of mutants derived from SBW25.

2. Experimental evolution of bacterial resistance to ionic copper.

This work was performed using a non-pathogenic strain of *P. fluorescens* SBW25 and a pathogenic strain of *P. aeruginosa* MPAO1. The two bacterial species were subjected to

- Broth-to-broth transfer in LB broth supplemented with $CuSO_4$ at sub-lethal concentrations.
- Colony-to-colony transfer in gradient agar plate containing low to high concentrations of $CuSO_4$.

This work is still on-going in Zhang's lab, but the levels of bacterial resistance to copper ions were determined at the end of this thesis work.

CHAPTER TWO: MATERIALS AND METHODS

2.1 Bacterial strains and growth conditions

Major bacterial strains and plasmids used in this study are provided in Table 2.1. These strains from the -80 ºC freezer were routinely inoculated into Luria Bertani (LB) broth, also referred to as lysogeny broth, which is a nutritionally rich medium. *P. aeruginosa* strains were grown at 37 ºC while *P. fluorescens* strains were grown at 28 ºC (Sambrook et al. 1989). *P. fluorescens* strains were also grown in minimal M9 minimal medium supplemented with histidine and succinate as the nitrogen and carbon sources, at the final concentration of 10 and 20 mM, respectively. Where appropriate, the following antibiotics and other supplements were also added to the growth media at the indicated concentrations except where specifically indicated: X-Gal (40 µg/ml), gentamicin (Gem), kanamycin (Km), tobramycin (Tb), nalidixic acid (Nal, 75 µg/ml), ampicillin (Amp), carbenicillin (Cb), neomycin (Nm), penicillin (Pen), streptomycin (Str), tetracycline (Te).

Table 2.1. List of bacterial strains and plasmids used in this study

Strains or plasmids	Genotypes and relevant characteristics	Source/reference
P. fluorescens		
SBW25	Wild type strain isolated from phyllosphere of a sugar beet plant grown at the University of Oxford farm	Bailey et al. 1995
MU30-5	Δ *mutS,* an allelic exchange *mutS* deletion mutant of *P. fluorescens* SBW25	X.-X. Zhang, unpublished
MU30-11	Δ*mutL*, an allelic exchange *mutL* deletion mutant of *P. fluorescens* SBW25	X.-X. Zhang, unpublished
MU6-16	Δ*cueA*, a SBW25-derived strain with a nonpolar *cueA* deletion	X.-X. Zhang and P. B. Rainey, 2007
SBW25-*lacZ*	SBW25 harboring a neutral, chromosomal *lacZ* marker in a phage locus	X.-X. Zhang and P. B. Rainey
MU6-61	Δ*pvdL*, SBW25 mutant with a deletion of *pvdL* defective in production of pyoverdine	Moon et al. 2008
C1	control group replicate 1 of the 320th evolution experiment transfer	unpublished

C2	control group replicate 2 of the 320th evolution experiment transfer	unpublished
C3	control group replicate 3 of the 320th evolution experiment transfer	unpublished
C4	control group replicate 4 of the 320th evolution experiment transfer	unpublished
C5	control group replicate 5 of the 320th evolution experiment transfer	unpublished
C6	control group replicate 6 of the 320th evolution experiment transfer	unpublished
C7	control group replicate 7 of the 320th evolution experiment transfer	unpublished
C8	control group replicate 8 of the 320th evolution experiment transfer	unpublished
D1	replicate 1 subjected to metallic copper contact-killing of the 320th transfer	unpublished
D2	replicate 2 subjected to metallic copper contact-killing of the 320th transfer	unpublished
D3	replicate 3 subjected to metallic copper contact-killing of the 320th transfer	unpublished
D4	replicate 4 subjected to metallic copper contact-killing of the 320th transfer	unpublished
D5	replicate 5 subjected to metallic copper contact-killing of the 320th transfer	unpublished
D6	replicate 6 subjected to metallic copper contact-killing of the 320th transfer	unpublished
D7	replicate 7 subjected to metallic copper contact-killing of the 320th transfer	unpublished
D8	replicate 8 subjected to metallic copper contact-killing of the 320th transfer	unpublished
P. aeruginosa		
MPAO1	Wild type strain obtained from B. Iglewski (Department of Microbiology, University of Rochester Medical Center, Rochester, NY)	Jacobs et al., 2003
Plasmids		

pUX-BF13	Helper plasmid for transposition of mini-Tn7 element, Ap^r	Bao et al., 1991
PhutuJ-mini-Tn7T-Gm-lacZ	Mini-Tn7 vector, Ap^r, Gm^r	Naren, unpublished
PhutF-mini-Tn7T-Gm-lacZ	Mini-Tn7 vector, Ap^r, Gm^r	Naren, unpublished
PntrB-mini-Tn7T-Gm-lacZ	Mini-Tn7 vector, Ap^r, Gm^r	Naren, unpublished
PcbrA-mini-Tn7T-Gm-lacZ	Mini-Tn7 vector, Ap^r, Gm^r	Naren, unpublished
PcbrB-mini-Tn7T-Gm-lacZ	Mini-Tn7 vector, Ap^r, Gm^r	Naren, unpublished
PplC-mini-Tn7T-Gm-lacZ	Mini-Tn7 vector, Ap^r, Gm^r	Naren, unpublished

2.2 Laboratory media

LB medium, KB medium and minimal M9 salt medium were prepared according to the preparation protocols listed in Table 2.2. They were sterilized by autoclaving at 121 ^oC for 20 minutes. When preparing KB medium, 1.5 g/l sterile magnesium sulphate ($MgSO_4$) was added after autoclaving all other medium components to avoid precipitation. For the preparation of M9 medium, magnesium sulfate ($MgSO_4$) stock solution was filter-sterilized and stored at 4 ^oC. Base M9 minimal salts were of standard composition. When *P. fluorescens* was grown in the minimal M9 salt medium (Sambrook et al., 1989), carbon source (succinate) and nitrogen source (histidine) was supplemented at the final concentration of 20 mM and 10 mM, respectively, except where indicated. Medium supplements such as copper sulfate and X-Gal solution were sterilized by syringe filters and then added after autoclaved LB agar had been cooled to around 50 ^oC at a water bash.

Bacterial strains were stored in glycerol-saline solution at -80 ^oC to remain structurally viable. Glycerol-saline stock in a 2 ml plastic screw top tube was prepared by mixing 1000 µl of the bacterial culture with 800 µl of the 70% glycerol solution which contains 8.5 g sodium chloride (NaCl) and 700 ml glycerol per liter.

Table 2.2. List of laboratory media used in this study

LB medium		Application
Tryptone (10 g/l) Yeast Extract (5 g/l) Sodium Chloride (10 g/l)	Agar (15 g/l)	Agar plates
	X-Gal (40 µg/ml)	Identification of strains with *lacZ* marker
KB medium		
Glycerol (10 g/ml) Proteose Peptone (10 g/l) Dipotassium Hydrogen Phosphate (1.5 g/l) Magnesium Sulphate. Heptahydrate (1.5 g/l)		
Minimal M9 salt medium		
M9 minimal salts (5 X) Magnesium sulfate (1 M) Histidine (10 mM) Succinate (20 mM)		

2.3 Bacterial susceptibility to copper sulfate in *P. fluorescens*

The minimal inhibitory concentration (MIC) of copper sulfate was determined on LB agar plates containing varying concentrations of $CuSO_4$. Two replicates were performed for each concentration to measure the most accurate MIC possible. The stock solution of 100 mM $CuSO_4$ was prepared by dissolving 1.25 g of pentahydrate $CuSO_4$ into 100 ml of sterile water and $CuSO_4$ stock solution was sterilized through a 0.22 µm syringe filter (Millipore) and stored at room temperature (around 20 ^oC). 20 ml LB agar was added into a petri dish supplemented with an appropriate amount of 100 mM $CuSO_4$ solution. Before use, agar plates were left at room temperature (around 20 ^oC) for more than 24 hours to let plates solidify and dry.

For inoculum preparation, 0.5 ml of the overnight bacterial culture of each strain was spun down for one minute. The supernatant of each tube was removed and each cell pellet was re-suspended with the same amount of sterile water. After making a 10-time dilution by adding 100 µl of the resuspension bacterial culture into 900 µl sterile water, 10 µl of the dilution was dropped onto the surface of LB agar plates containing different concentrations of $CuSO_4$. The bacterial growth was examined and photographed at 24, 48 and 72 hours

after inoculation at 28 ºC. In this study, MIC was defined as the minimum concentration of copper at which no visible bacterial growth was observed after 48 or 72-hour incubation.

2.4 Determining the minimal inhibitory concentration of antibiotics in *P. fluorescens*

The antibiotics used in this study were ampicillin (Thermo Fisher), carbenicillin (Sigma-Aldrich), penicillin (Thermo Fisher), gentamicin (Melford), kanamycin (Thermo Fisher), nalidixic acid (Sigma-Aldrich), neomycin (Fisher Bioreagents), streptomycin (Melford), tetracycline (Thermo Fisher) and tobramycin (Sigma-Aldrich). Recipes of antibiotic stock solution are shown in Table 2.3. After solubilizing the antibiotic powder, antibiotic stock solution was sterilized by membrane filtration and stored in 20 ml sterile vials in -20 ºC freezer. When preparing agar plates, 20 ml LB agar was added with each plate containing the following final concentrations of antibiotics: 128, 64, 32, 16, 8, 4, 2, 1, 0.5, 0.25, 0.06, 0 µg/ml.

Table 2.3. List of antibiotics used in this study

Antibiotic	Stock concentration	
Ampicillin	50 mg/ml	add 500 mg into 10 ml sterile water
Carbenicillin	50 mg/ml	add 500 mg into 10 ml sterile water
Penicillin	50 mg/ml	add 500 mg into 10 ml sterile water
Gentamicin	10 mg/ml	add 100mg into 10ml sterile water
Kanamycin	50 mg/ml	add 500 mg into 10 ml sterile water
Nalidixic acid	20 mg/ml	add 500 mg into 10 ml sterile water
Neomycin	50 mg/ml	add 500 mg into 10 ml sterile water
Streptomycin	10 mg/ml	add 100mg into 10ml sterile water
Tetracycline	10 mg/ml	add 100 mg into 10 ml 70% ethanol
Tobramycin	10 mg/ml	add 30 mg into 3 ml sterile water

To prepare the bacterial inoculants, strains stored in -80 ºC freezer were inoculated into 5 ml LB broth and incubated at 28 ºC in a shaker until they achieve a full growth before used in assay conditions. After about 20 hours, the overnight culture was subjected to a diluted a 100-fold dilution by adding 10 µl culture to 990 µl sterile water, resulting in a bacterial suspension with $1x10^6$ cfu ml^{-1}. After dilution, 10 µl of the cell solutions was inoculated onto agar plates supplemented with antibiotics, such that one drop contained around 10^4 cells. Two replicates were performed for each concentration. Colony growth was recorded and

photographed daily during the incubation for a period of 3 days at 28 ºC.

2.5 Measurement of growth kinetics in M9 minimal medium and LB medium supplemented with tobramycin

To ensure strains in growth curve comparisons were physiologically equal, wild type *P. fluorescens* SBW25, evolved copper treatment strains and evolved control strains were inoculated directly from bacterial stocks that had been stored at 80 ºC, grown in 5 ml LB broth at 28 ºC overnight and then re-grown in M9 broth or LB broth. When grown in LB medium, a 200 µl aliquot of each bacterial culture with varying concentrations of tobramycin was directly added into a 96-well microplate (3 replicates). When grown in M9 minimal medium supplanted with succinate (20 mM) as carbon source and histidine (10 mM) as nitrogen source, 1 ml of the overnight bacterial culture was pelleted and washed with M9 salts (1:100 dilution to 1 X) twice. A 200 µl aliquot of each bacterial culture with varying concentrations of tobramycin was added into a well of a 96-well microplate (3 replicates). Growth kinetics of SBW25 and evolved strains were monitored at 28 ºC using a Synergy™ 2 multi-mode plate reader equipped with Gen5 software (Bio-Tek). Absorbance at 450 nm was measured at 5 minutes intervals for a period of 24 hours when grown in LB medium or 48 hours in M9 minimal medium. The plate was shaken for 10 seconds prior to each read.

2.6 Assay for bacterial fitness

Relative fitness of evolved strains was determined by direct competition. Cells were prepared from cultures stored at −80 ◦C, first grown in 5 ml LB broth at 28 ◦C overnight. To initiate the competition, the wild type SBW25 strain used as the competitor was mixed 1:1 with the evolved strain and 5 µl of the mixed culture was inoculated into 5 ml fresh LB medium (each with four replicates). To count the starting ratio, mixed bacteria was subject to serial 10^6 and 10^7-fold dilution in sterile water and 100 µl of each dilution was inoculated onto LB plus X-Gal plates. After 24-hour incubation at 28 ◦C, the 10^{-6} and 10^{-7} dilutions of mixed bacteria were placed out onto LB plus X-Gal plates to count the end ratio. Two days after inoculation, colonies each plate were counted. Relative fitness was calculated as log ratio of Malthusian parameters of the two strains being compared (Lenski et al. 1991).

When measuring bacterial fitness in tobramycin, 5 µl of the mixed culture was inoculated into 5 ml LB medium supplemented with 2 µg/ml tobramycin and mixed bacteria was

subject to serial 10^4, 10^5 and 10^6-fold dilution in sterile water before being placed out.

2.7 Pyoverdine production measurement

To estimate the production of pyoverdine, the experimental culture was prepared by transferring 5 µl overnight culture of LB broth to 5 ml LB broth and KB broth, respectively. Four biological replicates were performed for each broth per strain culture. Following 24-hour and 48-hour incubation at 28 °C, the supernatant was transferred to a 96-well microtiter plate. In this step, four technical replicates were performed to minimize experimental errors. Pyoverdine production was measured in relative fluorescence units (RFU) by measuring fluorescence at the excitation wavelength of 360 nm and the emission wavelength of 460 nm using a Synergy™ 2 plate reader equipped with Gen5 software, with the mean pyoverdine production calculated. The respective broth media was used as the blank. Simultaneously, cell density was assayed in the absorbance at the wavelength of 600 nm (A_{600}).

2.8 Measurement of bacterial mutation rate

Mutation rate was measured using a so-called Luria-Delbrück fluctuation assay. In this study, the fluctuation assay was performed on single colonies from evolved strains of previous experimental evolution and wild type SBW25 strain. Evolved strains and wild type SBW25 strain stored in glycerol-saline at -80 ºC were streaked onto LB agar plates and grown at 28 °C for single colonies. After two-day incubation, a single colony picked up from the plate and inoculated into 5 ml of LB broth and grown for 24 hours at 28 °C with orbital shaking. Assuming the cell density of an overnight bacterial culture of LB broth is around $1x10^9$ cells/ml, the fluctuation test was set up by inoculating of the dilution containing around 500 cells into a 25 ml tube containing 6 ml LB broth. After 24-hour incubation with orbital shaking at 28 °C to stationary phase, the frequency of nalidixic acid mutants was measured. To measure the number of nalidixic acid resistance colonies, the overnight bacterial culture was subjected to 10^0, 10^{-1} and 10^{-2} dilution and 100 µl of each dilution was placed out onto LB agar plates supplemented with 75 µg/ml nalidixic acid. To measure the total number of colonies, serial dilution of 10^{-5}, 10^{-6} and 10^{-7} was performed on the overnight culture and 20 µl of each dilution was dropped onto the surface of the non-selective LB agar plates using drop count method (3 replicates).

Until colonies grew, the number of mutants resistant to nalidixic acid and total colonies per

plate were counted and the means were used in mutation rate calculations. The mutation rate was calculated online using an integrated web tool named as *bz-rates* (accessible at http://www.lcqb.upmc.fr/bzrates) which is based on Luria–Delbrück distribution-generating algorithm (Gillet-Markowska et al., 2015).

2.9 Electroporation technique

2.9.1 Preparation of electrocompetent *Pseudomonas aeruginosa* cells

Prior to electroporation, MPAO1 strain stored in glycerol saline in -80 ºC freezer was inoculated into 6 ml of LB broth medium and grown with orbital shaking overnight at 37 ºC. 1.5 ml of the overnight bacterial culture was centrifuged at 16 g for 2 minutes at room temperature (around 20 ºC). After removing the supernatant, the pellet was further washed with 1 ml of 300 mM sterile sucrose stock solution twice. Bacterial cells were resuspended in 100 µl of 300 mM sucrose solution and were ready for electroporation.

2.9.2 Transformation of *Pseudomonas aeruginosa* by electroporation

DNAs of the desired plasmid (5 µl, ~100 ng) and the pUX-BF13 helper plasmid (5 µl, ~100 ng) were added to 100 µl of electrocompetent cells (Bao, et al., 1991). After chilling on ice for 30 minutes, the bacterial and plasmid suspension was transferred and placed between electrodes of a pre-chilled 0.1 cm-gap Gene Pulser® electroporation cuvette (Bio-Rad) and electroporated using Electroporator 2510 (Eppendorf) at the following settings: 25 mF, 200 Ohms, 1.8 kV.

After transformation by electroporation, 600 µl of LB broth was immediately added into the 1 mm cuvette. Then, all the bacterial culture was transferred from the cuvette into a 1.5 ml sterile eppendorf tube and incubated for 1 hour at 37 ºC with orbital shaking. After being centrifuged and resuspended in 300 µl of LB broth, 150 µl of the bacterial culture was placed out onto LB plus X-Gal plates containing 30 µg/ml gentamicin and incubated at 37 ºC overnight. Until colonies grew, single colonies were picked up and inoculated into 5 ml LB broth with shaking overnight for long-term storage.

To check whether the mini-Tn7 element system had been successfully integrated into the genome of MPAO1, a 170 bp fragment was amplified by PCR reaction (described in Method 2.11) using a pair of strain-specific primers MLG048-PF and MLGO49-PR. Then

strains were stored in glycerol-saline in -80 °C freezer and used as ancestral strains in experimental evolution of bacterial resistance to copper sulfate.

2.10 Experimental evolution of bacterial resistance to ionic copper for *Pseudomonas aeruginosa* and *Pseudomonas fluorescens*

This experimental evolution work was performed using *P. fluorescens* strain SBW25 and *P. aeruginosa* strain MPAO1 marked with *lacZ*. SBW25 is a model bacterium of *P. fluorescens* normally used in the experimental evolution study and *P. aeruginosa* MPAO1 is a pathogenic micro-organism responsible for a wide range of HAIs.

To check potential cross contamination using PCR reaction, each ancestral strain was inserted the *lacZ* marker with a unique promoter in the genome by electroporation described in Method 2.9. All these strains were marked with the *lacZ* gene encoding the protein beta-galactosidase, and thus colonies formed by strains with lacZ marker would show blue color on LB agar plates in the presence of X-Gal (40 μg/ml), ensuring no extraneous contamination and allowing the rapid identification of the evolved bacterial strains.

In this work, we conducted both broth-to-broth transfer and colony-to-colony transfer to select for mutants with increased resistance to copper ions.

2.10.1 Broth-to-broth transfer in LB broth

As outlined in Figure 3.12 (see Results), we set up six independent cell lines for evolution experiment, with each carrying a *lacz* marker with a unique promoter in the genome. To ensure the sequestration between copper and the thiol-containing of LB broth (Nies and Herzberg, 2013), 5 ml LB broth supplemented with appropriate amount of 100 mM $CuSO_4$ were prepared in advance and subjected to orbital shaking for two hours before transfer. 5 μl of the overnight culture of each line, prepared from the ancestral strain stored in -80 °C freezer, was then transferred to a 30 ml plastic tube containing 5 ml LB broth supplemented with subinhibitory concentration of $CuSO_4$. As a control, six evolutionary lines of SBW25 strains were transferred into 5 ml LB broth but without copper sulfate.

During the process of broth-to-broth transfer, evolved bacterial strains were examined every ten transfers. First, bacterial culture was streaked onto LB plus X-Gal plates to check

if there is any possible extraneous microbial contamination. Secondly, to examine whether cross contamination between different lines occurred, identity of the *P. fluorescens* strains were confirmed by polymerase chain reaction (PCR), with each strain using six pairs of primers. Forward primers and reverse primers used as the reagent of PCR reaction are shown in Table 2.4 with the respective fragment length. Thirdly, bacterial cultures were streaked out onto LB plus X-gal plates supplanted with 30 µg/ml gentamicin to further verify the strain identity.

After being verified by both streak plate method and PCR, strains were permanently stored in glycerol saline in -80 ^{o}C freezer for further whole genome sequencing to identify the mutations conferring copper resistance and phenotypic analysis.

2.10.2 Colony-to-colony transfer on gradient LB agar plates

2.10.2.1 Preparation of gradient LB agar plates supplemented with copper sulfate

Colony-to-colony transfer was conducted by using linear gradient plates supplanted with sub-inhibitory concentration of copper sulfate. For the preparation of a linear gradient plate, two layers of LB agar were poured into each plate. 10 ml LB medium with 1.5% agar was added when the Petri plate was elevated. In this way, bottom layer formed a triangular wedge and the entire bottom was covered. The tilt direction was marked with an arrow. After 10 minutes to ensure the bottom layer completely harden, another 10 ml melted LB agar (around 60 ^{o}C) with appropriate amount of 100 mM $CuSO_4$ solution was poured on the top of the bottom layer with the plate in the horizonal position. Linear gradient plates were prepared one day before applying spread plate technique, such that copper sulfate in the top layer diffused vertically and the surface of agar plates contained gradually varying concentration of $CuSO_4$ along the gradient axis (Figure 2.1).

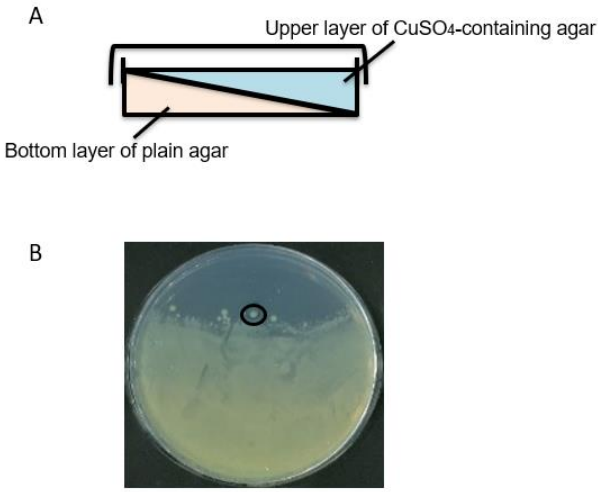

Figure 2.1. Gradient LB agar plate consisting of two agar layers. Figure A shows the gradient plate, with the top layer supplemented with sub-inhibitory concentration of $CuSO_4$ solution and bottom layer of plain LB agar. Figure B is a representative photo of gradient agar inoculated with SBW25 and the mutant colony was circled.

2.10.2.2 Serial passages on gradient LB agar plates

As outlined in Figure 3.15 (see Results), similar to broth-to-broth transfer, we set up six independent cell lines for evolution experiment, with each carrying a *lacz* marker with a unique promoter in the genome. 24 hours after the preparation of gradient LB agar plates, 100 µl overnight culture of copper sulfate free LB broth of each line was placed evenly out onto gradient plates. SBW25 and MPAO1 was incubated at 28 ºC and 37 ºC, respectively. Until mutant grew, a single mutant near to the inhibition zone (cultured with subMICs) was picked up from the gradient plate and then streaked out onto a LB plus X-Gal plate for purification. After incubation for one or two days at 28 ºC or 37 ºC, a single colony showing blue color on LB plus X-Gal plate was inoculated into 5 ml LB broth and grown overnight for the next round of colony-to-colony transfer.

During the process of colony-to-colony transfer, the mutant strain of each line after each cycle was stored in glycerol-saline at -80 ºC freezer and the information of each line was recorded, including storage location, the date of place out and storage.

Table 2.4. List of forward primers and reverse primers

	Forward Primer	Reverse Primer	Fragment length
PhutuJ	PhutuJ	lacz7	790 bp
PhutF	PhutF-F	lacz7	705 bp
PntrB	PntrB-1	lacz7	586 bp
PcbrA	cbrA-FB	lacz7	1170 bp
PcbrB	cbrB-FB	lacz7	1030 bp
PplC	plc-R	lacz7	770 bp

Table 2.5. Sequence of primers used in this study

Primer	Sequence (5' - 3')[a]
MLG048-PF	CAACCTGGCCAAGTCGGTCACC
MLG049-PR	CAGCATAACTGGACTGATTTCAG
PhutuJ	gactagtAATGCCCCAGCGTGGCGCAAAACC
PhutF-F	aactagtACAAGGGCGCCGGACTTTCG
PntrB-1	CAGGGCTTGCACGCTTCTTTTC
cbrA-FB	gaagaTCTACCTGCAGGAACTGCTCG
cbrB-FB	gaagatCTGATCGTCGAAGATGAAGGT
plc-R	ggactagtGGACTTCAGTTCTTGTGGATTC
lacz7	ATCTGCCAGTTTGAGGGGAC

2.11 Standard PCR and agarose gel electrophoresis

The reagents of PCR reaction are listed in Table 2.5. The final total volume of one PCR reaction is 50 µl, containing 1 x PCR reaction buffer, 1.5 mM $MgCl_2$, 0.2 mM dNTP, 0.2 pmol/µl of each forward primer and reverse primer and one unit Taq DNA polymerase. Taq DNA polymerase for PCR amplification was purchased from Invitrogen and the 10 mM deoxyribonucleotide triphophate (dNTP) stock solution was prepared from a 100 mM dNTP set purchased from Bioline by mixing all the four dNTP in equal proportions. Template DNA was prepared by spinning down overnight culture of bacteria in LB broth in microcentrifuge and resuspending within 1 ml sterile water, with 5 µl added to the reaction as template DNA for PCR.

PCR reaction was performed using a gradient thermal Palm-Cycler™ (Corbett Life Science) and thermocycling conditions for a PCR reaction are shown in Table 2.6.

Table 2.6. Reagents of PCR reaction

Reagent	Volume (µl)	Final Concentration
10x PCR Running Buffer	5.0	1 x
$MgCl_2$ (50 mM)	1.5	1.5 mM
dNTP (10 mM)	1	0.2 mM
Forward Primer (10 µM)	1	0.2 µM
Reverse Primer (10 µM)	1	0.2 µM
Taq DNA Polymerase (5 U/µl)	0.2	1 U
Template DNA	5	1 ~ 5 ng per 50 µl
MilliQ H_2O	35.3	
Total Volume	50	

Table 2.7. Standard PCR setup

Stage	Temperature	Time	Cycles
Initial Denaturation	94 °C	3 min	1
Denaturation	94 °C	45 sec	30
Annealing	56 °C	45 sec	
Elongation	72 °C	1 min per kb	
Final Elongation	72 °C	10 min	1
Hold	4 °C	-	-

For the separation of DNA fragments, amplified DNA samples were mixed with 6 x DNA gel loading dye (Thermo Fisher) at the ratio of 1:5 and then loaded into indentations of 1% agarose gel supplanted with 1X SYBR™ Safe DNA gel stain (Invitrogen). To estimate the length of DNA fragments, the ready-to-use GeneRuler 1kb DNA Ladder (Thermo Fisher) was also loaded onto the gel. Gel electrophoresis was carried out in 1 x TBE buffer (UltraPure™, Invitrogen) at 140 volts for 24 minutes. After DNA fragments were separated, we examined the gel by placing the gel under Ultraviolet (UV) light produced by a High-Performance UV transilluminator, and thus DNA became visible. The photograph of gel was taken by using the DigiDoc-It Imaging Systems installed with Doc-It LS Image Analysis Software (UVP, LLC).

CHAPTER THREE: RESULTS

3.1 Evolving *P. fluorescens* SBW25 on the surfaces of metallic copper

This long-term research of experimental evolution forms the basis of the experimental work described in the following sections of this master's thesis. This work was performed by previous researchers in Zhang's lab, and results of a proof-of-concept study were published by Liu and Zhang (2016).

As outlined in Figure 3.1, the work involved two treatments with and without copper contact killing. Eight independent evolutionary lines of strains were subject to continued selection on metallic copper, named as copper treatment strains (D1 to D8). As a control, strains were subject to serial daily transfer in the Luria-Bertani (LB) broth without copper treatment by 1000-times dilution in eight lines, named as control strains (C1 to C8). 320 transfers (around 3200 generations) were performed in total, with the first 200 transfers on a brass coupon (63.5% Cu) and the following 100 transfers on a pure copper coupon (99.99% Cu).

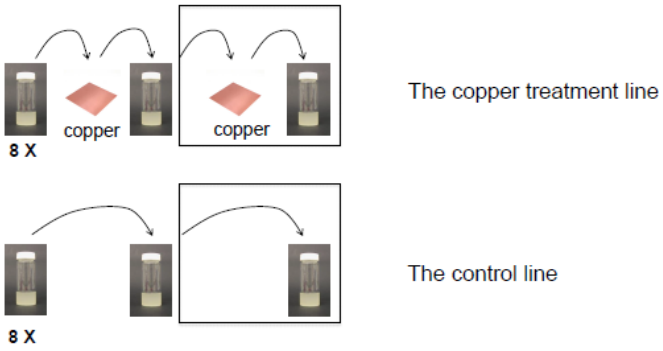

Figure 3.1. Outline of the mutation accumulation experiment. *P. fluorescens* SBW25 was subjected to daily passage of sub-lethal conditions on the surfaces of brass or pure copper. For copper treatment line, bacterial cells from the overnight culture were washed once with sterile water, and then 20 µl added onto a metal coupon. After 60 min treatment at room temperature, all surviving cells on the coupon were suspended into 2 ml of fresh LB medium and subject to next round of copper treatment on the following day. In the control line, bacterial cells were subject to serial daily transfer in parallel without the treatment of contact killing on copper surfaces (Liu et al., 2016).

Bacterial cultures of every 10 transfers were stored in glycerol stock at -80 ℃ freezer and their ability to survive from contact killing on brass and pure copper was then determined. Results are shown in Figure 3.2 and survival rates of evolved strains from the 320th transfer

on copper are summarized in Table 3.1. Survival rates of strains from the control lines without copper treatment remained the low levels during the whole process of evolution. In the contrast, the survival rate of copper treatment lines increased from 0.035±0.001% to 30.982±2.468% during the first 200 transfers on brass, and further increased to 37.795±4.293% from the 320th transfer on pure copper.

Genome of the evolved strains have been sequenced, and a comparison with genome sequence of the ancestral *P. fluorescens* SBW25 identified over 200 mutations. These included *mutS* associated with mutation rates, and many genes involved in pyoverdine production (data not shown).

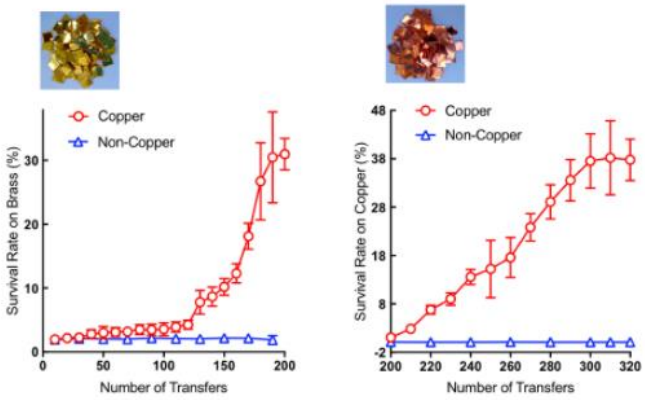

Figure 3.2. Dynamic changes in bacterial resistance to copper. A non-pathogenic strain of *P. fluorescens* SBW25 was subjected to daily passage of sub-lethal conditions (1-hour copper treatment) on the surface of brass during the first 200 transfers and on the surface of pure copper after 200 transfer. As a control, the LSWS-lacZ strain was subjected to the same treatment but without the copper. The survival rate was determined every 20 transfers.

3.1.1 Examining bacterial susceptibility to copper ions

To determine whether evolved strains display higher resistance to copper sulphate, we evaluated the minimal inhibitory concentration of copper ions (MIC-Cu^{2+}) of all evolved strains, wild type SBW25 and mutants derived from SBW25. A *cueA* deletion mutant derived from SBW25 which showed a twofold reduction in its resistance to copper ions, referred to as Δ*cueA*, was used as a control in this study (Zhang & Rainey, 2006).

Representative plate figures are shown in Figure 3.3 with results summarized in Table 3.1 (and all images of 10^{-3}, 10^{-4} and 10^{-2} dilutions are available in Appendix 1). The figures

clearly indicated that evolved copper treatment strains (D1 to D8), especially D3 and D4 (MIC-Cu^{2+}, 3750 μM), were more tolerant to copper ions than wild type SBW25. However, evolved control strains (C1 to C8) displayed the similar levels of resistance to copper ions when compared with the wide type ancestor, with a MIC value of 3250 μM.

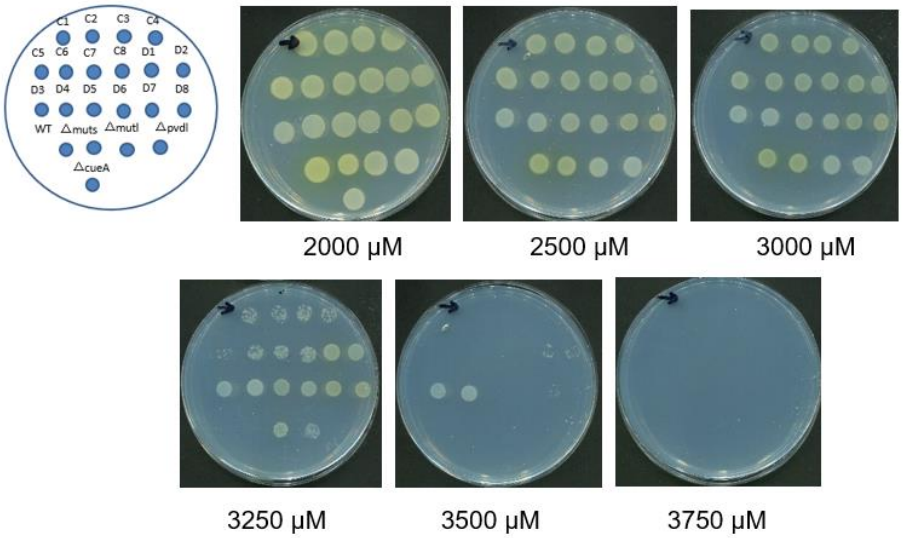

Figure 3.3. Representative plate photos for copper MIC tests. Concentration of $CuSO_4$ is indicated below each agar plate. For each strain, 10 μl of the diluted culture (10^{-4}) was inoculated, and photos were taken after 48 hours incubation at 28 °C.

3.1.2 Measuring pyoverdine production by the evolved strains

Pyoverdine produced by *Pseudomonas* species is a yellow green fluorescent and high affinity siderophore responsible for iron transport, metabolism and heavy metal resistance system (Meyer, 2000; Hannauer et al. 2011). Comparison of the whole genome sequence of the ancestral SBW25 strain and copper treatment strains showed that metallic copper killing caused the mutation on several genes, *pvsA*, *pvdj* and *pvdL*, involved in pyoverdine synthesis in *P. fluorescens*. Thus, we decided to compare the pyoverdine production between evolved strains and wild type SBW25.

In this work, a SBW25 mutant carrying the deletion of *pvdL* which displays a decreased ability to produce pyoverdine was included as a negative control (Zhang & Rainey, 2012).

The results are summarized in Table 3.1. We first measured the pyoverdine production in LB medium after 24-hour and 48-hour incubation. The data for 48-hour incubation is shown in Figure 3.4 and the full dataset for both 24-hour and 48-hour incubation are available in

Appendix 2 - 3. Fluorescence was measured at 460 nm with an excitation wavelength at 360 nm. Result showed that all copper treatment strains produced significantly less pyoverdine compared to wild-type SBW25 after 48-hour growth ($P < 0.05$) (Figure 3.4B). Similar results were obtained for single colonies of the respective evolved strains (Figure 3.4A).

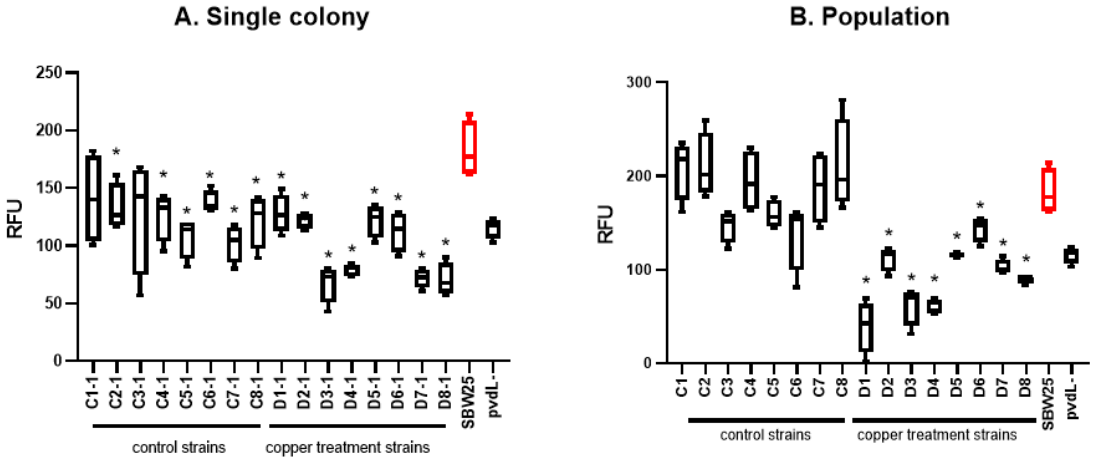

Figure 3.4. Pyoverdine production (RFU) by the evolved strains when grown in LB medium. Pyoverdine production of single colony strains (A) and their respective evolved population strains (B) was measured after 48-hour growth in LB medium. Data are means and standard errors of four biological replicates. Asterisks denote significant difference compared with wild-type SBW25 ($P<0.05$). The line in the middle of the box represents the median; the bottom and top boxes represent the 25th and 75th percentiles, respectively; and the lower and upper whiskers indicate the smallest and the largest values, respectively. Strains included in this assay: control strains from the 320th transfer of evolutionary experiment and their respective single colonies; copper treatment strains and their respective single colonies; wild type SBW25; SBW25 mutant with the deletion of *pvdL* gene.

Next, we preformed pyoverdine production measurements in King's B medium. King's B (KB) medium described by King et al. (1954) is a non-selective medium which can promote the production and excretion of pyoverdine.

After 48 hours incubation, evolved control strains and wild type SBW25 produced characteristic green color while copper treatment strains showed only little greenish yellow fluorescent. As indicated in Figure 3.5, compared with wild type SBW25 strain, copper treatment strains displayed reduced fluorescence in the culture supernatant (Of note, all the details are available in Appendix 4 - 5). Significant but smaller difference was found between evolved control strains and SBW25. Single colonies of copper treatment strains showed the similar pattern to the respective evolved strains whereas among evolved

control strains, only single colonies of C1 and C2 produced significantly lower level of pyoverdine (RFU, 715.000 and 462.500, respectively, *P*<0.001).

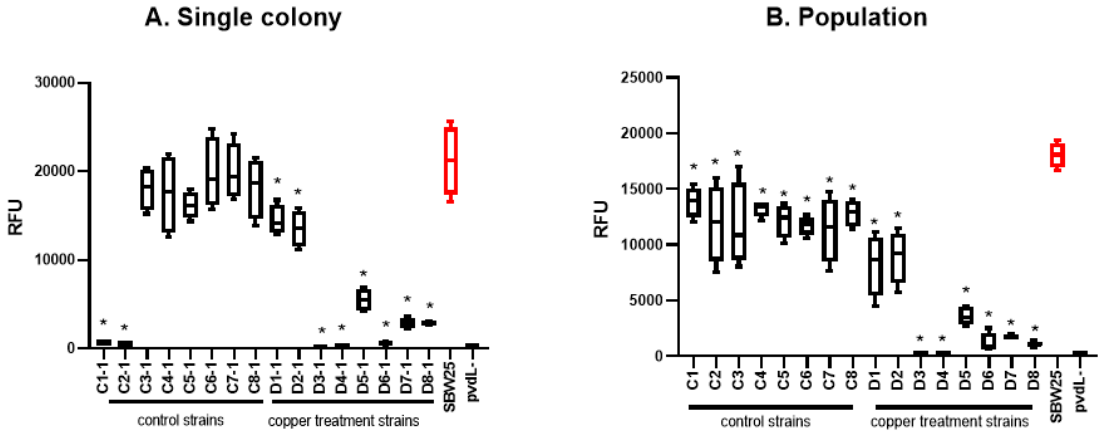

Figure 3.5. Pyoverdine production (RFU) by the evolved strains when grown in KB medium. Pyoverdine production of single colony strains (A) and their respective evolved population strains (B) was measured after 48-hour growth in KB medium. Data are means and standard errors of four biological replicates. Asterisks denote significant difference compared with wild-type SBW25 (*P*<0.05). The line in the middle of the box represents the median; the bottom and top boxes represent the 25th and 75th percentiles, respectively; and the lower and upper whiskers indicate the smallest and the largest values, respectively. Strains included in this assay: control strains from the 320th transfer of evolutionary experiment and their respective single colonies; copper treatment strains and their respective single colonies; wild type SBW25; SBW25 mutant with the deletion of *pvdL* gene.

3.1.3 Using fluctuation test to determine mutation rate of the evolved strains

The data of mutation rates is shown in Figure 3.6 and summarized in Table 3.1 (details are available in Appendix 6). Results of *bz-rates* clearly showed that compared with wild type SBW25, all evolved strains exhibited an average threefold increase in mutation rate. However, there is no significant difference between the mutation rates of evolved control strains and evolved copper treatment strains.

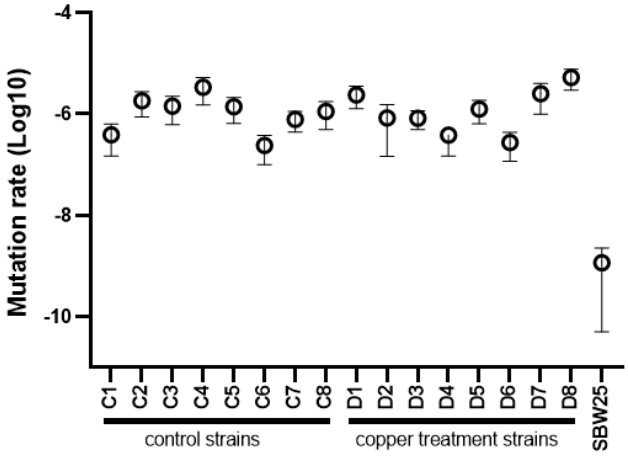

Figure 3.6. Rates of mutation in evolved strains at 320th transfer and in their common ancestor SBW25. Mutation rate was determined by fluctuation test to nalidixic acid resistance and calculated by *bz-rates* web tool. Each bar represents six replicates per population. The line in the middle of the box represents the median; the bottom and top boxes represent the lower and upper 95% confidence limit.

Table 3.1. A summary of phenotypic analysis of wild-type bacteria *P. fluorescens* SBW25 and the evolved strains.

	Resistance to metallic copper (survival rate, %)	Resistance to ionic copper (MIC, μM)	Pyoverdine production (RFU)		Mutation rate (log10)	Resistance to tobramycin (MIC, μg/ml)
			LB	KB		
C1	0.05	3250	208.000	13830.000	-6.41	1
C2	0.04	3250	210.000	11897.500	-5.74	1
C3	0.20	3250	146.500	11687.500	-5.85	1
C4	0.14	3250	194.000	13245.000	-5.47	1
C5	0.04	3250	158.500	12177.500	-5.86	1
C6	0.07	3250	137.250	11750.000	-6.62	1
C7	0.04	3250	187.750	11400.000	-6.11	1
C8	0.17	3250	209.750	12830.000	-5.95	1
D1	41.72	3500	39.000	8237.500	-5.62	2
D2	47.79	3500	111.750	8907.500	-6.08	2
D3	60.00	3750	62.000	130.000	-6.09	2
D4	34.21	3750	58.500	160.000	-6.42	2
D5	22.50	3500	116.000	3580.000	-5.91	2
D6	38.75	3500	143.000	1175.000	-6.57	2

D7	30.93	3500	102.750	1740.000	-5.60	2
D8	26.45	3500	89.500	1052.500	-5.28	2
SBW25		3250	182.750	18045.000	-8.94	1
Δ*cueA*		2500				1
Δ*pvdL*		3250	115.750	175.0		
Δ*mutS*		3250				1
Δ*mutL*		3250				1

3.2 Exploring antimicrobial resistances to antibiotics and copper

3.2.1 Using agar dilution method to determine the minimal inhibitory concentration (MIC) of antibiotics

It might be argued that prolonged use of metallic copper surfaces in hospitals would not only select for resistance traits against copper but also would favor co-selection with innate antibiotic resistance genes. Therefore, in this work we investigated the probable overlapping antimicrobial resistance to copper and antibiotics by determining *in vitro* MIC of various types of antibiotics following agar dilution method (Wiegand et al., 2008).

Antibiotics used in this study are listed in Table 2.3 with the receipts of their stock solution (See Methods). In total, we selected ten types of antibiotics from different classes varying in mechanisms of killing bacteria and all these antibiotics are commonly prescribed to human and highly utilized for medical use in hospitals to minimize diseases. LB agar plates were supplemented with the following concentrations of different antibiotics: 0, 0.06, 0.25, 0.5, 1, 2, 4, 8, 16, 32, 64, 128, 256 μg/ml.

All the results are summarized in Table 3.2 and photos are shown in Appendix 7. Wild type SBW25 shows natural resistance to carbenicillin (Cb), penicillin (Pen) and ampicillin (Amp). As the *lacZ* marker was inserted into the ancestral strain of evolution experiment through mini-Tn7 system, all evolved strains are tolerant to gentamicin (Gem). Thus, these four antibiotics are useless for examining the difference of antibiotic resistances between evolved strains and wild type SBW25. Although evolved copper treatment strains exhibited increased MIC of neomycin (Nm), nalidixic acid (Nal), tetracycline (Tet), streptomycin (Str), kanamycin (Km) and tobramycin (Tob) compared with SBW25, these results may be not accurate due to the spontaneous mutants.

It is interesting to note that the deletion of *mutS* and *mutL* gene for the DNA mismatch repair system and of *cueA* gene encoding a copper homeostasis P-type ATPase increased bacterial resistance to Str.

Thus, we proceeded to subject the overnight bacterial cultures to 10^{-4} and 10^{-5} dilution and inoculate dilutions onto LB agar plates containing varying concentrations of Tob. As shown in Figure 3.7, evolved copper treatment strains were more resistant to Tob (MIC, 2 μg/ml) whereas control strains showed similar MIC of Tob (1 μg/ml) to SBW25. This suggests that there was co-selection of metallic copper resistance and resistance against tobramycin.

Table 3.2. Minimal inhibitory concentrations (MICs, μ g/ml) of antibiotics for the evolved strains and mutants derived from SBW25.

	Pen	Cb	Amp	Nm	Gem	Nal	Str	Tet	Km	Tob
C1	-	-	-	32	>256	64	32	8	16	8
C2	-	-	-	32	256	64	32	8	16	8
C3	-	-	-	32	>256	64	32	8	16	8
C4	-	-	-	32	>256	64	32	8	16	8
C5	-	-	-	32	>256	64	32	8	16	8
C6	-	-	-	32	256	64	32	8	16	8
C7	-	-	-	32	>256	64	32	8	16	8
C8	-	-	-	32	256	64	32	8	16	4
D1	-	-	-	64	>256	64	32	8	32	8
D2	-	-	-	32	>256	64	32	8	16	8
D3	-	-	-	64	>256	64	32	4	32	16
D4	-	-	-	64	>256	64	32	8	32	16
D5	-	-	-	64	>256	64	32	4	32	8
D6	-	-	-	32	>256	64	32	4	16	8
D7	-	-	-	32	>256	64	32	4	16	8
D8	-	-	-	32	>256	64	32	4	16	8
SBW25	-	-	-	16	4	16	8	8	4	2
Δ*mutS*	-	-	-	32	8	64	32			
Δ*mutL*	-	-	-	32	8	32	32			
Δ*cueA*	-	-	-	16	4	16	>64			

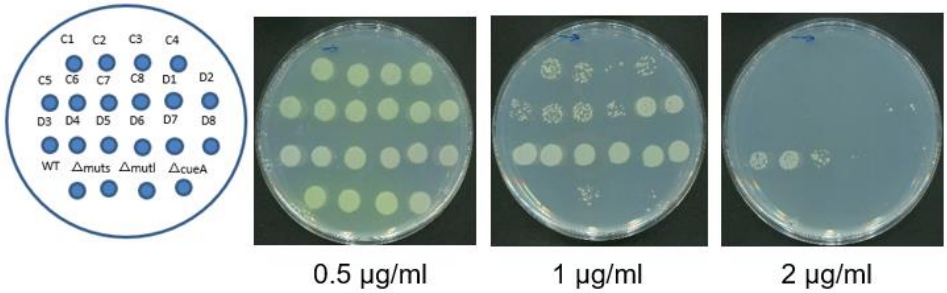

Figure 3.7. Representative photos for the sensitivity of *P. fluorescens* strains to tobramycin. Concentration of tobramycin is indicated below each agar plate. For each strain, 10 µl of the diluted culture (10^{-4}) was inoculated, and photos were taken after 48 hours incubation at 28 °C.

3.2.2 Determining bacterial resistance to tobramycin in broth medium

To further investigate the potential overlapping antimicrobial resistances to copper and antibiotics, we assayed the growth of wild type SBW25 and the evolved strains in broth medium with varying concentrations of antibiotics. This work involved two types of broth medium: LB medium and M9 minimal medium with succinate (20 mM) as the sole carbon source and with histidine (10 mM) as the sole nitrogen source. We selected tobramycin (Tob) as the antibiotic tested in this assay.

The full dataset is available in Appendix 9 - 10 for LB medium and Appendix 11 - 12 for M9 minimal medium. In general, evolved copper treatment strains exhibited altered levels of resistance to Tob. More specifically, in LB medium, evolved copper treatment strains exhibited longer lag phase and higher yield than wild type SBW25 at 2 µg/ml Tob concentration, the condition under which wild type SBW25 showed a significantly reduced but not abolished growth (Figure 3.8A).

In M9 medium with 2 µg/ml Tob, growth pattern of copper treatment lines was not significantly influenced whereas the growth of wild type SBW25 was fully inhibited (Figure 3.9A). Interestingly, D7 and D8 was not grown even in fresh M9 medium without the supplementation of antibiotic (Figure 3.9A), and results of whole-genome sequencing showed that mutations occurred on genes responsible for histidine uptake and transport, such as *hutF*, *cbrB* and *ntrBC*, in these two strain lines.

However, it should be noted that differences were also found between tobramycin resistance of evolved control strains and wild type SBW25: in LB medium and M9 medium

with 2 μg/ml Tob, evolved control strains except C5 grew well than SBW25 and exhibited higher resistance to Tob (Figure 3.8B and Figure 3.9B).

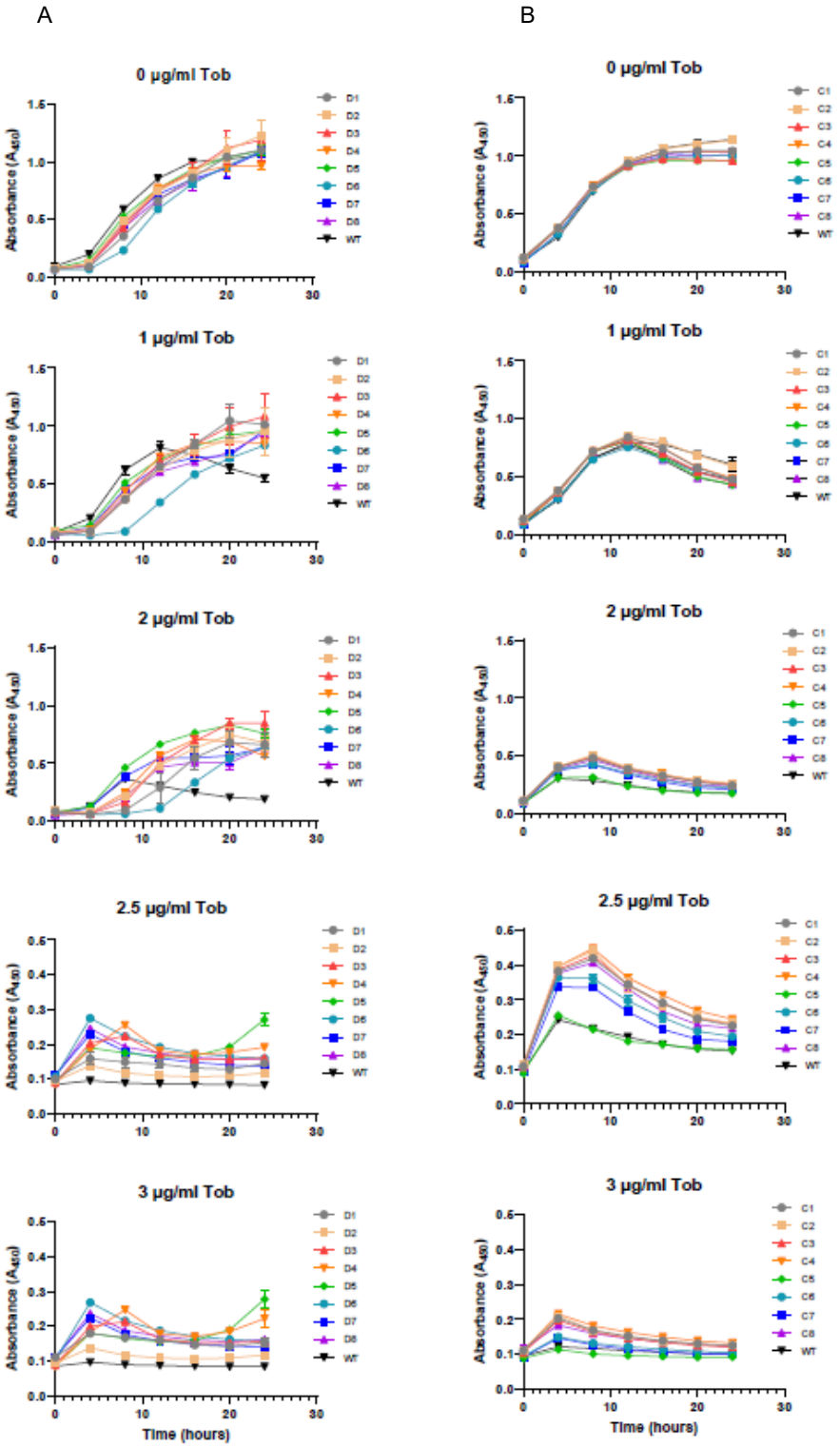

Figure 3.8. Growth kinetics of wild-type SBW25 and the evolved strains (A: copper treatment strains; B: control strains) in LB medium with tobramycin. The concentration of tobramycin is 0,1, 2, 2.5 and 3 μg/ml. Data are means and standard errors

of 3 independent cultures.

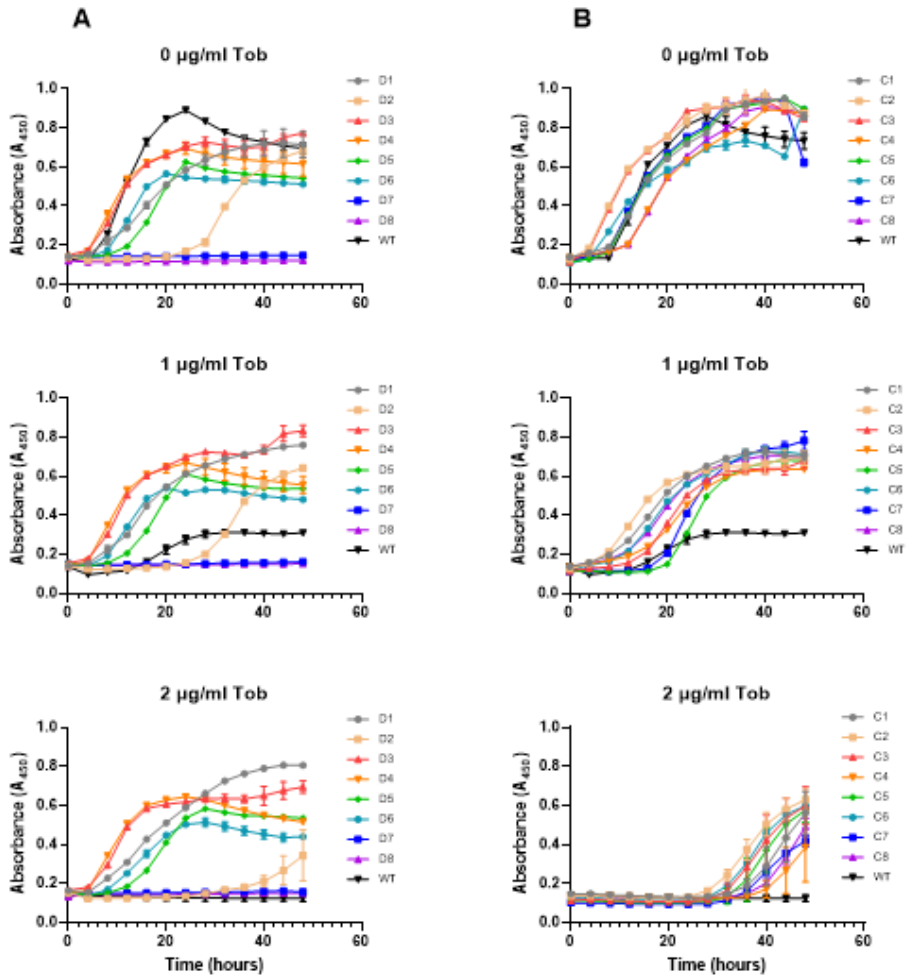

Figure 3.9. Growth kinetics of wild-type SBW25 and the evolved strains (A: copper treatment strains; B: control strains) in M9 minimal salt medium with tobramycin. 20 mM succinate and 10 mM histidine are added into medium as the sole carbon source and nitrogen source, respectively. The concentration of tobramycin is 0,1 and 2 µg/ml. Data are means and standard errors of 3 independent cultures.

3.2.3 Measuring fitness of the evolved strains relative to the wild-type ancestor

To examine the possible impact of copper treatment on microbial antibiotic resistance, we further measured relative fitness of the evolved strains when they were grown in LB medium with and without Tob (2 µg/ml).

The result was summarized in Figure 3.10. The full dataset is available in Appendix 13 for LB medium and Appendix 14 for LB medium with Tob. In unsupplemented LB, relative

fitness of evolved copper treatment strains to wild type SBW25 is lower than that of evolved control strains. In LB medium with subinhibitory concentration of Tob (2 μg/ml), relative fitness of copper treatment strains is greater than that of control strains.

Taken together all the fitness assay data presented above, we can conclude that the copper evolved strains (D1 to D8) showed restively higher levels of resistance when compared with evolved strains without copper treatment (C1 to C8).

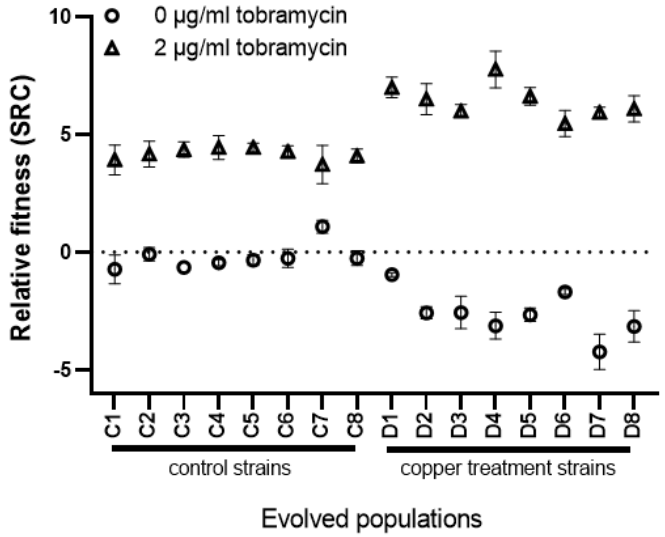

Figure 3.10. Fitness of evolved strains in LB medium with and without 2 μg/ml tobramycin. Fitness of evolved strains was determined relative to the wild type SBW25 after 24h growth in fresh LB medium or LB medium supplemented with 2 μg/ml tobramycin. Fitness data (mean and SEs of four biological replicates) are log10 transformed ratios of the Malthusian parameters for each competitor.

3.3 Evolution of bacterial resistance to ionic copper

3.3.1 Broth-to-broth transfer

In this work, broth-to-broth transfer relied on the stepwise cultivation of bacterial cells in LB media supplemented with subinhibitory concentrations of copper sulphate. To decide the initial copper concentration, we first measured the cell density of wild type *P. aeruginosa* MPAO1 and *P. fluorescens* SBW25 in LB broth supplemented with varying concentrations of copper sulfate. Based on this proof-of-concept study (Figure 3.11), the initial copper concentration of the broth-to-broth transfer was set up as 2.5 mM for SBW25 and 4 mM for MPAO1, which is permissive but subinhibitory for all strain lines. Also, we decided to transfer the bacterial cultures every two days.

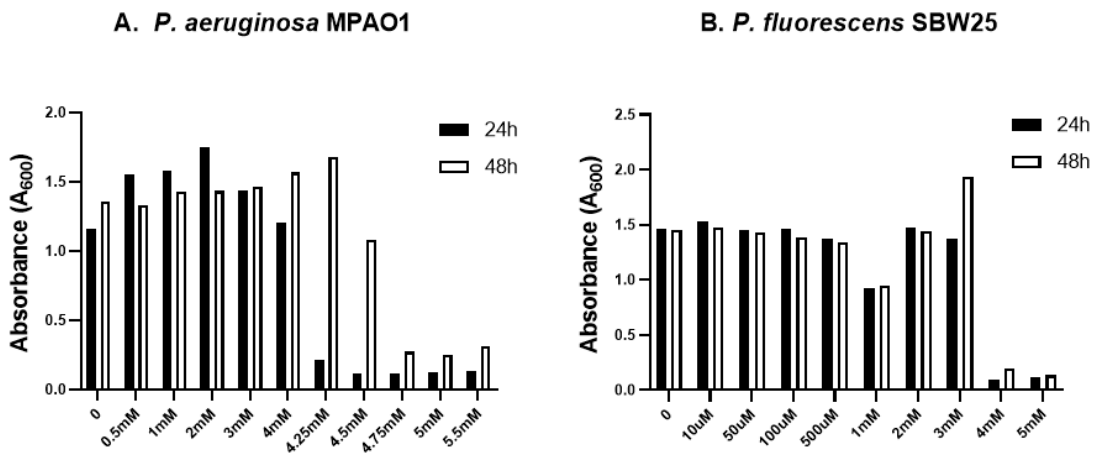

Figure 3.11. Yield of *P. aeruginosa* MPAO1 and *P. fluorescens* SBW25 grown in LB broth supplemented with varying concentrations of copper sulphate. Absorbance (A_{600}) was measured at 24 hrs and 48 hrs after inoculation.

As outlined in Figure 3.12, broth-to-broth transfer started by growing six independent lines of MPAO1 and six lines of SBW25 in 5 ml LB broth and transferring 5 µl of the overnight bacterial cultures in LB medium supplemented with subinhibitory concentration of ionic copper. At each transfer, bacterial cultures were grown for 48 hours before next round of transfer. Every ten transfers, the concentration of ionic copper in LB medium was progressively increased. For SBW25, the starting condition was LB medium with 2.5 mM $CuSO_4$ and the following steps were in LB medium with 3 mM $CuSO_4$ and LB medium with 3.25 mM $CuSO_4$. For MPAO1, the stepwise conditions of broth-to-broth transfer were as follows: LB medium with 4 mM, 4.5 mM, 4.75 mM and 5 mM $CuSO_4$. Treatment B was set up as a control for bacterial adaptation in the LB medium, which was performed in parallel with Treatment A but without copper ions at the sub-lethal concentration.

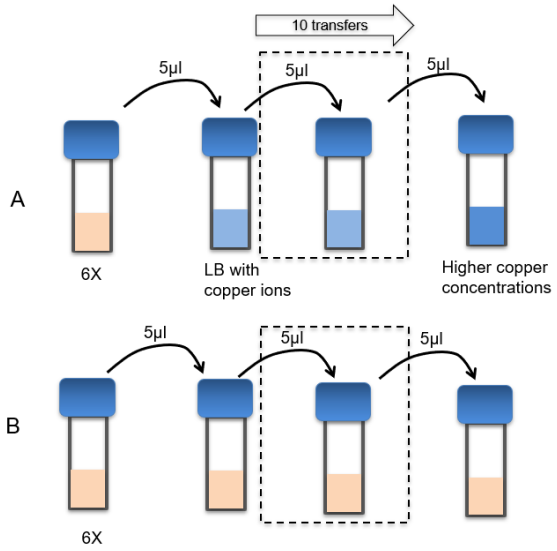

Figure 3.12. Outline of experimental evolution by broth-to-broth transfer. A. For each transfer, 5 µl of bacterial cultures grown in 5 ml LB mediums was inoculated into 5 ml LB medium with subinhibitory concentration of ionic copper. 5 µl of the bacterial cultures will subject to the next round of transfer after two-day incubation. Every ten transfers, concentrations of copper sulphate added into LB medium will be progressively increased. B. A control without the supplement of ionic copper in LB broth.

In this work, ancestral strains were marked with the *lacZ* marker through the mini-Tn7 system, and thus, they form distinctive blue colonies on LB agar plates supplemented with X-Gal and 30 µg/ml Gem (Figure 3.13). These characters were used to verify the strain identity during the process of experimental evolution and ensure that there was no external microbial contamination. In addition, as each ancestral strain was marked with a unique *lacZ* promoter by electroporation, PCR amplification of each strain-specific gene was conducted to verify the strain identity and make sure that there was no cross contamination (Figure 3.14). It should be pointed out that during the course of transfer, one of control lines (EC line) was contaminated, and thus, there were only five control lines for SBW25 at the end of this work.

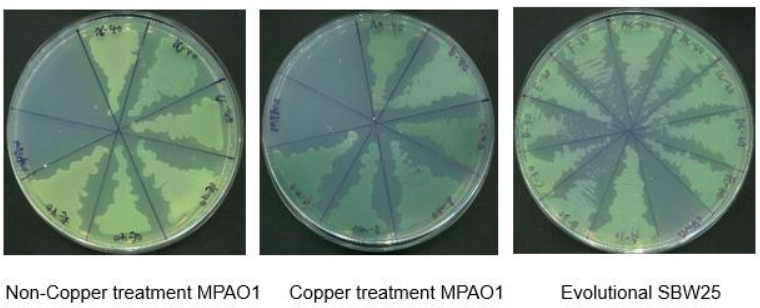

Figure 3.13. Verification of *P. fluorescens* SBW25 and *P. aeruginosa* MPAO1 strains from

the 30th and 40th broth-to-broth transfer, respectively. Copper treatment cultures and control cultures were inoculated onto LB plus X-Gal plates supplemented with 30 μg/ml Gem by streaking. On each plate, the respective ancestral strain was used as the negative control. SBW25 was incubated at 28 ℃ for two days and MPAO1 was incubated at 37 ℃ for one day.

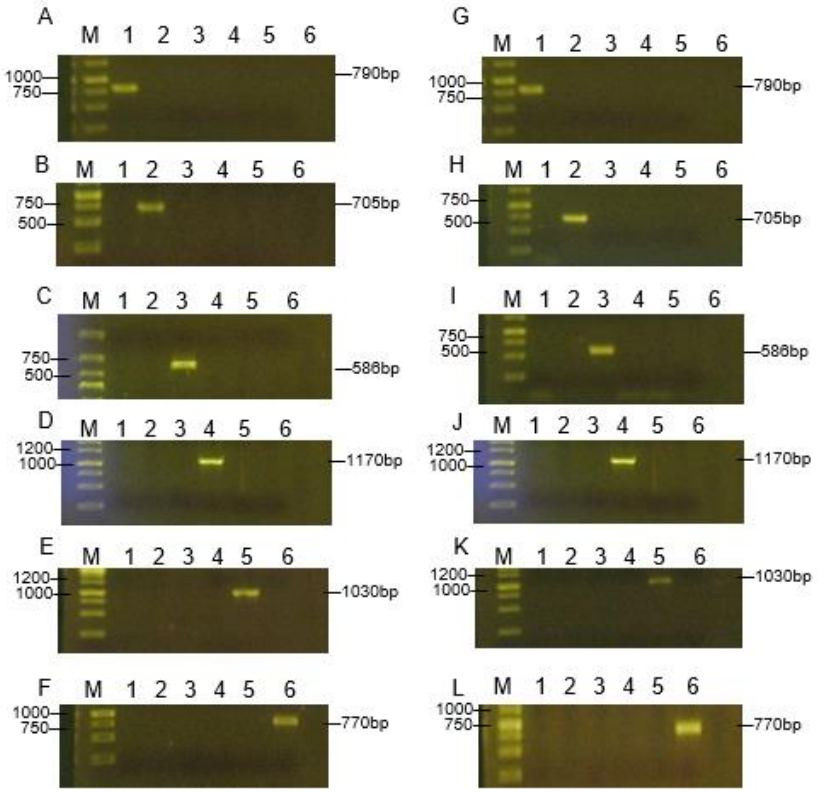

Figure 3.14. PCR verification of each strain line from broth-to-broth transfer. Each unique gene fragment was amplified by PCR using six pairs of primers. Gel electrophoresis was performed in 1 x TBE buffer at 140 volts using GeneRuler DNA ladder. **Lane M**, GeneRuler DNA ladder (1kb). **(A)**, A30. Lane 1 is amplified by primers PhutuJ and lacz7. **(B)**, B30. Lane 2 is amplified by PhutuF-F and lacz7. **(C)**, C30. Lane 3 is amplified by PntrB-1 and lacz7. **(D)**, D30. Lane 4 is amplified by cbrA-FB and lacz7. **(E)**, E30. Lane 5 is amplified by cbrB-FB and lacz7. **(F)**, F30. Lane 6 is amplified by plc-R and lacz7. **(G)**, a40. Lane 1 is amplified by primers PhutuJ and lacz7. **(H)**, b40. Lane 2 is amplified by PhutuF-F and lacz7. **(I)**, c40. Lane 3 is amplified by PntrB-1 and lacz7. **(J)**, d40. Lane 4 is amplified by cbrA-FB and lacz7. **(K)**, e40. Lane 5 is amplified by cbrB-FB and lacz7. **(L)**, f40. Lane 6 is amplified by plc-R and lacz7.

Bacterial cultures of every 10 transfers were stored in glycerol stock at -80℃ freezer and their tolerance towards copper ions was measured at the end of this work. Results are summarized in Table 3.3 with all plate photos available in Appendix 17 and 18. Strains from

the copper treatment line (referred to as a40 - f40 for the 40th evolutional MPAO1 and A30 - F30 for the 30th evolutional SBW25) tolerated up to higher concentrations of ionic copper. In the contrast, the MIC-Cu^{2+} of strains from the control line (without copper treatment, referred to as ac-40 - fc40 for the 40th evolutional MPAO1 and AC30 – FC30 for the 30th evolutional SBW25) remained the similar levels to wild type ancestral strain after the whole process of broth-to-broth transfer (4.5 mM for MPAO1 and 3 mM for SBW25).

Table 3.3. Minimal inhibitory concentrations (MICs) of copper sulphate for the evolved strains by broth-to-broth transfer. As EC line was contaminated during broth-to-broth transfer, MIC of EC30 was not measured.

Strain		Resistance to ionic copper (MIC, μM)
P. fluorescens		
Control lines	AC30	3000
	BC30	3000
	CC30	3000
	DC30	3000
	FC30	3000
Copper treatment lines	A30	3300
	B30	3400
	C30	3400
	D30	3400
	E30	3400
	F30	3400
Wild type SBW25		3000
P. aeruginosa		
Control lines	ac40	4500
	bc40	4500
	cc40	4500
	dc40	4500
	ec40	4500
	fc40	4500
Copper treatment lines	a40	4600
	b40	4700
	c40	4600
	d40	4600
	e40	4600
	f40	4600
Wild type MPAO1		4500

3.3.2 Colony-to-colony transfer using the gradient-plate method

To determine the initial concentration of copper ions for colony-to-colony transfer, we first prepared gradient LB agar plates with the following concentrations of copper sulfate: 4 mM, 5 mM, 6 mM and 7 mM and inoculated MPAO1 and SBW25 onto gradient plates.

On the gradient LB agar plate with 6 mM copper ions and then inoculated with MPAO1, two distinct regions were observed after 48-hour incubation: an area of continuous dense growth and an area of discrete colonies (Figures are available in Appendix 19). Compared with the plate prepared two days before inoculation, there were more single colonies on the LB agar plate prepared only one day before inoculation. Similar results were obtained after three-day incubation on the gradient plate with 5 mM copper ions and inoculated with SBW25 (available in Appendix 19). Therefore, we set up the initial concentration as 5 mM ionic copper for SBW25 and 6 mM for MPAO1 and decided to prepare the gradient plates one day before inoculation.

For the colony-to-colony transfer, we followed the steps outlined in Figure 3.15. In brief, 100 µl overnight bacterial cultures of six independent strain lines were spread out onto gradient plates with copper ions. After several days, a discrete mutant colony was picked and inoculated into fresh LB broth following purification onto LB plus X-Gal plate. The overnight bacterial culture was subject to the next round of colony-to-colony transfer.

A.

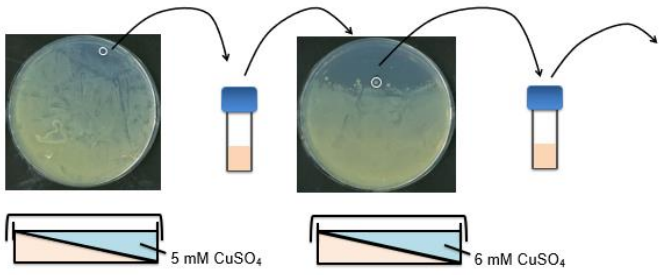

B. *P. fluorescens* SBW25

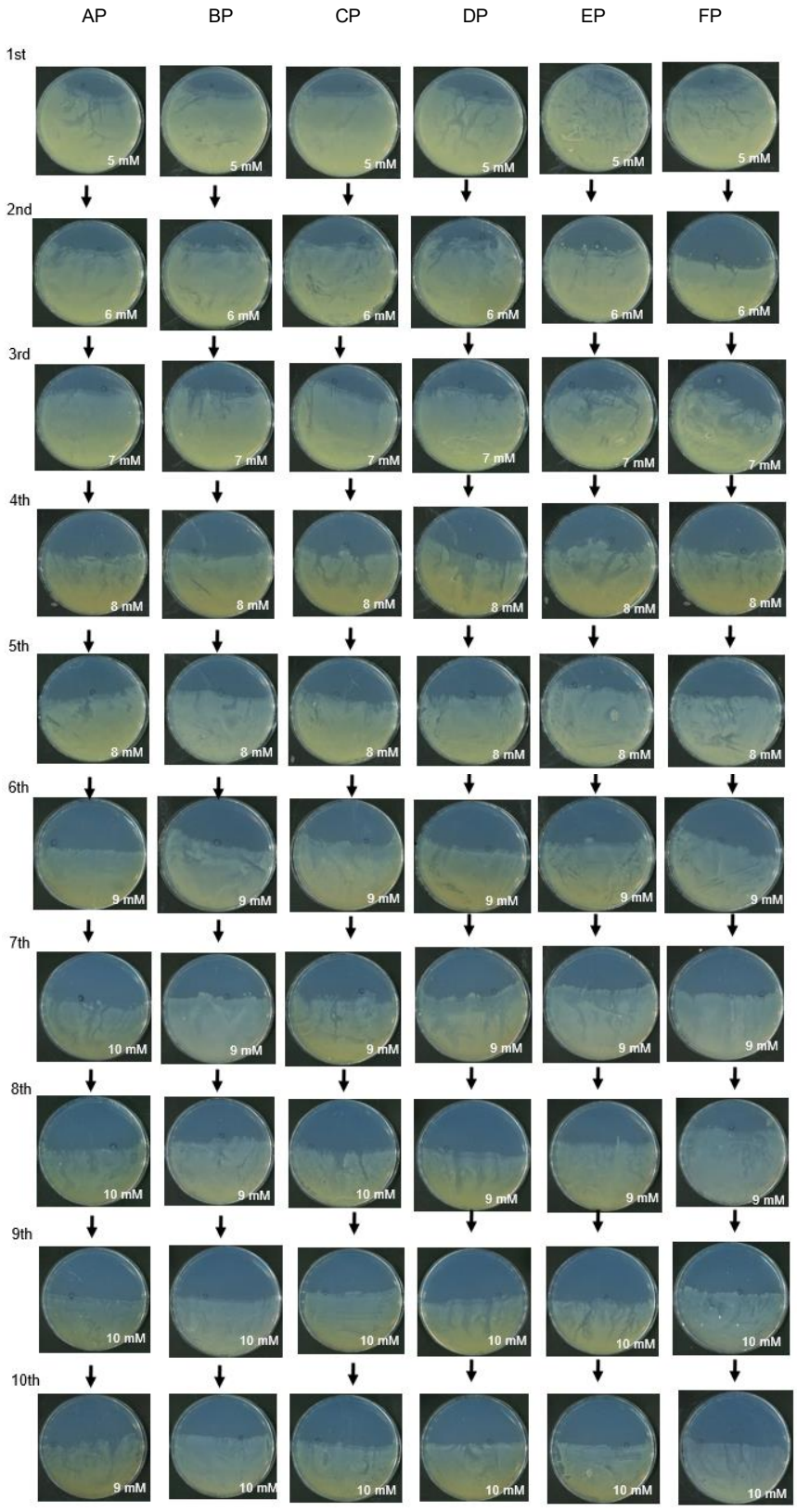

C. *P. aeruginosa* MPAO1

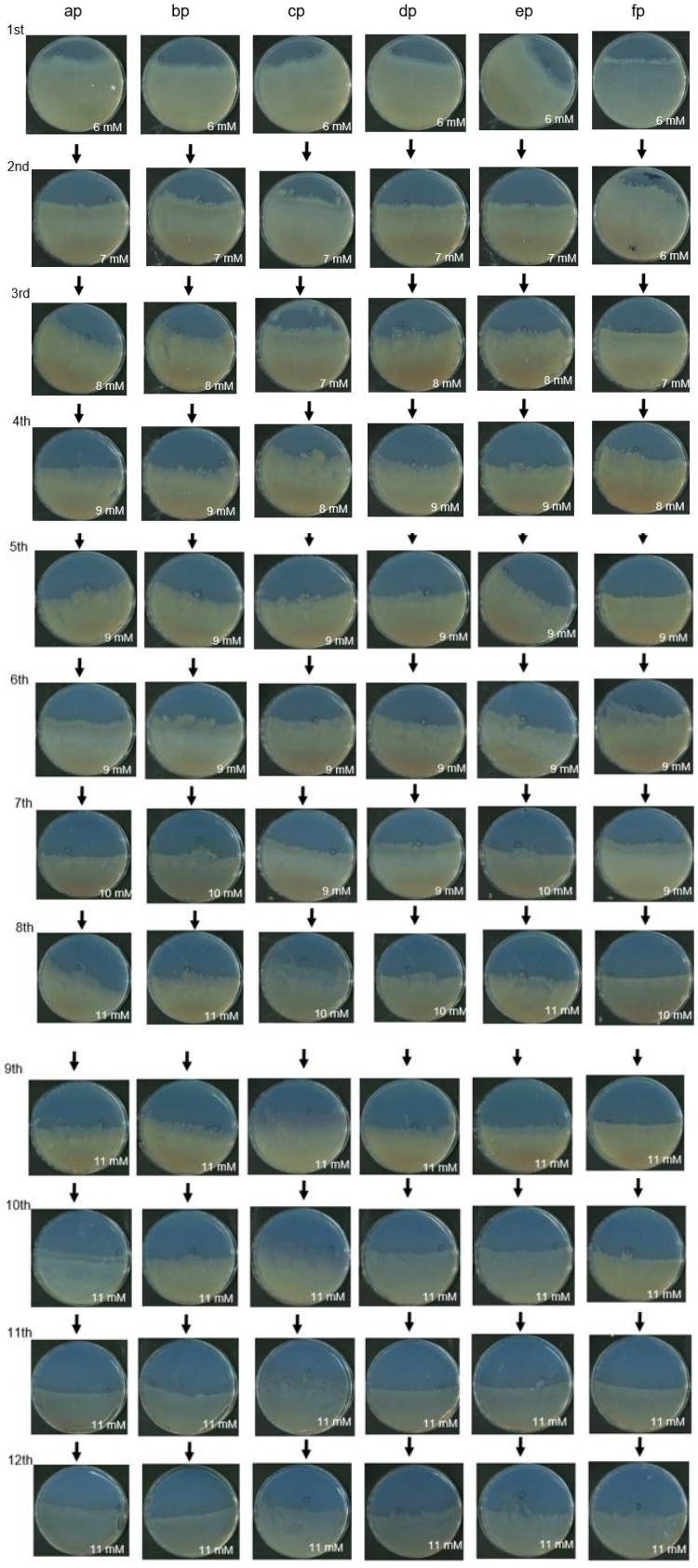

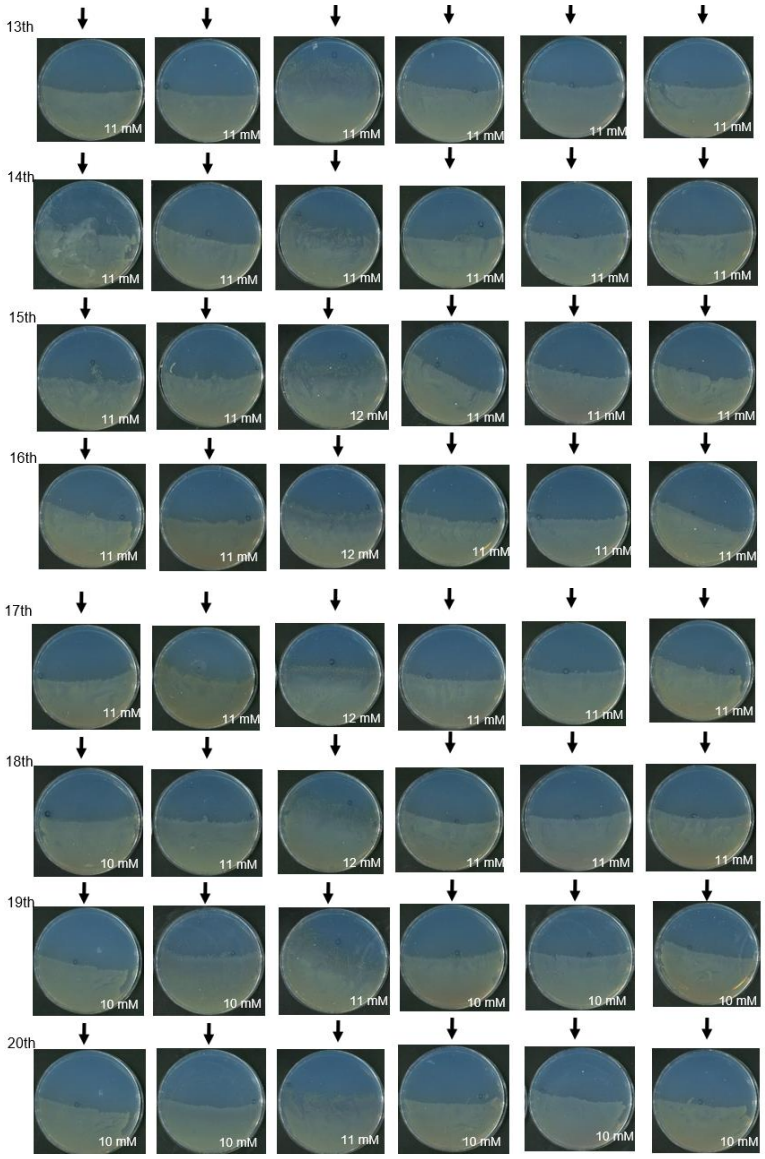

Figure 3.15. Colony-to-colony transfer performed on gradient LB agar plates.

(A) Outline of colony-to-colony transfer. 100 µl of the overnight bacterial cultures was spread onto gradient LB agar plate containing $CuSO_4$ prepared 24h before inoculation and then incubated until mutants grew. Then a single colony from gradient plate was picked and purified on LB plus X-Gal plate by streaking. After purification, a colony was inoculated into 5 ml LB broth and overnight bacterial culture was subject to the next round of colony-to-colony transfer. In total, 10 and 20 transfers were performed on SBW25 and MPAO1, respectively.

(B) Mutants of SBW25 on gradient plates during colony-to-colony transfer. Concentration of $CuSO_4$ is indicated on the corner of each agar plate. In total, SBW25 lines were subject to 10 transfers. The colony picked for the next round of transfer and stored in -80 ºC freezer was circled.

(C) Mutants of MPAO1 on gradient plates during colony-to-colony transfer. Concentration of $CuSO_4$ is indicated on the corner of each agar plate. In total, MPAO1 lines were subject to 20 transfers. The colony picked for the next round of transfer and stored in -80 ºC freezer was circled.

All evolved strains of every transfer were stored in glycerol stock at -80 ℃ freezer. At the end of this experimental work, we preformed PCR (Figure 3.17) and streaked the bacterial cultures onto LB plus X-Gal plates with 30 μg/ml Gem (Figure 3.16) to verify the strain identity. However, the 10th evolutional BP line was wrong as it was amplified by the pair of primers of EP line (Figure 3.17B). By conducting PCR on previous strains of BP line, we found this mistake occurred from the third transfer of BP line during the passage of colony-to-colony transfer.

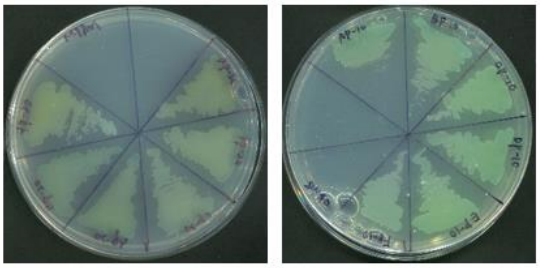

Figure 3.16. Verification of *P. fluorescens* SBW25 and *P. aeruginosa* MPAO1 strains obtained from the 10th and 20th colony-to-colony transfer, respectively. Copper treatment cultures and control cultures were inoculated onto LB plus X-Gal plates supplemented with 30 μg/ml Gem by streaking. On each plate, the respective ancestral strain was used as the negative control. SBW25 was incubated at 28 ℃ for two days and MPAO1 was incubated at 37 ℃ for one day.

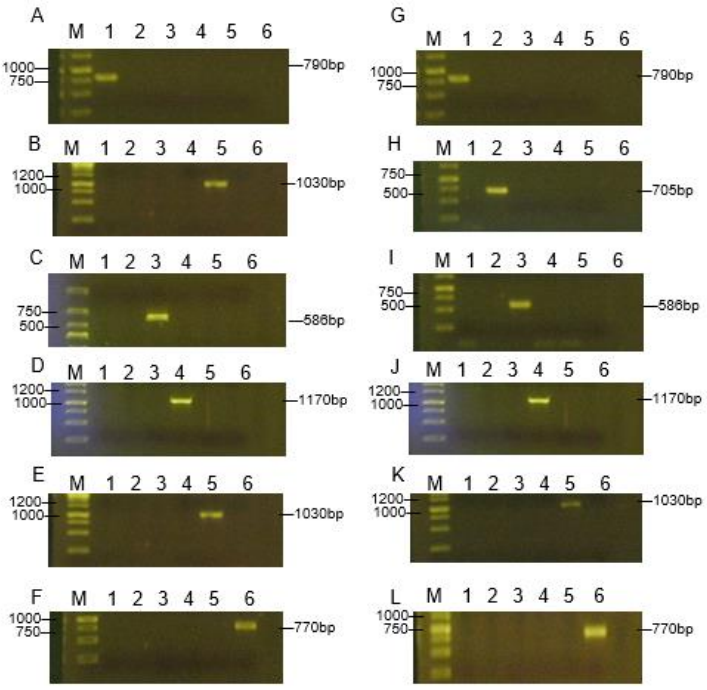

Figure 3.17. PCR verification of each strain line from colony-to-colony transfer. Each

unique gene fragment was amplified by PCR using six pair of primers. Gel electrophoresis was performed in 1 x TBE buffer at 140 volts using GeneRuler DNA ladder (1kb). **Lane M**, GeneRuler DNA ladder. **(A)**, AP10. Lane 1 is amplified by primers PhutuJ and lacz7. **(B)**, BP10. Lane 5 is wrong as it is amplified by cbrB-FB and lacz7. **(C)**, CP10. Lane 3 is amplified by PntrB-1 and lacz7. **(D)**, DP10. Lane 4 is amplified by cbrA-FB and lacz7. **(E)**, EP10. Lane 5 is amplified by cbrB-FB and lacz7. **(F)**, FP10. Lane 6 is amplified by plc-R and lacz7. **(G)**, ap20. Lane 1 is amplified by primers PhutuJ and lacz7. **(H)**, bp20. Lane 2 is amplified by PhutuF-F and lacz7. **(I)**, cp20. Lane 3 is amplified by PntrB-1 and lacz7. **(J)**, dp20. Lane 4 is amplified by cbrA-FB and lacz7. **(K)**, ep20. Lane 5 is amplified by cbrB-FB and lacz7. **(L)**, fp20. Lane 6 is amplified by plc-R and lacz7.

Finally, in this work, we have also conducted an experiment to assay the tolerance towards ionic copper of evolved strains from the colony-to-colony transfer (referred to as AP10 - FP10 for the 10^{th} evolutional SBW25 and ap20 – fp20 for the 20^{th} evolutional MPAO1). Overnight cultures of all strain lines were subject to 10^{-3}, 10^{-4} and 10^{-5} dilution before inoculation. Results are summarized in Table 3.4 and plate photos are available in Appendix 20 and 21. We observed that evolved MPAO1 strains and evolved SBW25 strains obtained from colony-to-colony transfer were able to proliferate up to at least 3.9 mM and 3.75 mM $CuSO_4$, respectively.

Table 3.4. Minimal inhibitory concentrations (MICs) of copper sulphate for the evolved strains by colony-to-colony transfer.

Strain	Resistance to ionic copper (MIC, μM)
P. fluorescens	
AP10	3750
BP10	3750
CP10	3750
DP10	3750
EP10	3750
FP10	3750
Wild type SBW25	3000
P. aeruginosa	
ap20	3900
bp20	4000
cp20	4250
dp20	4000
ep20	4000
fp20	4000
Wild type MPAO1	3700

CHAPTER FOUR: DISCUSSION

4.1 Evolution of bacterial resistance to metallic copper

HAIs are a serious public health problem worldwide and a novel strategy for HAI prevention is to apply antimicrobial metallic copper surfaces within hospitals. Given the expenses of introduction of copper surfaces, it is essential to conduct risk assessment, to optimize the handling of copper surfaces and avoid the potential evolution of metallic copper resistant pathogens. To examine the evolutionary effects of long-term contacts with copper surfaces on bacterial resistance, previous researchers in our lab conducted an evolution experiment on metallic copper. This experimental evolution allowed us to investigate physiological differences involved in acquired copper tolerance that we briefly summarize and discuss in the following.

There has been no doubt that copper ions play a major role in the process of bacterial contact killing on metallic copper. Recent research demonstrated that defense systems against copper ions are attributable to the survival of bacteria on copper cast alloys in *P. aeruginosa* (Elguindi et al., 2009). Previous work showed that in most case, MIC scores of copper ions are positively correlated with survival rate on metallic copper (Liu & Zhang, 2016). We therefore reasoned that evolved strains with higher survival rate on metallic copper are more tolerant to ionic copper. Our own data presented in this study showed that evolved copper treatment strains exhibited higher MIC of copper ions when compared with wild type SBW25.

When measuring MIC-Cu^{2+}, we first inoculated overnight bacterial cultures subjected to serial 100-fold dilution onto LB agar plates supplanted with the following ionic copper concentrations: 1.5, 1.75, 2.0, 2.5, 3.0, 3.5, 3.6, 3.7, 3.75, 3.8, 3.85, 3.9, 3.95, 4.0, 4.1, 4.2, 4.3, 4.4, 4.5, 4.6, 4.7, 4.8, 4.9, 5.0, 5.1 mM. MIC-Cu^{2+} units were determined after incubated three days. However, results were complicated by the rise of spontaneous mutants in evolved strains due to the passage of long-term experimental evolution (Figures are available in Appendix 1).

As the mutation rate is constant, we decided to subject the overnight bacterial cultures to serial 1000-fold and 10000-fold dilution to reduce the number of inoculated bacterial cells, thus minimizing the interference of mutants on the measurement of MIC-Cu^{2+}. Also, considering that bacteria forms bacterial lawn whereas mutants form single colonies under

the inhibitory concentration, we monitored the growth statuses and took photos from day one to day three after inoculation. Thirdly, the standardization of the number of bacterial cells used for susceptibility testing is critical for obtaining accurate and reproducible results. Thus, concentration of copper ions was set up starting from 0μM.

High mutation rates have been reported in *Escherichia coli* undergoing experimental evolution (Sniegowski, et al., 1997). Furthermore, it has been established that chronic exposure to sublethal levels of a metal can substantially increase the rate at which large-scale heritable mutations arise in genomes (Chain et al., 2019). Armed with the knowledge that metal stress can impair DNA replication and DNA repair system (Baer et al., 2007), we then assayed for spontaneous mutation rates in the common ancestral strain SBW25 and in the evolved strains by the fluctuation test for nalidixic acid resistance. Consistent with previous research, our results illustrated that evolved strains were associated with higher mutation rates than ancestral strain, with around triple the rates of mutation.

In this work, we also identified decreased pyoverdine production subsequent to long-term copper treatment. Previous research by Zhang and Rainey (2012) has shown that strains defective in pyoverdine production gained advantage under the conditions where pyoverdine was not required and another research by Jin et al. (2018) demonstrated that *P. aeruginosa* suppressed secretion of pyoverdine and accumulated pyoverdine in the periplasm when exposed to environmental stresses. One explanation might be that the pyoverdine-mediated iron uptake results in oxidative stress and thus kills cells faster in the presence of copper ions.

4.2 Overlapping antimicrobial mechanisms of antibiotics and metallic copper

Copper has been domestically used for thousands of years. Applying copper surfaces with antimicrobial activities onto surfaces commonly touched in hospital facilities, such as doorknobs and toilet seats will certainly be a significant economic commitment. However, there is a chance that introduction of copper alloys may facilitate multi drug resistance, resulting in the failure of medical antibiotic treatment and other hospital hygiene controls. Considering that possible impacts of metallic copper on the medical use of antibiotics have rarely been explored, it is critically important to analyse the potential impact of copper alloys on antibiotic resistance.

Minimum inhibition concentrations are the gold standards in determining the susceptibilities of bacteria to antibiotics and other antimicrobial drugs. There are two general methods reported in literature for assaying MIC: agar dilution method and broth dilution method (Wiegand et al., 2007). In this work, we first measured MIC using agar dilution method. However, the mutation rates of evolved strains are significantly increased; thus, it is not appropriate to compare MIC of evolved strains with wild type SBW25 without sufficient dilution, and it would be technically difficult due to the large amount of manual handling needed to run the test. Thus, we decided to compare the growth curve under different concentrations of antibiotics.

Tobramycin displays a narrow spectrum of activity similar to gentamicin, but is less nephrotoxic. Tobramycin works by preventing the formation of 70S complex and thus blocking the translation of mRNA (Haddad et al., 2002). Tobramycin is especially effective against species of *Pseudomonas* and consequently is commonly prescribed to treat cystic fibrosis associated with *P. aeruginosa* infection. Therefore, we selected tobramycin in this part of work.

We found that copper treatment strains still grew well in mediums with inhibitory concentration of tobramycin. Although control strains could be cultured under inhibitory concentration of tobramycin, they exhibited different changes in growth patterns compared with copper treatment strains. For example, in LB medium with 2μg/mL tobramycin, most evolved copper treatment strains showed a significant lag phase extension while lag phase of evolved control strains was not altered. Previous research indicated that extension in the lag-time allows bacteria to survive under high antibiotic concentrations and accommodate the selective antibiotic pressures as an advantageous trait (Fridman et al., 2014; Li et al., 2016). Hence, we can suggest that altered levels of resistance to tobramycin of copper treatment strains results from long-term copper contact rather than other spontaneous mutations occurring during the experimental evolution. Additionally, the difference between growth patterns in different mediums may be due to changes in fitness of the populations relative to their ancestral strain. Taken together, our data support the overlapping antimicrobial resistance to copper and tobramycin.

4.3 Evolution of bacterial resistance to ionic copper

In addition to its use as a commonly touch surface in healthcare settings, the antimicrobial effect of copper is being exploited in liquids and potent liquid formulations containing

copper ions might therefore be of potential use to control the spread of pathogens found in the healthcare environment responsible for HAIs. Recently, the biocidal effects of several copper-based liquid formulations have been assessed, confirming their efficacy against organisms highly relevant to HAIs (Gant et al., 2007). However, there may be chance that pathogens can evolve resistance to ionic copper due to large-scale application of these copper-based liquid formulations. In addition, considering the essential role of copper ions in copper contact killing, it is crucial to assess the potential of bacterial pathogens to develop resistance to copper ions. In this work, we have conducted an experimental evolution to examine the evolutionary effects of long-term subinhibitory concentration of copper ions on bacterial resistance to ionic copper and potential resistance to metallic copper and antibiotics. This part of work involves broth-to-broth transfer and colony-to-colony transfer on copper gradient agar plate. While this work is currently ongoing, our primary data indicates that bacteria has evolved higher resistance to copper ions compared with ancestral strains.

CHAPTER FIVE: CONCLUSION AND FUTURE RESEARCH

5.1 Evolved strains show different functional traits associated with the evolution of copper resistance

Copper and copper alloys exhibit intrinsic antimicrobial activities to a wide range of pathogens and consequently, have a great potential in reducing the incidence of hospital-acquired infections (HAIs) when applied to commonly touched surfaces in healthcare settings such as door handle, pushing plate and toilet seats. However, there is a concern about the emergence of copper-resistant pathogens.

Previous researchers in Zhang's lab conducted experimental evolution, whereby eight independent lines of the non-pathogenic model bacterium – *P. fluorescens* SBW25 marked with a *lacZ* gene were daily treated with brass or pure copper for a period of 320 days in total. The data of rate of contact killing indicates that the evolved strains exhibit an increase of resistance to metallic copper. In this work, phenotypic characterization shows that all evolved strains subjected to long-term metallic copper treatment have enhanced mutation rate and decreased abilities to produce pyoverdine. Also, evolved copper treatment strains are more tolerant to ionic copper. This result suggests overlapping mechanisms conferring metallic and ionic copper resistances.

5.2 Resistance to metallic copper is overlapped with resistance to tobramycin.

Data of agar dilution method presented in this thesis indicates that evolved copper treatment strains have increased MIC of tobramycin compared with wild type SBW25. In addition, results of growth curve show that evolved copper treatment strains exhibit altered levels of resistance to tobramycin. All these data support the overlapping antimicrobial resistance to copper and tobramycin.

5.3 Bacteria has evolved increased resistance to copper ions through evolutionary experiment

Given the important role of copper ions in copper contact killing, it is critically important to assess the potential of bacterial pathogens to develop resistance to ionic copper and analyse physiological and genomic changes enabling bacterium to survive under sub-lethal

concentrations of copper ions.

In this work, we have subjected a non-pathogenic model bacterium *P. fluorescens* SBW25 and a common nosocomial pathogenic bacteria *P. aeruginosa* MPAO1 to a long-term experimental evolution, including broth-to-broth transfer and colony-to-colony transfer whereby bacterial cells were treated with sub-inhibitory concentration of copper ions in LB broth and on LB agar plates, respectively. Our primary data suggests that all the evolved copper treatment strains show an increased resistance to copper ions when compared with ancestral strains.

5.4 Future research

In this thesis, we have tested the potential of pathogens to develop resistance to metallic copper using experimental evolution and examined several functional traits associated with the evolution of copper resistance. Our data indicates the increased rate of mutation in evolved strains, perhaps resulting from the defects in their ability to repair DNA caused by copper contact killing. However, direct evidence on reactions between DNA and metallic copper are still lacking. Visualization of the DNA damages caused by contact killing can potentially be achieved using comet assay (Singh et al., 1988). Also, we observed that long-term contact with copper surfaces reduced pyoverdine production of SBW25. To better understand the role of pyoverdine in copper contact killing, we can compare the death rate of mutant defective in pyoverdine production on copper surface with SBW25 following the wet incubation method (Warnes & Keevil, 2011).

Secondly, we have examined the resistance to tobramycin of the evolved strains and explored possible correlation with resistance to metallic copper. Although it can be concluded from my thesis that copper resistance is associated with tobramycin resistance, we have not tested whether this is true for other antibiotics. Therefore, future work will first involve the analysis of growth curve of evolved strains when exposed to other antibiotics and Epsilometer test by using ready-to-use antibiotic stripes to measure antibiotic MIC (Glupczynski et al., 1991). Also, we can measure the growth curve of evolved copper treatment strains in M9 medium with other nitrogen source, such as ammonium chloride.

Finally, we have used the experimental evolution to examine the potential of a pathogenic bacteria of *P. aeruginosa* PAO1 and a model organism of *P. fluorescens* SBW25 to develop resistance to copper ions. During the course of broth-to-broth transfer, even when the

concentration of copper ions is same as last transfer, bacterial cells may be not capable of growing. It is assumed that bacterial cells might undergo the viable but nonculturable (VBNC) condition occurring in response to adverse circumstances. To determine cell status, we can use the Live/Dead BacLight bacterial viability kit methodologies with fluorescent microscopy (Ordax et al., 2006).

While promising results for experimental evolution have already been obtained in this thesis, it should be noted that the experimental evolution work has only been performed for around four months in total due to the time limit of my master program. Consequently, the long-term experimental evolution work initiated in this work to develop bacterial resistance to ionic copper is still ongoing in Zhang's lab. According to the original experimental design, extensive genotypic and phenotypic characterizations will be performed with the evolve strains at the end of this experiment (e.g. after 50^{th} transfer for colony-to-colony transfer and 100^{th} transfer for broth-to-broth transfer). More specifically, whole genome sequencing will be used to identify the mutations accumulated during the process of experimental evolution and characterization of their functionalities will be performed. Together, it is anticipated that new data from longer term experimental evolution will help us better understand the mechanisms of bacterial resistance to antimicrobial metallic copper surfaces and evaluate the potentials of bacterial resistance to antimicrobial copper surfaces and ionic copper.

APPENDICES: 1-21

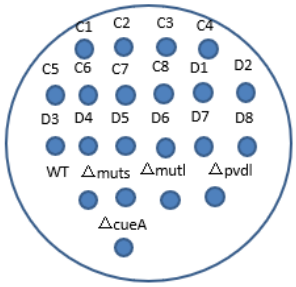

Dilution: 10^{-3}

24 hours

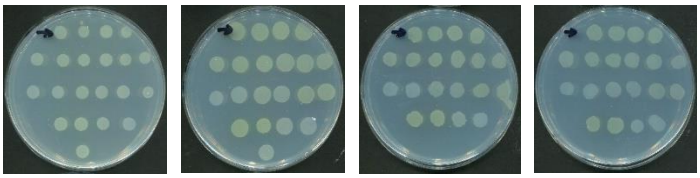

0 μM 1000 μM 2000 μM 2500 μM

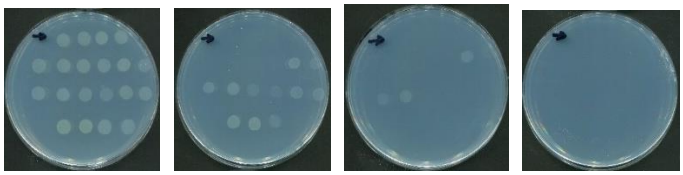

3000 μM 3250 μM 3500 μM 3750 μM

48 hours

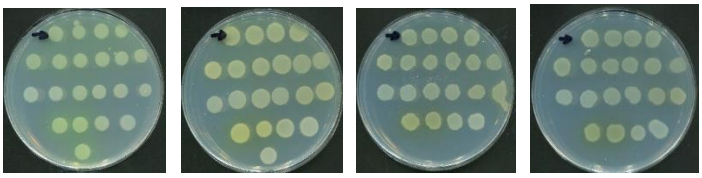

0 μM 1000 μM 2000 μM 2500 μM

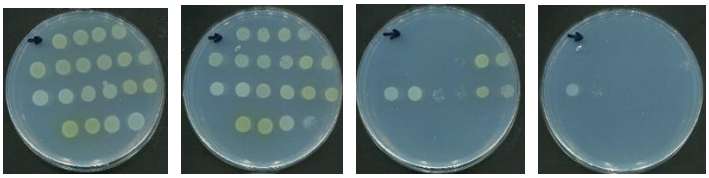

3000 μM 3250 μM 3500 μM 3750 μM

72 hours

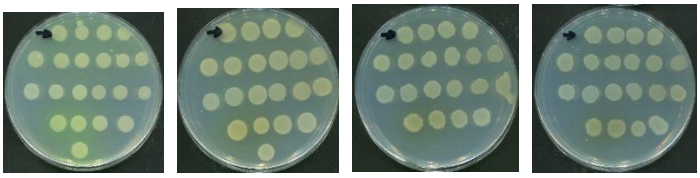

0 µM 1000 µM 2000 µM 2500 µM

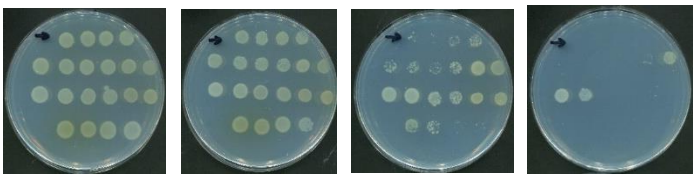

3000 µM 3250 µM 3500 µM 3750 µM

Dilution: 10^{-4}

24 hours

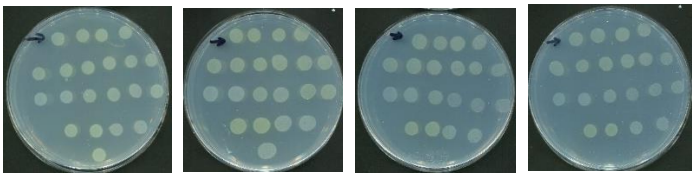

0 µM 1000 µM 2000 µM 2500 µM

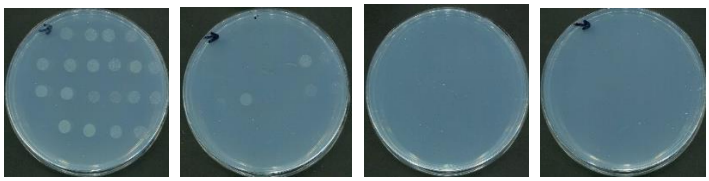

3000 µM 3250 µM 3500 µM 3750 µM

48 hours

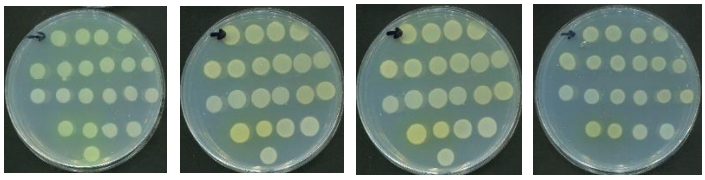

0 µM 1000 µM 2000 µM 2500 µM

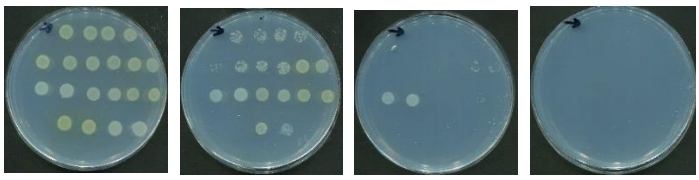

3000 µM 3250 µM 3500 µM 3750 µM

72 hours

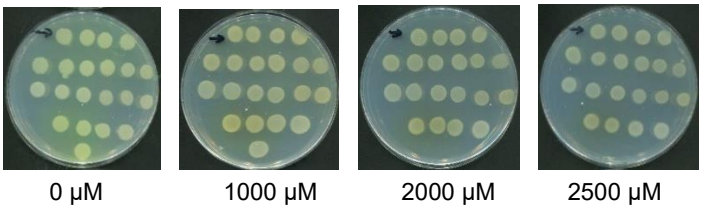

0 µM 1000 µM 2000 µM 2500 µM

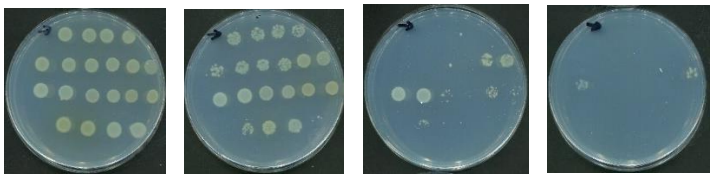

3000 µM 3250 µM 3500 µM 3750 µM

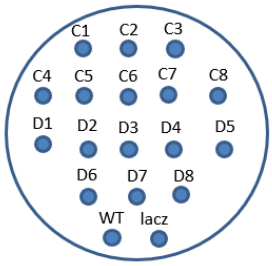

Dilution: 10^{-2}

24 hours

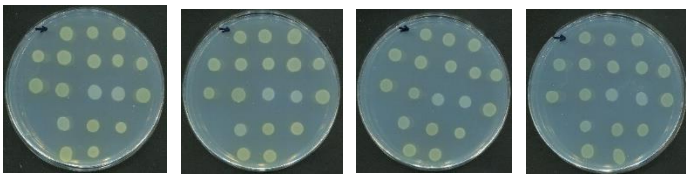

2000 µM 2500 µM 3000 µM 3500 µM

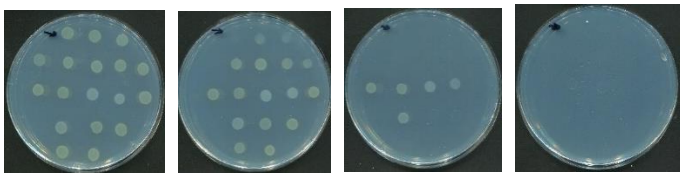

3750 µM 4000 µM 4500 µM 5000 µM

48 hours

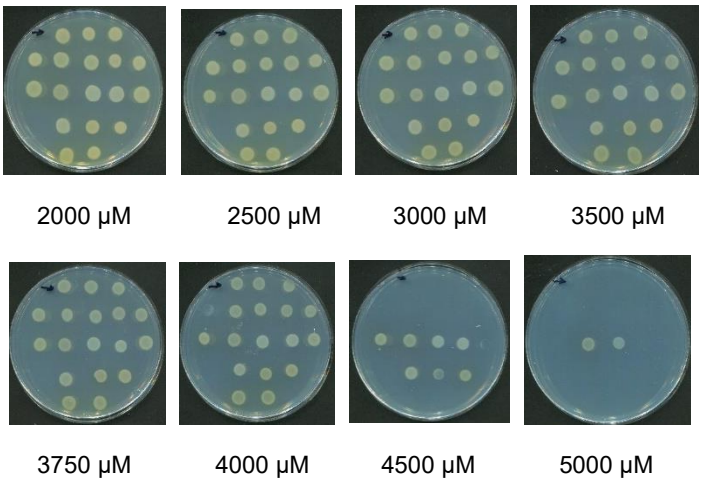

72 hours

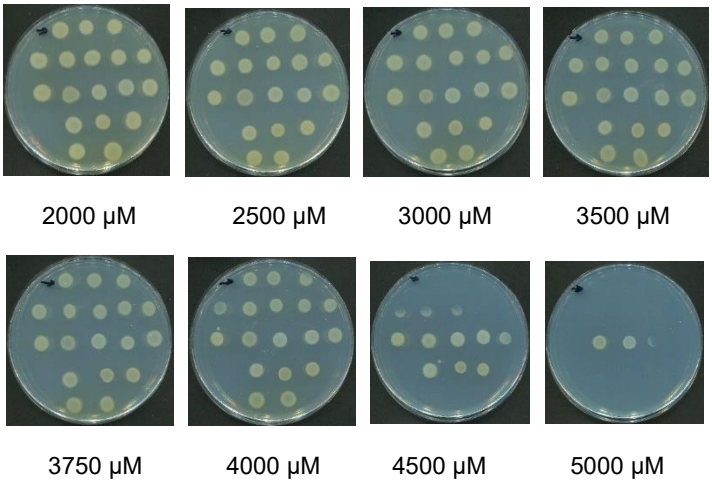

Appendix 1. Plate photos for copper MIC tests. The layout of strains is shown in the figure above agar plates. Concentration of $CuSO_4$ is indicated below each agar plate. Overnight bacterial cultures were subjected 10^{-2}, 10^{-3} and 10^{-4} dilution, and 10 µl was dropped onto an agar plate. Photos were taken after incubation at 28 °C for 24, 48 and 72 hours.

Appendix 2. Pyoverdine production (RFU) of evolved strains after 24-hour and 48-hour growth in LB medium. Data are means and standard errors of four biological replicates. Strains included in this assay: evolved control strains from the 320th transfer of evolutionary experiment and their respective single colonies; evolved copper treatment strains and their respective single colonies; wild type SBW25; SBW25 mutant with the deletion of *pvdL* gene.

Strain	24h		48h	
	population	single colony	population	single colony
C1	108.250	52.750	208.000	140.750
C2	102.000	27.250	210.000	132.750
C3	55.250	70.500	146.500	127.500
C4	87.500	46.250	194.000	126.000
C5	56.750	32.250	158.500	107.500
C6	38.500	88.250	137.250	137.500
C7	78.250	74.250	187.750	102.000
C8	86.750	84.500	209.750	122.000
D1	25.000	129.250	39.000	127.750
D2	78.750	83.750	111.750	122.250
D3	1.000	26.000	62.000	67.500
D4	3.000	34.500	58.500	77.250
D5	74.250	84.750	116.000	122.000
D6	81.750	85.250	143.000	112.250
D7	52.250	59.500	102.750	71.750
D8	57.250	44.000	89.500	70.750
Wild type SBW25	44.500	122.250	182.750	182.750
Δ*pvdL*	29.250	29.250	115.750	115.750

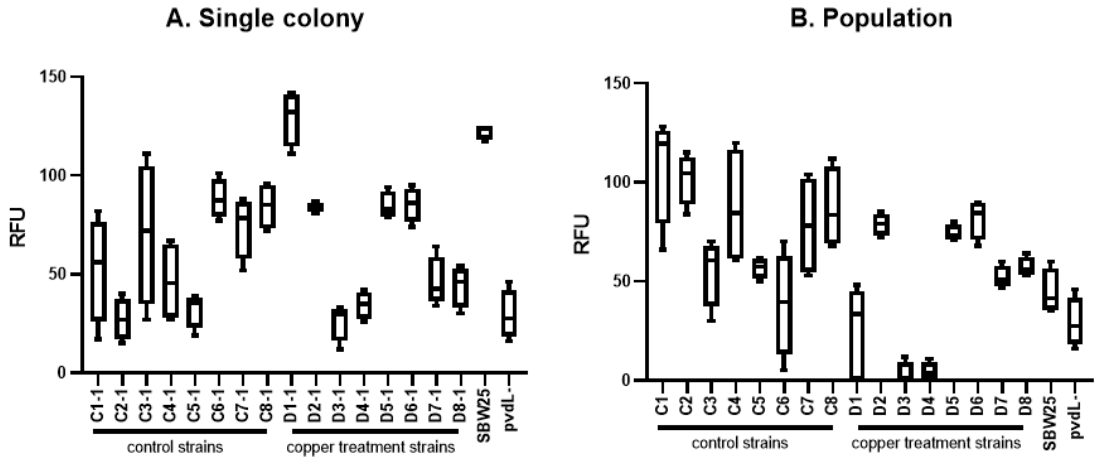

Appendix 3. Pyoverdine production (RFU) of evolved strains after 24-hour in LB medium. Data are means and standard errors of four biological replicates. The line in the middle of the box represents the median; the bottom and top boxes represent the 25th and 75th percentiles, respectively; and the lower and upper whiskers indicate the smallest and the largest values, respectively. Strains included in this assay: evolved control strains from the 320th transfer of evolutionary experiment and their respective single colonies; evolved copper treatment strains and their respective single colonies; wild type SBW25; SBW25 mutant with the deletion of *pvdL* gene.

Appendix 4. Pyoverdine production (RFU) of evolved strains after 24-hour and 48-hour growth in KB medium. Data are means and standard errors of four biological replicates. Strains included in this assay: evolved control strains from the 320th transfer of evolutionary experiment and their respective single colonies; evolved copper treatment strains and their respective single colonies; wild type SBW25; SBW25 mutant with the deletion of *pvdL* gene.

Strain	24h		48h	
	population	single colony	population	single colony
C1	4602.50	165.000	13830.000	715.000
C2	3662.50	95.000	11897.500	462.500
C3	3752.50	9962.500	11687.500	18025.000
C4	3972.50	9245.000	13245.000	17455.000
C5	3320.00	11025.000	12177.500	16130.000
C6	3772.50	12040.000	11750.000	19700.000
C7	4950.00	15372.500	11400.000	19942.500
C8	3917.50	11027.500	12830.000	18150.000
D1	3875.00	10190.000	8237.500	14472.500
D2	6340.00	9310.000	8907.500	13522.500
D3	72.50	87.500	130.000	52.500
D4	87.50	90.000	160.000	172.500
D5	3922.50	3320.000	3580.000	5510.000
D6	362.50	175.000	1175.000	585.000
D7	1480.00	1887.500	1740.000	2860.000
D8	800.00	1452.500	1052.500	2912.500
Wild type SBW25	6257.50	15725.000	18045.000	21200.000
Δ*pvdL*	60.000	60.000	175.000	147.500

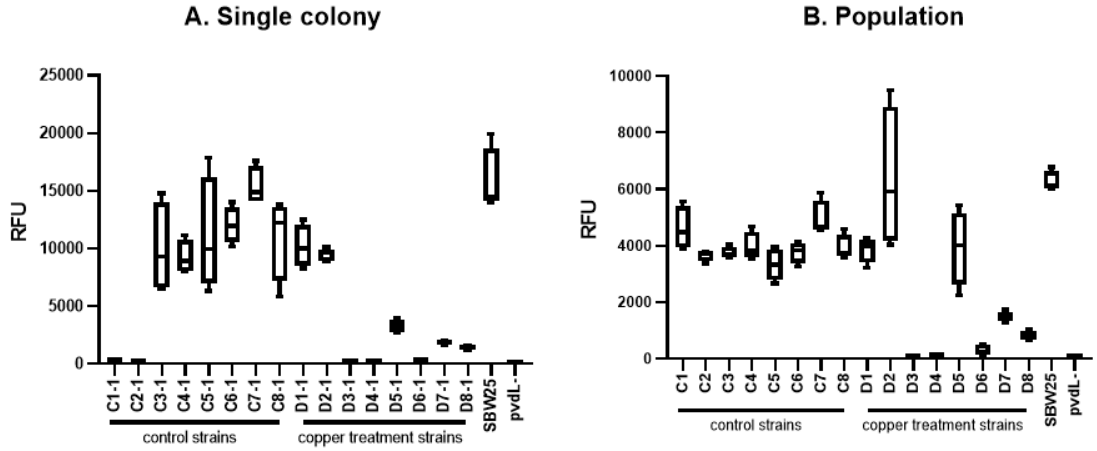

Appendix 5. Pyoverdine production (RFU) of evolved strains after 24-hour growth in KB medium. Data are means and standard errors of four biological replicates. The line in the middle of the box represents the median; the bottom and top boxes represent the 25th and 75th percentiles, respectively; and the lower and upper whiskers indicate the smallest and the largest values, respectively. Strains included in this assay: evolved control strains from the 320th transfer of evolutionary experiment and their respective single colonies; evolve copper treatment strains and their respective single colonies; wild type SBW25; SBW25 mutant with the deletion of *pvdL* gene.

Appendix 6. Rates of mutation in evolved control strains and copper treatment experimental populations (C1 to C8 and D1 to D8) at 320th transfer and in their common ancestor SBW25.

	Mutation rate	Lower confidence 95% limit	Upper confidence 95% limit
C1	3.8816490E-07	1.48E-07	6.29E-07
C2	1.81276990E-06	8.64E-07	2.76E-06
C3	1.4196642E-06	6.10E-07	2.23E-06
C4	3.38072620E-06	1.51E-06	5.25E-06
C5	1.3808108E-06	6.46E-07	2.12E-06
C6	2.3736020E-07	9.99E-08	3.75E-07
C7	7.8047210E-07	4.36E-07	1.13E-06
C8	1.1151465E-06	4.96E-07	1.73E-06
D1	2.37696200E-06	1.26E-06	3.49E-06
D2	8.289661E-07	1.44E-07	1.51E-06
D3	8.1972300E-07	4.91E-07	1.15E-06
D4	3.8412940E-07	1.47E-07	4.48E-07
D5	1.2397308E-06	6.33E-07	1.85E-06
D6	2.7215160E-07	1.15E-07	4.29E-07
D7	2.4899151E-06	9.89E-07	3.99E-06
D8	5.26879720E-06	2.93E-06	7.61E-06
Wild type SBW25	1.1476E-09	5.00E-11	2.25E-09

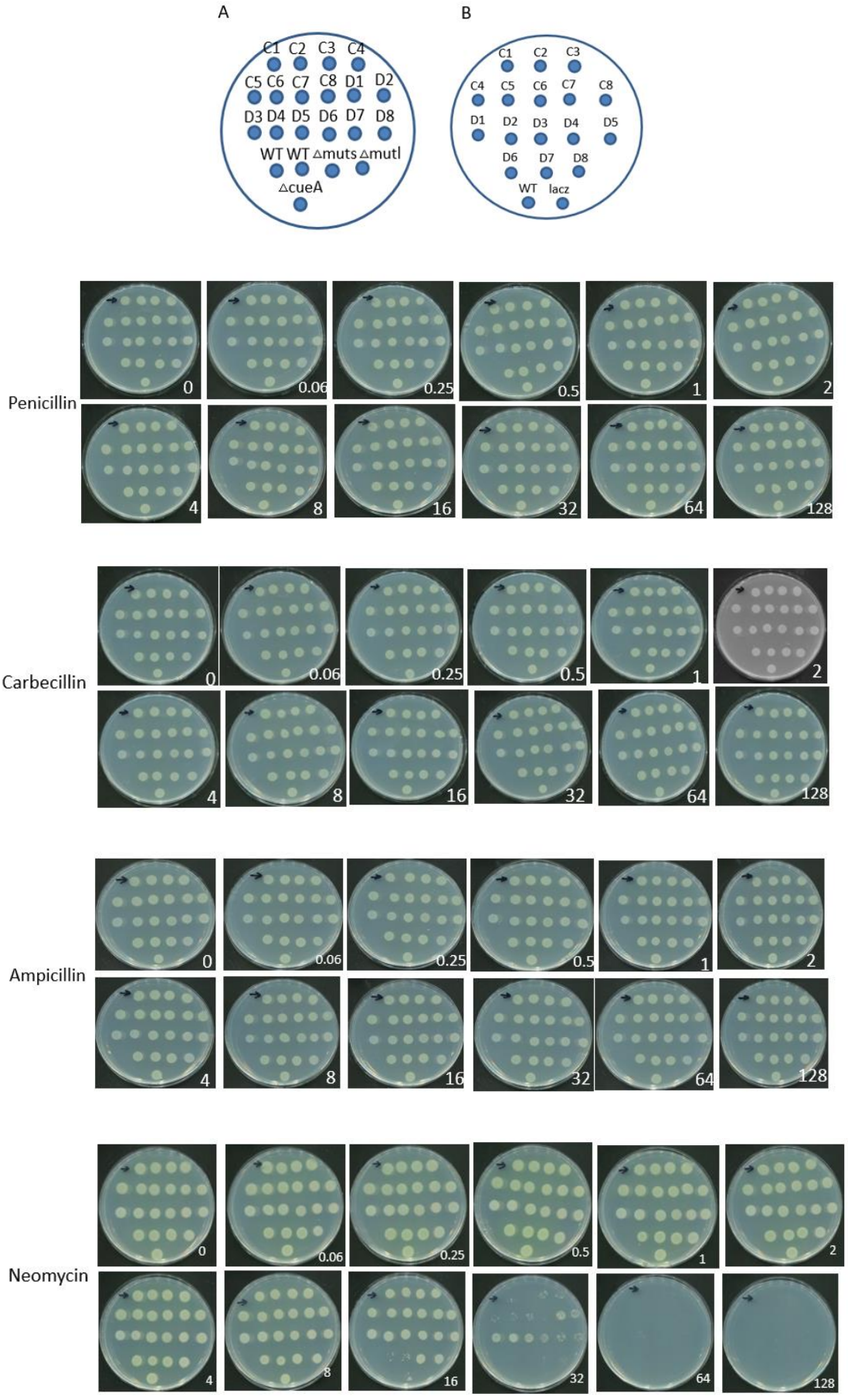
A
C1 C2 C3 C4
C5 C6 C7 C8 D1 D2
D3 D4 D5 D6 D7 D8
WT WT ΔmutS ΔmutL
ΔcueA
B
C1 C2 C3
C4 C5 C6 C7 C8
D1 D2 D3 D4 D5
D6 D7 D8
WT lacz
Penicillin
0 0.06 0.25 0.5 1 2
4 8 16 32 64 128
Carbecillin
0 0.06 0.25 0.5 1 2
4 8 16 32 64 128
Ampicillin
0 0.06 0.25 0.5 1 2
4 8 16 32 64 128
Neomycin
0 0.06 0.25 0.5 1 2
4 8 16 32 64 128

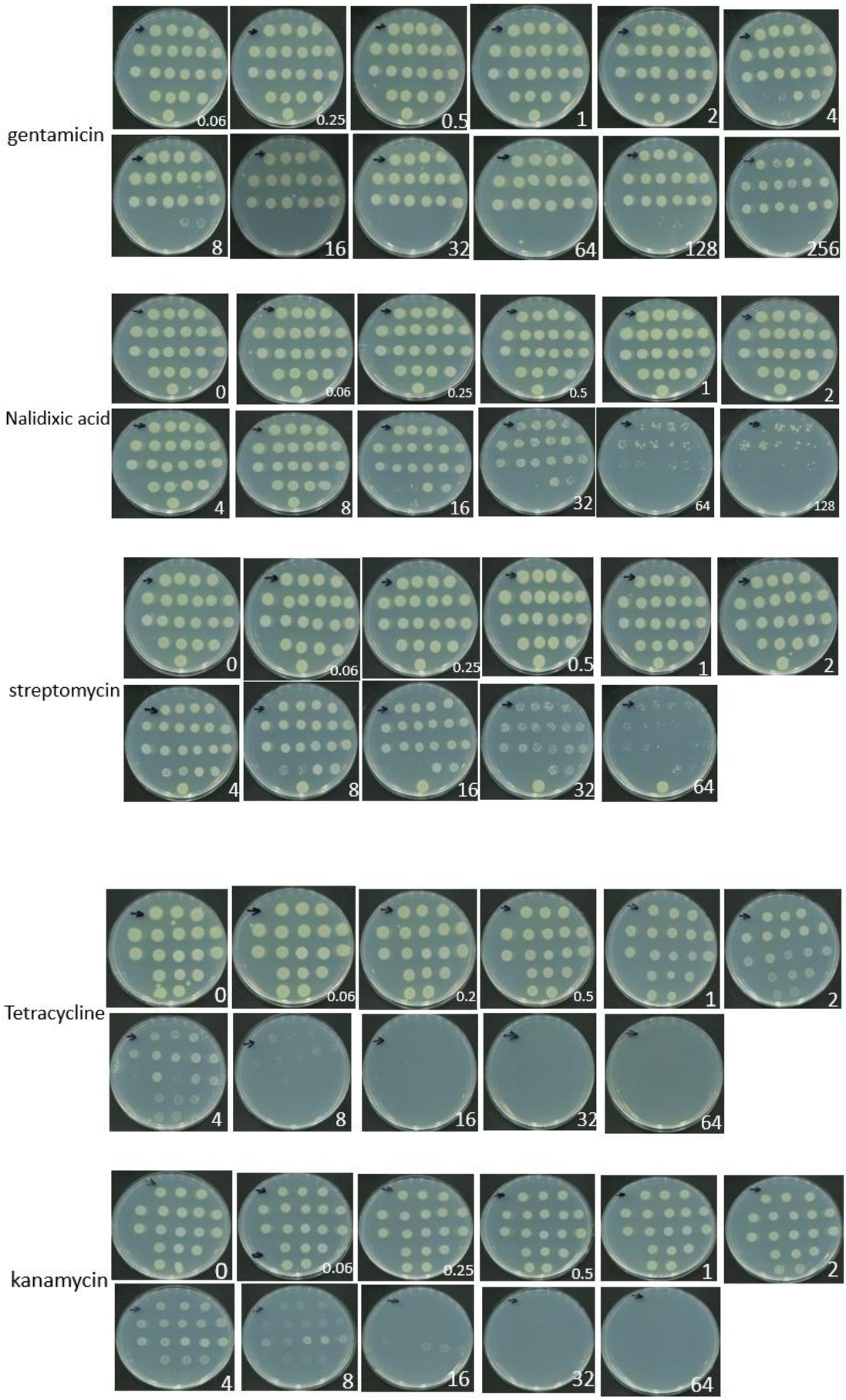
gentamicin
0.06
0.25
0.5
1
2
4
8
16
32
64
128
256
Nalidixic acid
0
0.06
0.25
0.5
1
2
4
8
16
32
64
128
streptomycin
0
0.06
0.25
0.5
1
2
4
8
16
32
64
Tetracycline
0
0.06
0.2
0.5
1
2
4
8
16
32
64
kanamycin
0
0.06
0.25
0.5
1
2
4
8
16
32
64

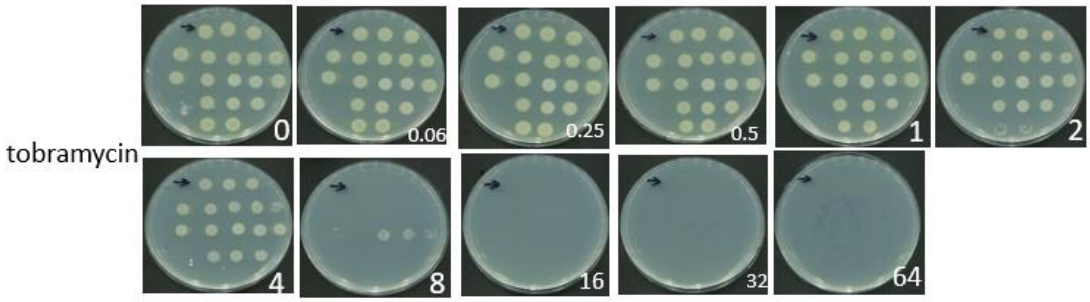

Appendix 7. Plate photos for antibiotic MIC tests. The layout of strains on LB agar plates supplemented with penicillin, carbenicillin, ampicillin, neomycin, gentamicin, streptomycin and nalidixic acid is shown in (A) and with tetracycline, kanamycin, tobramycin in (B). Concentration of antibiotic (μg/ml) is indicated on the corner of each agar plate. Overnight bacterial cultures were subjected 10^{-2} dilution, and 10 μl was dropped onto an agar plate. Photos were taken after incubation at 28 ^{o}C for 48 hrs.

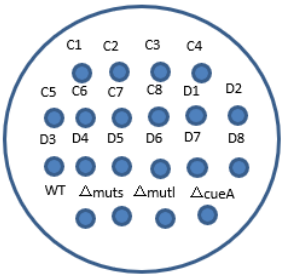

Dilution: 10^{-4}

24 hours

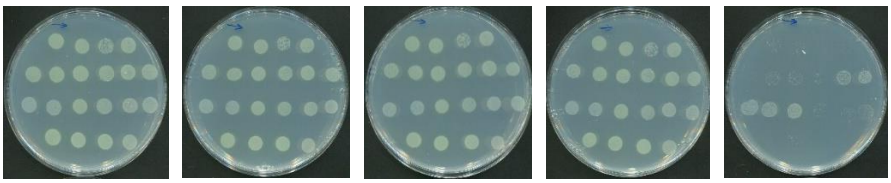

0 µg/ml 0.05 µg/ml 0.25 µg/ml 0.5 µg/ml 1 µg/ml

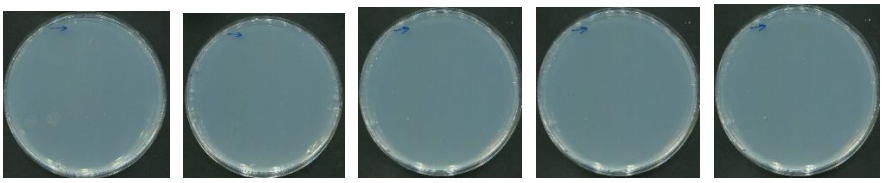

2 µg/ml 4 µg/ml 8 µg/ml 16 µg/ml 32 µg/ml

48 hours

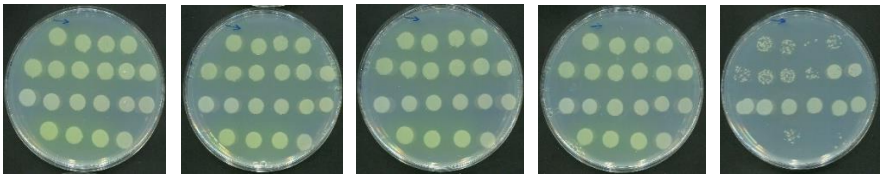

0 µg/ml 0.05 µg/ml 0.25 µg/ml 0.5 µg/ml 1 µg/ml

2 µg/ml 4 µg/ml 8 µg/ml 16 µg/ml 32 µg/ml

Dilution:10^{-5}

24 hours

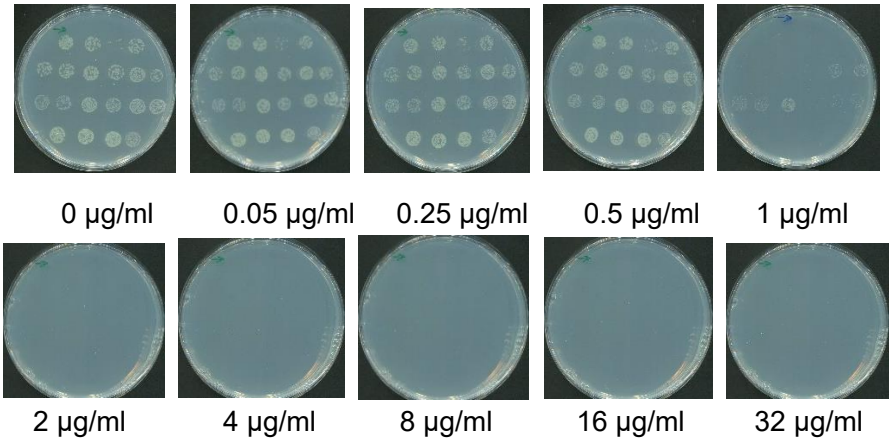

48 hours

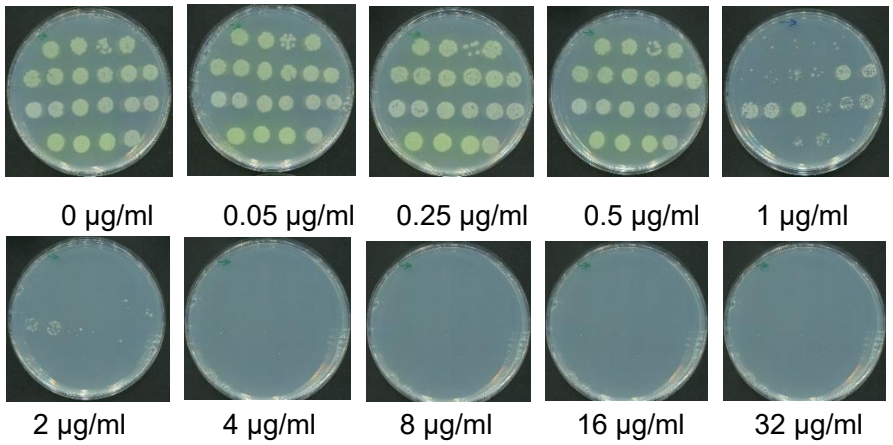

Appendix 8. Plate photos for tobramycin MIC tests. The layout of strains is shown in the figure above agar plates. Concentration of tobramycin is indicated below each agar plate. Overnight bacterial cultures were subjected to 10^{-4} and 10^{-5} dilution, and 10 µl was dropped onto an agar plate. Photos were taken after incubation at 28 ^{o}C for 24 and 48 hrs.

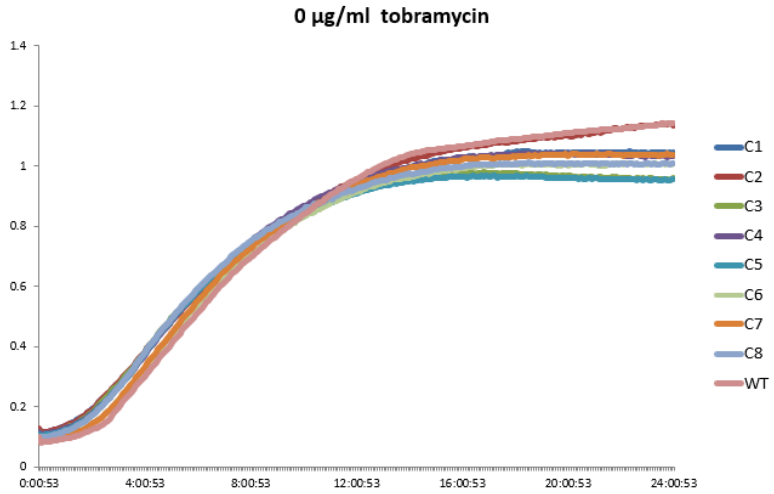
0 µg/ml tobramycin
1.4
1.2
1
0.8
0.6
0.4
0.2
0
0:00:53
4:00:53
8:00:53
12:00:53
16:00:53
20:00:53
24:00:53
C1
C2
C3
C4
C5
C6
C7
C8
WT

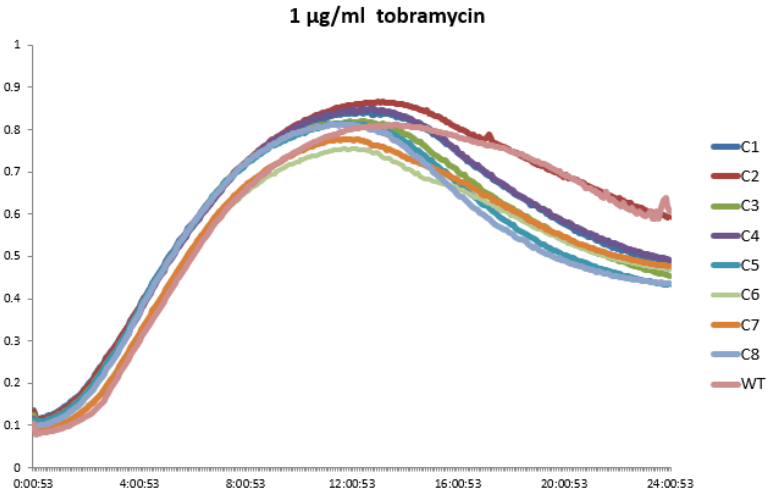
1 µg/ml tobramycin
1
0.9
0.8
0.7
0.6
0.5
0.4
0.3
0.2
0.1
0
0:00:53
4:00:53
8:00:53
12:00:53
16:00:53
20:00:53
24:00:53
C1
C2
C3
C4
C5
C6
C7
C8
WT

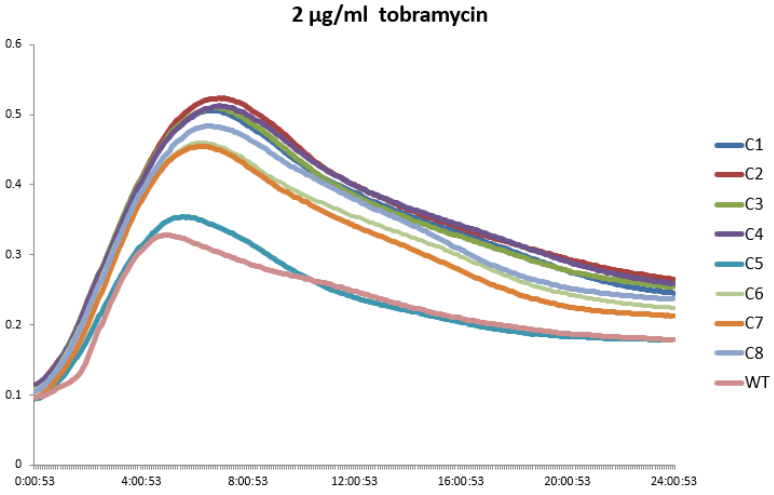
2 µg/ml tobramycin
0.6
0.5
0.4
0.3
0.2
0.1
0
0:00:53
4:00:53
8:00:53
12:00:53
16:00:53
20:00:53
24:00:53
C1
C2
C3
C4
C5
C6
C7
C8
WT

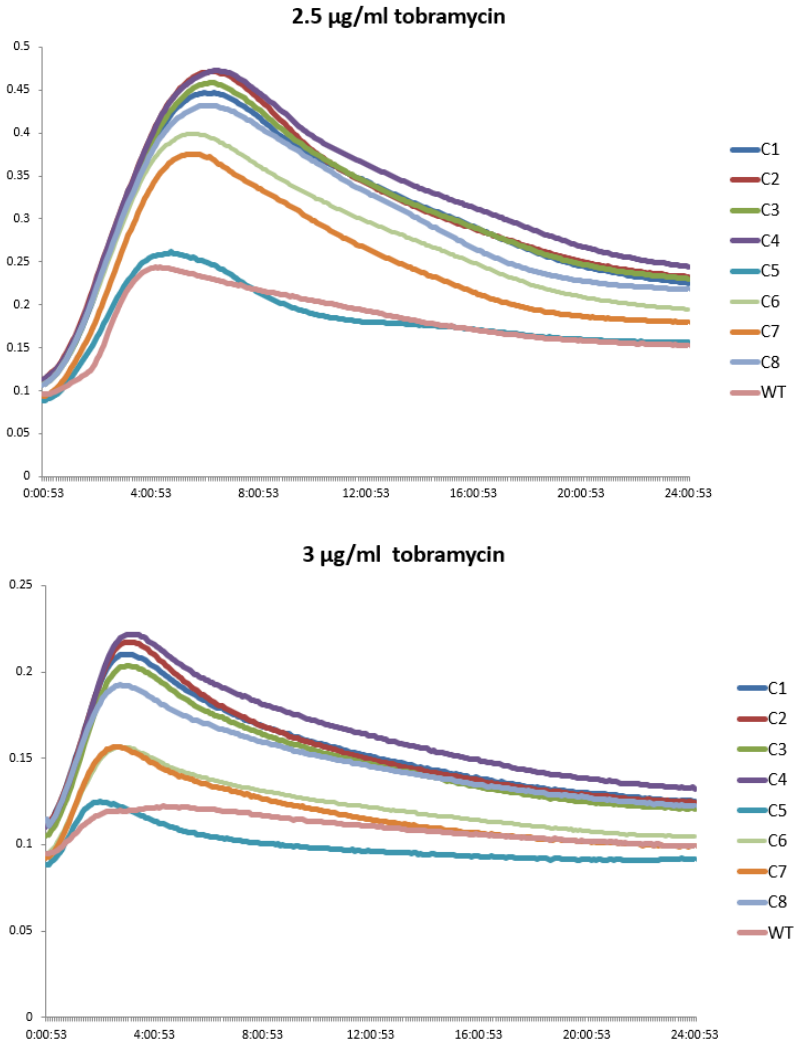

Appendix 9. Growth kinetics of wild-type SBW25 and evolved control strains in LB medium. LB medium was supplemented with 0, 1, 2, 2.5 and 3 µg/ml tobramycin. Data are means and standard errors of 3 independent cultures.

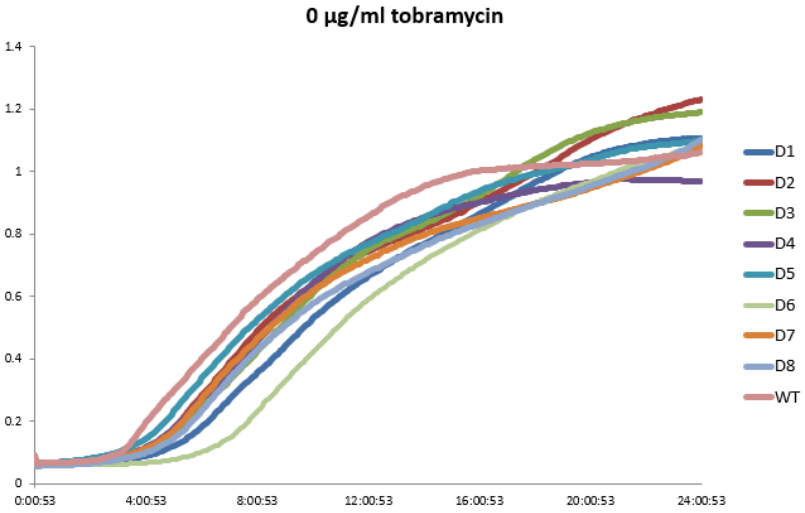
0 µg/ml tobramycin
1.4
1.2
1
0.8
0.6
0.4
0.2
0
0:00:53
4:00:53
8:00:53
12:00:53
16:00:53
20:00:53
24:00:53
D1
D2
D3
D4
D5
D6
D7
D8
WT

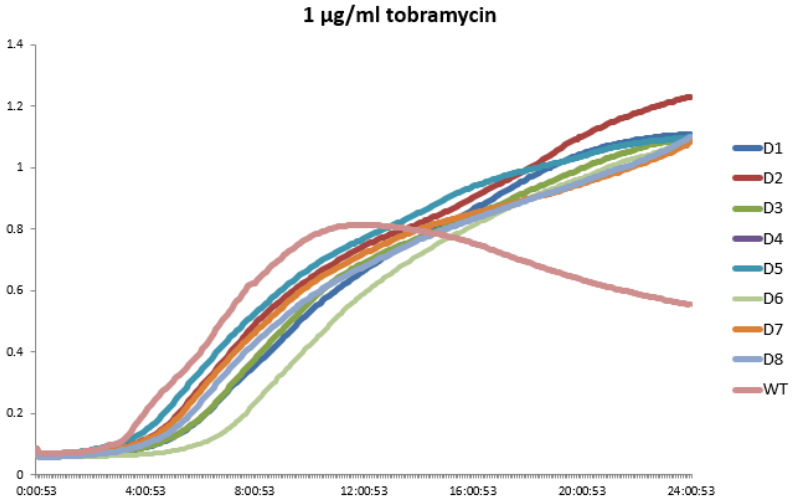
1 µg/ml tobramycin
1.4
1.2
1
0.8
0.6
0.4
0.2
0
0:00:53
4:00:53
8:00:53
12:00:53
16:00:53
20:00:53
24:00:53
D1
D2
D3
D4
D5
D6
D7
D8
WT

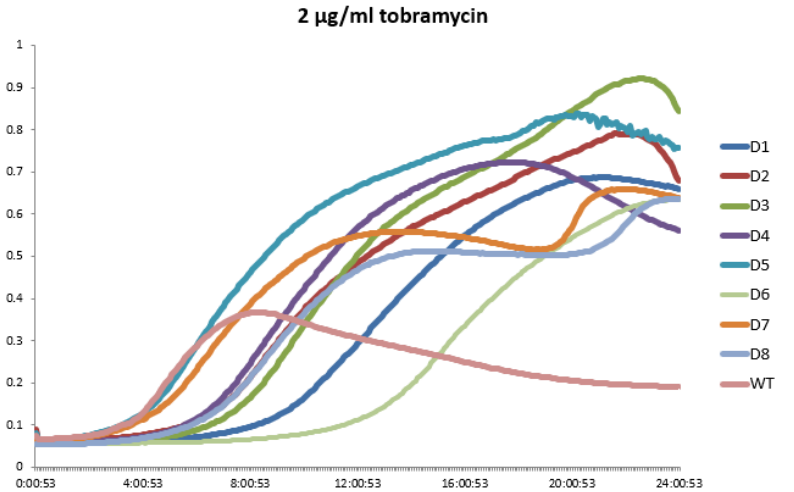
2 µg/ml tobramycin
1
0.9
0.8
0.7
0.6
0.5
0.4
0.3
0.2
0.1
0
0:00:53
4:00:53
8:00:53
12:00:53
16:00:53
20:00:53
24:00:53
D1
D2
D3
D4
D5
D6
D7
D8
WT

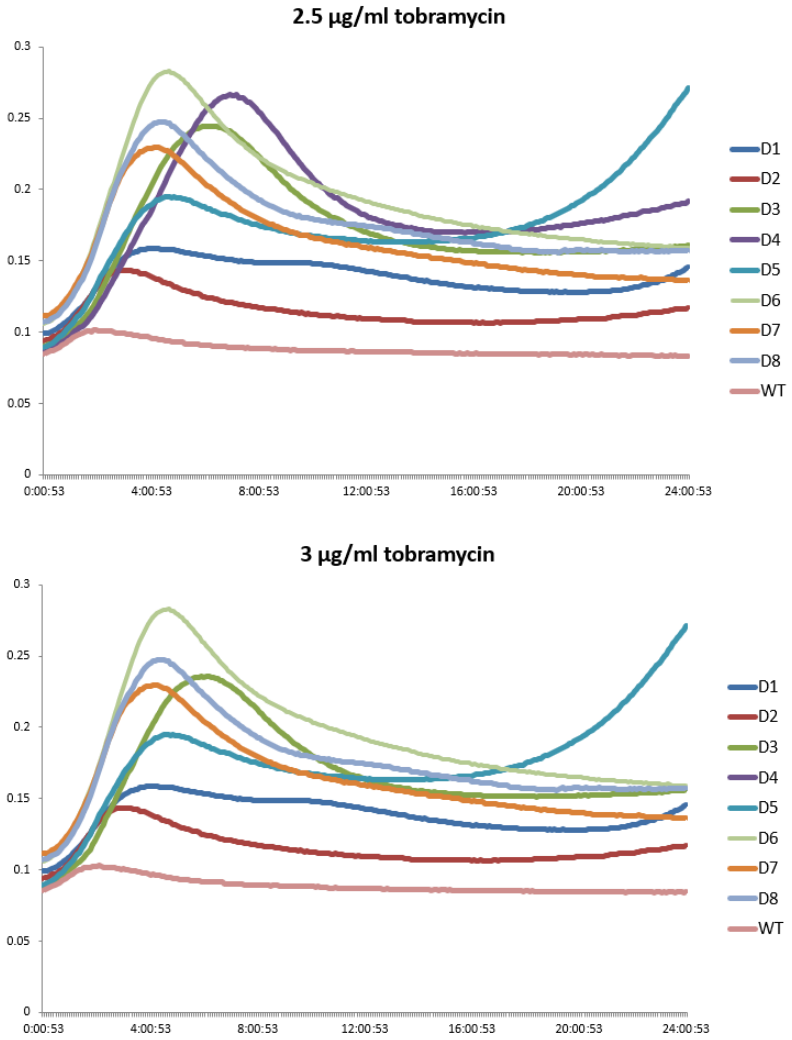

Appendix 10. Growth kinetics of wild-type SBW25 and evolved copper treatment strains in LB medium. LB medium was supplemented with 0, 1, 2, 2.5 and 3 µg/ml tobramycin. Data are means and standard errors of 3 independent cultures.

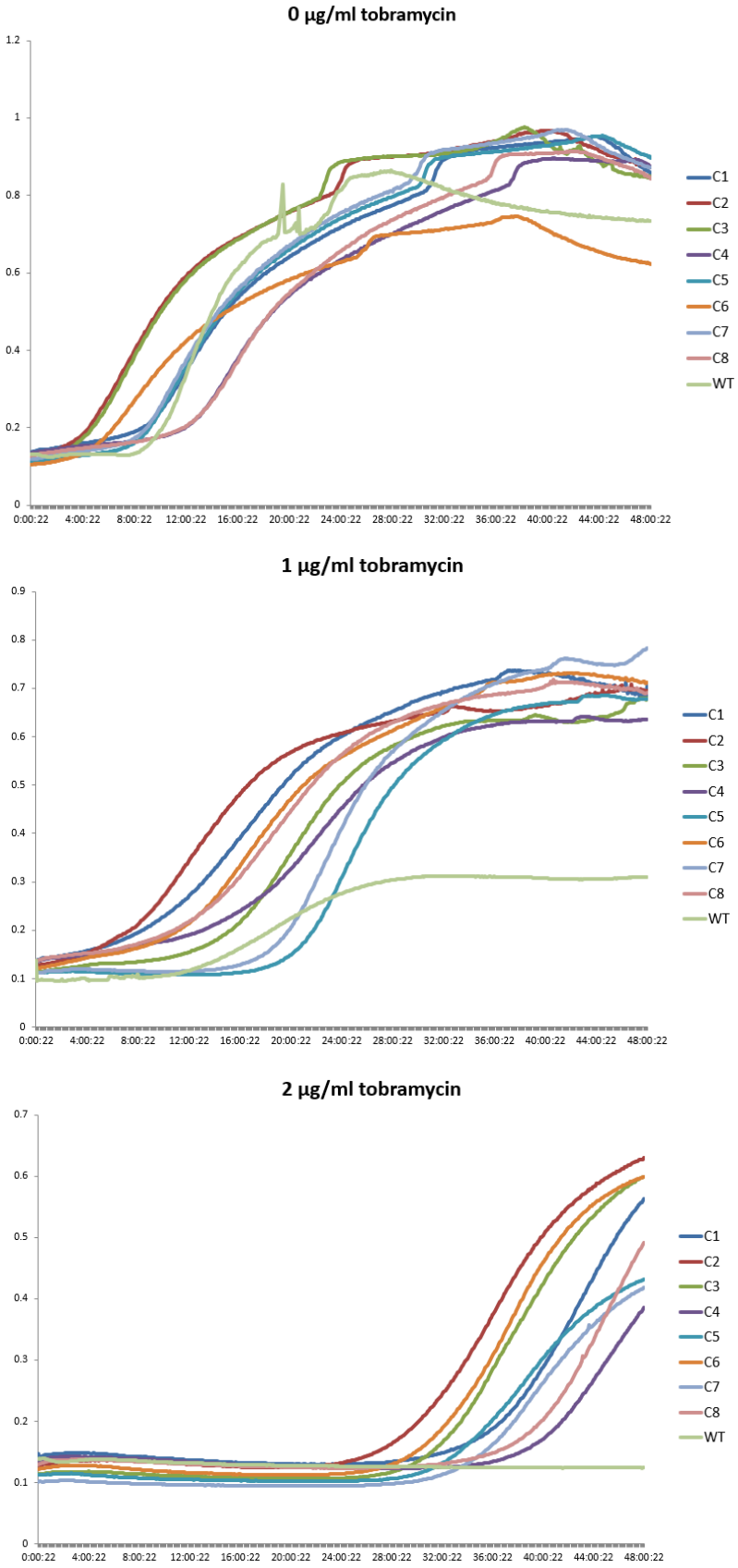

Appendix 11. Growth kinetics of wild-type SBW25 and evolved control strains in M9 minimal salt medium. 20 mM succinate and 10 mM histidine are added into medium as the sole carbon source and nitrogen source, respectively. The concentration of

tobramycin is 0,1 and 2 µg/ml. Data are means and standard errors of 3 independent cultures.

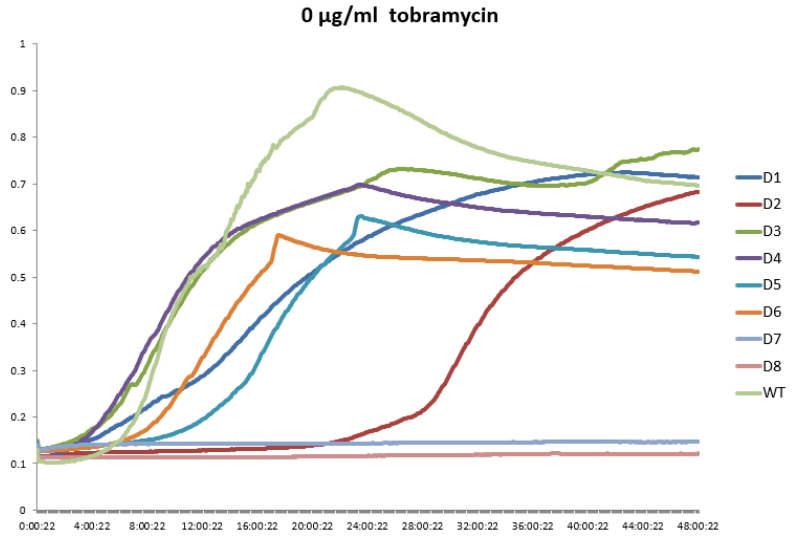

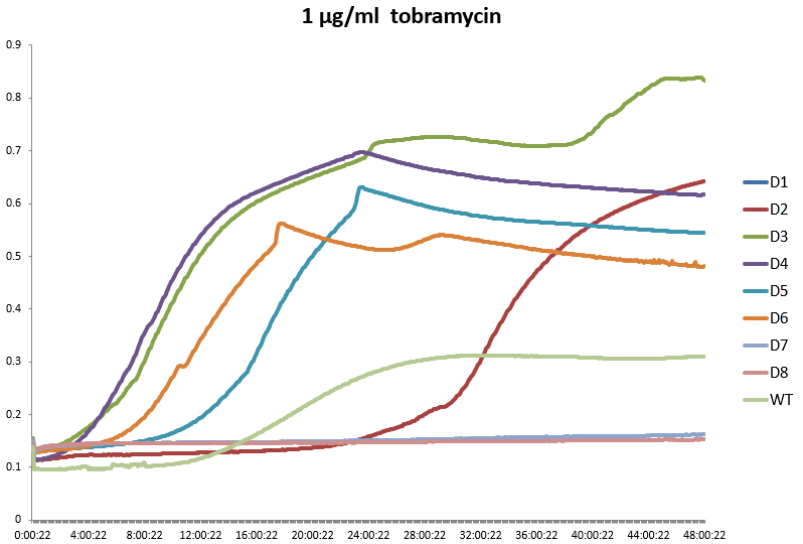

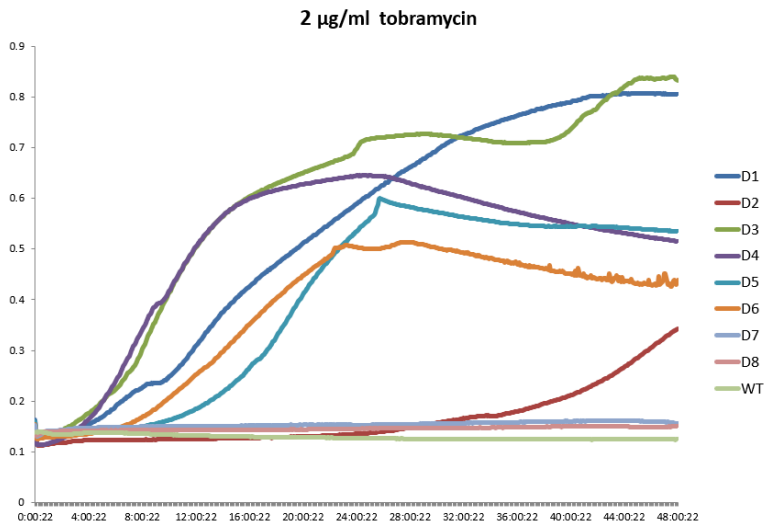

Appendix 12. Growth kinetics of wild-type SBW25 and evolved copper treatment strains in M9 minimal salt medium. 20 mM succinate and 10 mM histidine are added into medium as the sole carbon source and nitrogen source, respectively. The concentration of tobramycin is 0,1 and 2 µg/ml. Data are means and standard errors of 3 independent cultures.

Appendix 13. Fitness of evolved strains in LB medium. Fitness of evolved strains was determined relative to the wild type SBW25 after 24h growth in fresh LB medium. Fitness data (mean and SEs of four biological replicates) are log10 transformed ratios of the Malthusian parameters for each competitor.

	Replicate 1	Replicate 2	Replicate 3	Replicate 4
C1	-0.254169	-1.6171519	-0.4285716	-0.6184181
C2	-0.1686227	-0.4405564	0.06334875	0.19229852
C3	-0.5281049	-0.7021048	-0.6539265	-0.7037743
C4	-0.3629737	-0.6410063	-0.3657248	-0.4178262
C5	-0.3106773	-0.1055403	-0.2549437	-0.6655902
C6	-0.2101136	-0.8127467	-0.0943528	0.07351069
C7	1.15199865	1.42232502	0.95547257	0.79812466
C8	0.02120221	-0.3928466	-0.0084096	-0.6386590
D1	-0.8746031	-1.0596837	-0.9571503	-0.9297589
D2	-2.3237823	-2.9093735	-2.6415673	-2.4238438
D3	-1.9808079	-3.3015846	-2.9986350	-1.9676814
D4	-3.2633095	-3.8345669	-2.8781291	-2.5085647
D5	-2.5518558	-2.9599362	-2.7974173	-2.3065294
D6	-1.6879504	-1.6197065	-1.8458534	-1.5795298
D7	-3.6557106	-3.5276778	-4.9675933	-4.7780166
D8	-3.7815701	-3.6596803	-2.4788299	-2.6714161

Appendix 14. Fitness of evolved strains in LB medium with 2 µg/ml tobramycin. Fitness of evolved strains was determined relative to the wild type SBW25 after 24h growth in LB medium supplemented with 2 µg/ml tobramycin. Fitness data (mean and SEs of four biological replicates) are log10 transformed ratios of the Malthusian parameters for each competitor.

	Replicate 1	Replicate 2	Replicate 3	Replicate 4
C1	4.36004773	4.08561088	2.98699859	4.25468721
C2	3.76897485	3.63794659	4.55022930	4.71635617
C3	3.88106078	4.43255744	4.57042724	4.55515977
C4	4.76983681	3.88253361	4.15823949	4.96514556
C5	4.51847496	4.26619482	4.68031799	4.34154426
C6	4.05717580	4.15380263	4.60219278	4.29534280
C7	3.55950607	4.40388422	4.29265859	2.65336771
C8	3.65610521	4.18518427	4.16165377	4.34044176
D1	7.39659645	6.64111754	7.35276473	6.59873832
D2	5.90991949	6.17439866	7.41908078	6.47084503
D3	6.21264524	5.61294276	6.00307655	6.15642434
D4	7.23291376	8.00269416	8.74774920	7.05940283
D5	6.91007816	6.88422478	6.10666026	6.58697326
D6	5.46806014	5.75574221	5.94433338	4.68274250
D7	5.63788126	6.09230096	5.91446779	6.09230096
D8	6.63866128	5.48153138	5.75642010	6.46658897

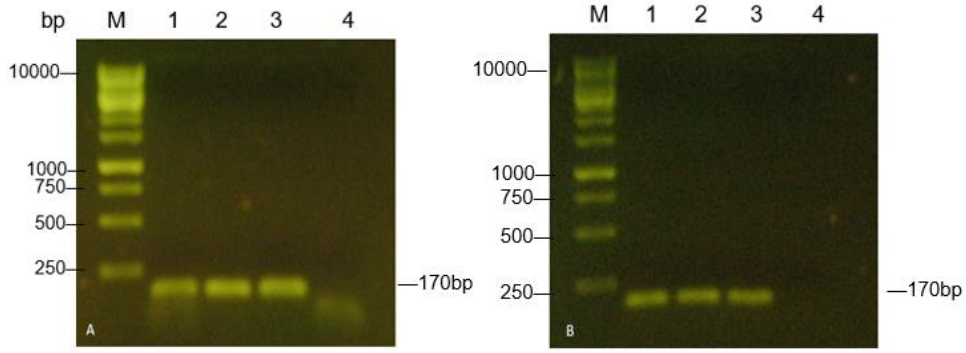

Appendix 15. PCR verification of the integration of Mini-Tn7 element carrying *lacZ* fusion in *P. aeruginosa* MPAO1. To verify integration of the mini-Tn7 element into the unique chromosomal integration sites located downstream of *glmS* gene. *P. aeruginosa* MPAO1 transconjugants were subjected to PCR amplification using the forward primer MLG048-PF and the reverse primer MLG049-PR. Gel electrophoresis was performed in 1x TBE buffer at 140 volts using GeneRuler DNA ladder (1kb). DNA was visualized under UV lights. **Lane M in (A) and (B)**, GeneRuler DNA ladder purchased from Thermo Scientific Ltd (Auckland). **Lane 1-3 in (A)**, cultures of bacteria marked with PhutuJ-lacZ, PhutF-lacZ and PntrB-lacZ. **Lane 1-3 in (B)**, cultures of bacteria marked with PcbrA-lacZ, PcbrB-lacZ and PplC-lacZ. **Lane 4 in (A) and (B)**, negative control.

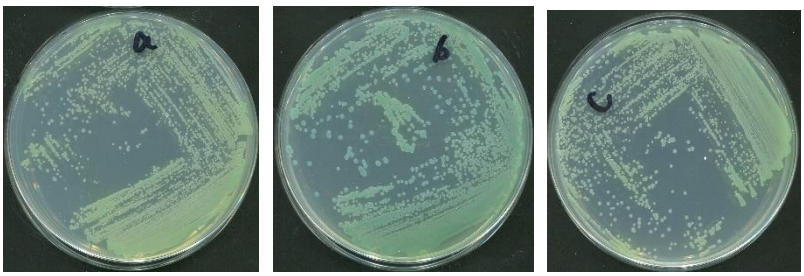

ac40 bc40 cc40

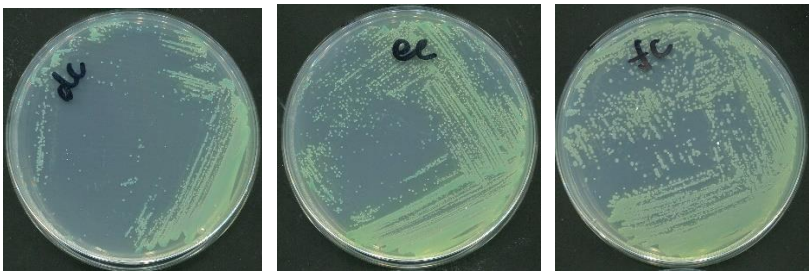

dc40 ec40 fc40

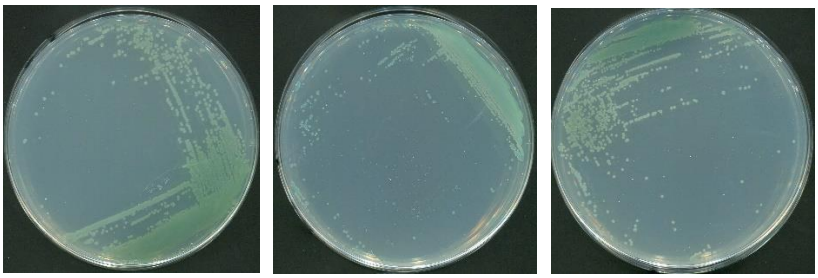

a40 b40 c40

d40 e40 f40

AC30 BC30 CC30

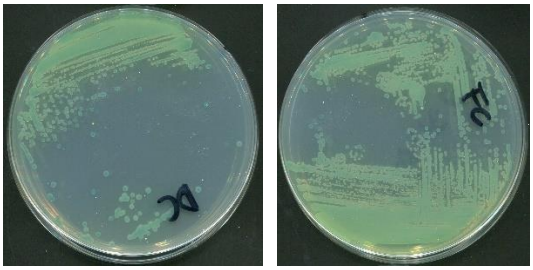

DC30 FC30

A30 B30 C30

D30 E30 F30

Appendix 16. Blue colonies formed by the 30th evolutional SBW25 strain and the 40th evolutional MPAO1 strain from broth-to-broth transfer. Bacterial cultures were inoculated onto LB plus X-Gal (40 μg/ml) plates by streaking. SBW25 was incubated at 28℃ for two days and MPAO1 was incubated at 37℃ for one day.

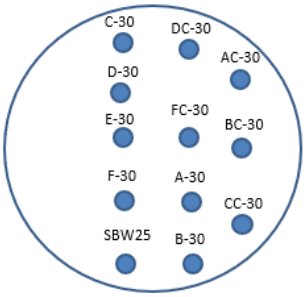

Dilution: 10^{-3}

24 hours

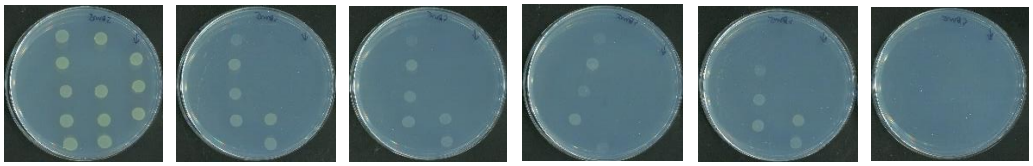

2500 µM 3000 µM 3100 µM 3200 µM 3300 µM 3400 µM

48 hours

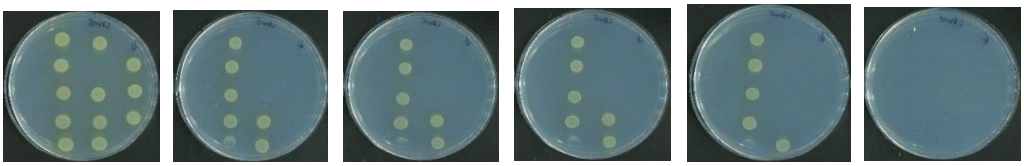

2500 µM 3000 µM 3100 µM 3200 µM 3300 µM 3400 µM

72 hours

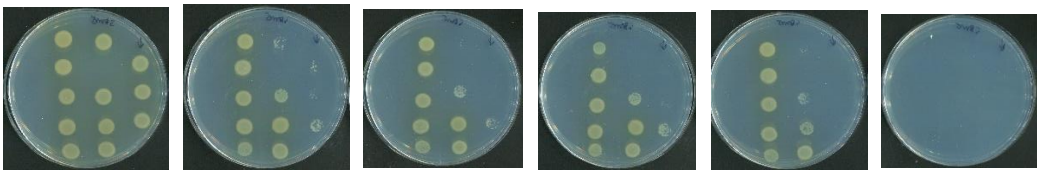

2500 µM 3000 µM 3100 µM 3200 µM 3300 µM 3400 µM

Dilution: 10^{-4}

24 hours

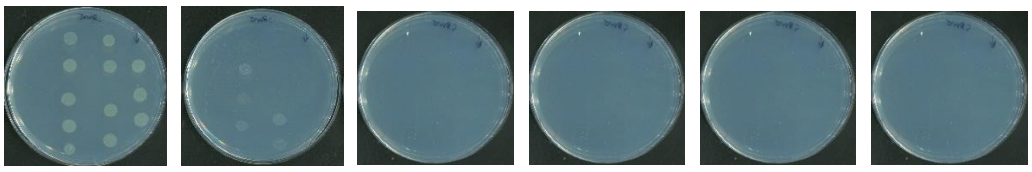

2500 µM 3000 µM 3100 µM 3200 µM 3300 µM 3400 µM

48 hours

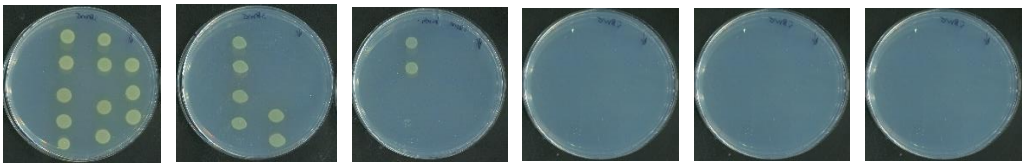

2500 μM 3000 μM 3100 μM 3200 μM 3300 μM 3400 μM

72 hours

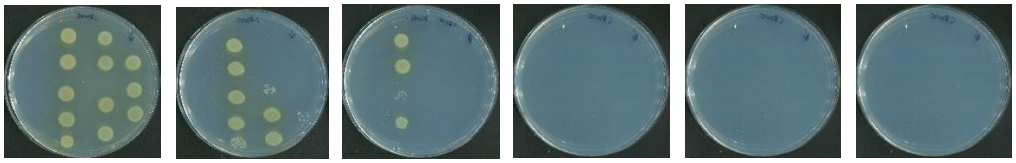

2500 μM 3000 μM 3100 μM 3200 μM 3300 μM 3400 μM

Appendix 17. Plate photos for copper MIC tests for the evolved SBW25 strains from broth-to-broth transfer. The layout of strains is shown in the figure above agar plates. Concentration of $CuSO_4$ is indicated below each agar plate. The overnight bacterial cultures were subjected to 10^{-3} and 10^{-4} dilution, and 10 μl was dropped onto an agar plate. Photos were taken after 24, 48 and 72-hour incubation. Minimal inhibitory concentration (MIC) units were determined after 48-hour incubation.

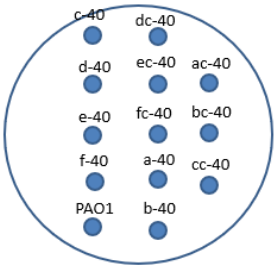

Dilution:10^{-3}

24 hours

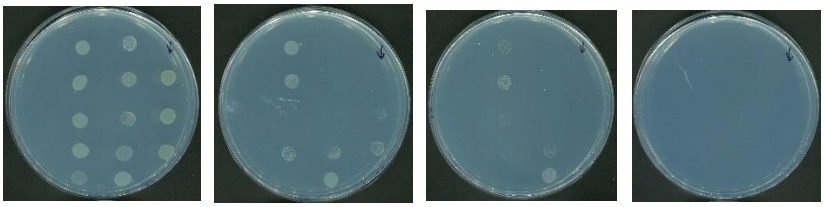

4250 μM 4500 μM 4600 μM 4700 μM

48 hours

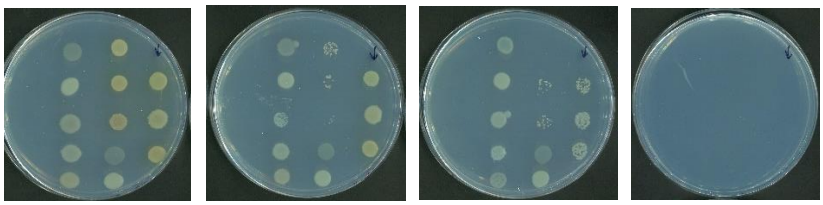

4250 μM 4500 μM 4600 μM 4700 μM

Dilution:10^{-4}

24 hours

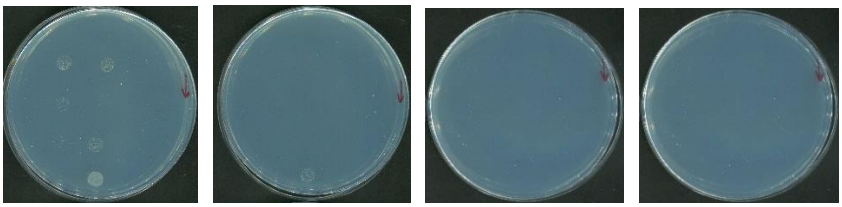

4250 μM 4500 μM 4600 μM 4700 μM

48 hours

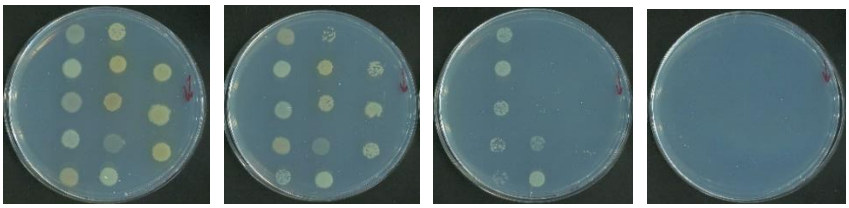

4250 μM 4500 μM 4600 μM 4700 μM

Appendix 18. Plate photos for copper MIC tests for the evolved MPAO1 strains from broth-to-broth transfer. The layout of strains is shown in the figure above agar

plates. Concentration of $CuSO_4$ is indicated below each agar plate. The overnight bacterial cultures were subjected to 10^{-3} and 10^{-4} dilution, and 10 µl was dropped onto an agar plate. Photos were taken after 24 and 48-hour incubation. Minimal inhibitory concentration (MIC) units were determined after 48-hour incubation.

A. SBW25

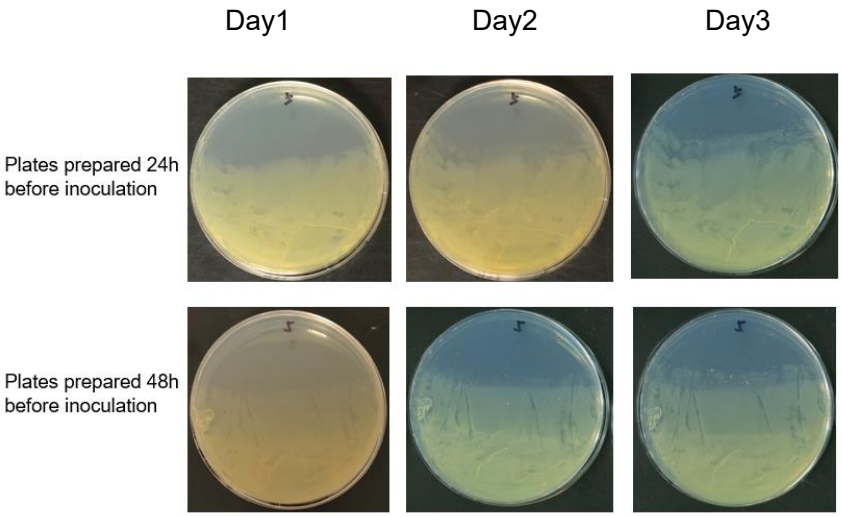

B. SBW25

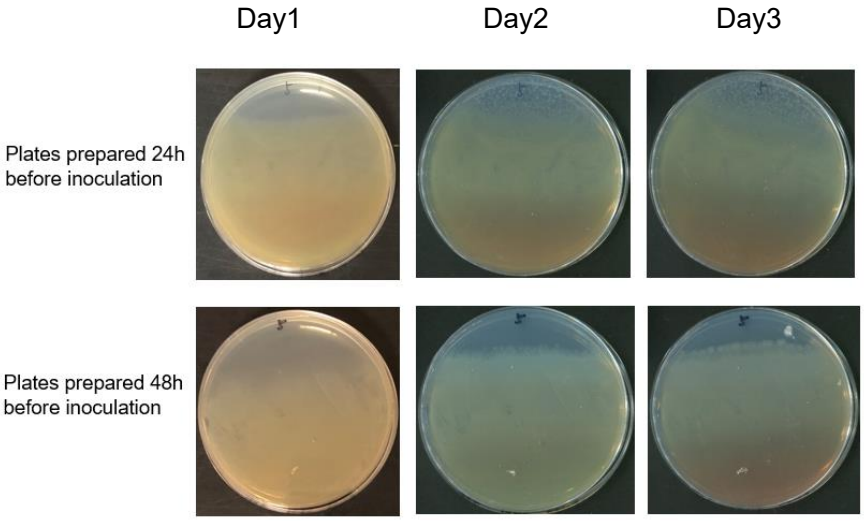

Appendix 19. Distribution of colonies on gradient LB agar plates with ionic copper. To decide the experiment condition of colony-to-colony transfer, plates were prepared 24h and 48h before inoculation. MPAO1 and SBW25 was inoculated onto gradient LB agar plate supplemented with 6 mM and 5 mM copper ions, respectively. The growth statuses of MPAO1 were recorded from day one to day three at 37 ℃ while the growth statuses of SBW25 were recorded at 28 ℃.

24 hours

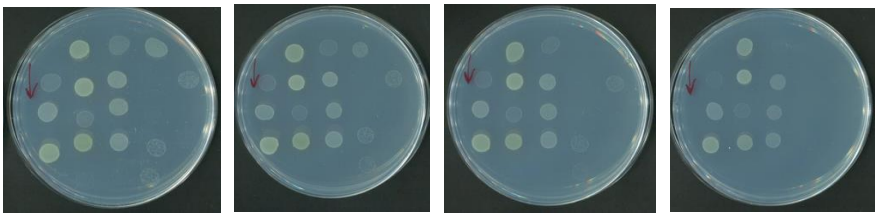

2900 µM 3000 µM 3100 µM 3200 µM

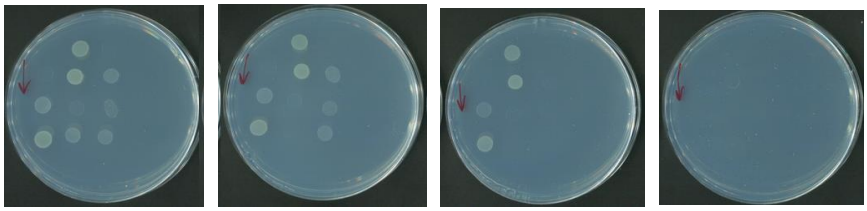

3300 µM 3400 µM 3500 µM 3750 µM

48 hours

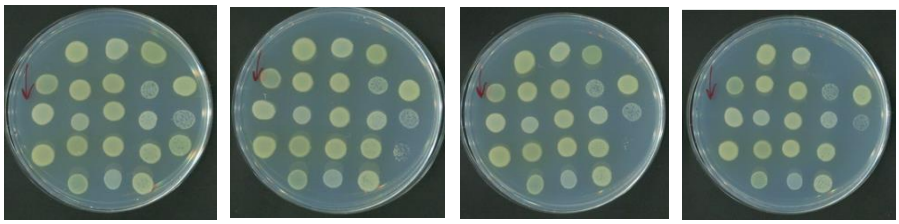

2900 µM 3000 µM 3100 µM 3200 µM

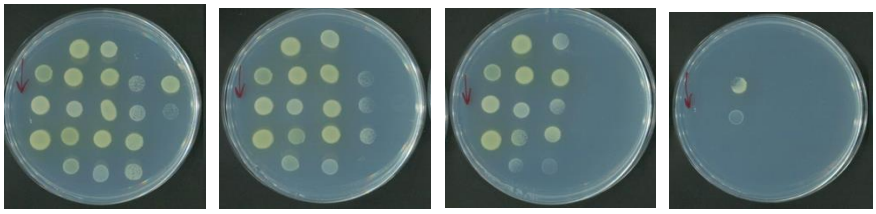

3300 µM 3400 µM 3500 µM 3750 µM

72 hours

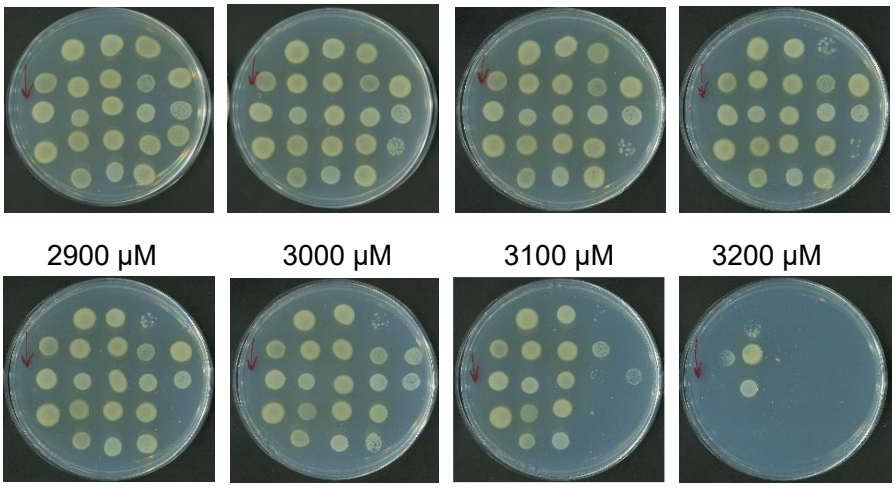

Appendix 20. Plate photos for copper MIC tests for the evolved SBW25 strains from colony-to-colony transfer. The layout of strains is shown in the figure above agar plates. Concentration of $CuSO_4$ is indicated below each agar plate. The overnight bacterial cultures were subjected to 10^{-3},10^{-4} and 10^{-5} dilution, and 10 µl was dropped onto an agar plate. Photos were taken after 24, 48 and 72-hour incubation. Minimal inhibitory concentration (MIC) units were determined after 72-hour incubation.

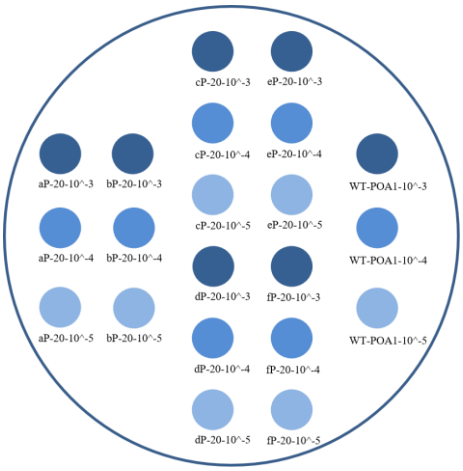

24 hours

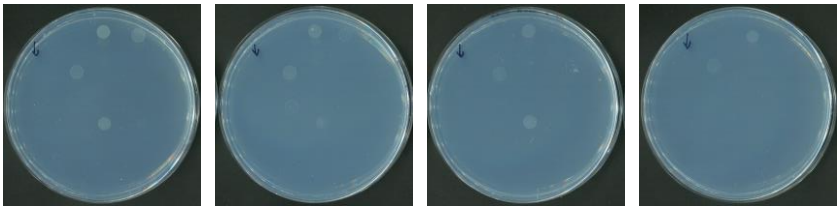

3600 μM 3700 μM 3750 μM 3800 μM

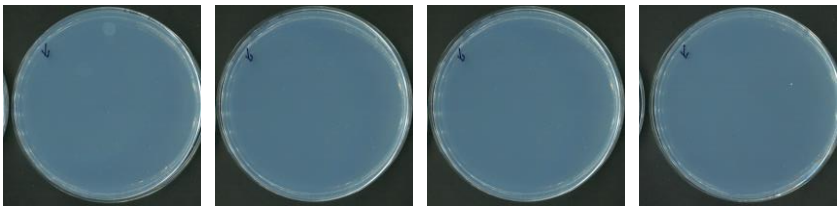

3900 μM 4000 μM 4250 μM 4500 μM

48 hours

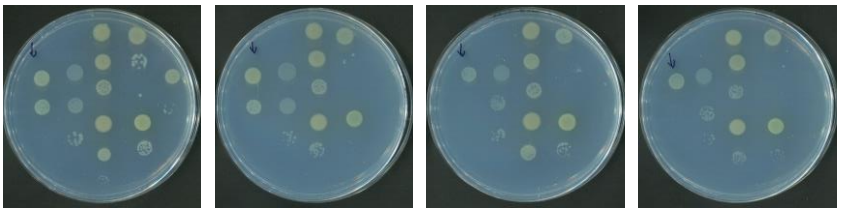

3600 μM 3700 μM 3750 μM 3800 μM

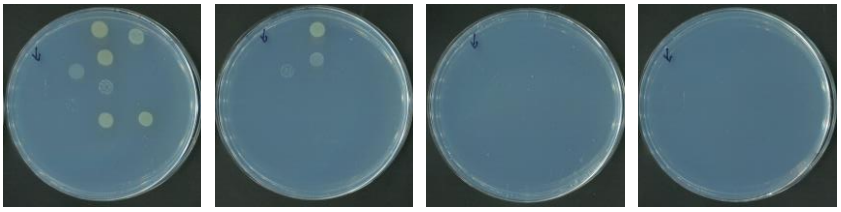

3900 μM 4000 μM 4250 μM 4500 μM

72 hours

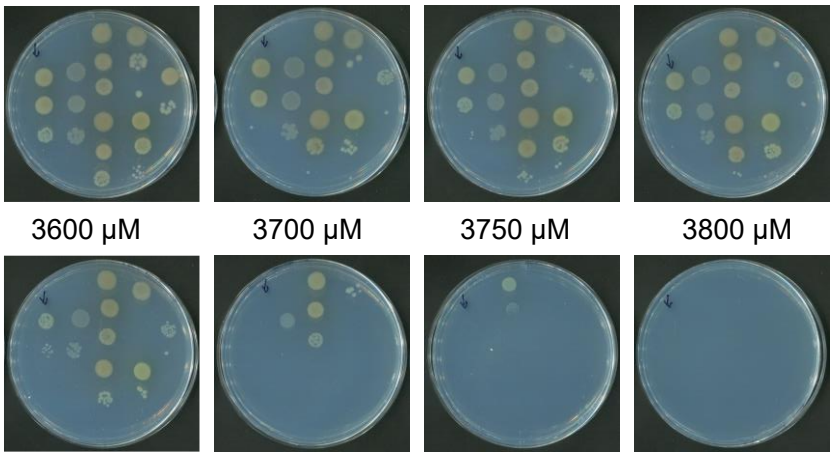

Appendix 21. Plate photos for copper MIC tests for the evolved MPAO1 strains from colony-to-colony transfer. The layout of strains is shown in the figure above agar plates. Concentration of $CuSO_4$ is indicated below each agar plate. The overnight bacterial cultures were subjected to 10^{-3}, 10^{-4} and 10^{-5} dilution, and 10 µl was dropped onto an agar plate. Photos were taken after 24, 48 and 72-hour incubation. Minimal inhibitory concentration (MIC) units were determined after 48-hour incubation.

References:

Al-Tawfiq, J. A., & Tambyah, P. A. (2014). Healthcare associated infections (HAI) perspectives. *Journal of infection and public health*, *7*(4), 339-344.

Baer, C. F., Miyamoto, M. M., & Denver, D. R. (2007). Mutation rate variation in multicellular eukaryotes: causes and consequences. *Nature Reviews Genetics*, *8*(8), 619.

Bao, Y., Lies, D. P., Fu, H., & Roberts, G. P. (1991). An improved Tn7-based system for the single-copy insertion of cloned genes into chromosomes of gram-negative bacteria. *Gene*, *109*(1), 167-168.

Blondeau, J. M. (1999). A review of the comparative in-vitro activities of 12 antimicrobial agents, with a focus on five new 'respiratory quinolones'. *Journal of Antimicrobial Chemotherapy*, *43*(suppl_2), 1-11.

Borkow, G. (2014). Using copper to improve the well-being of the skin. *Current chemical biology*, *8*(2), 89-102.

Casadaban, M. J., Martinez-Arias, A., Shapira, S. K., & Chou, J. (1983). [21] β-Galactosidase gene fusions for analyzing gene expression in Escherichia coli and yeast. In *Methods in enzymology* (Vol. 100, pp. 293-308). Academic Press.

Chain, F. J., Flynn, J. M., Bull, J. K., & Cristescu, M. E. (2019). Accelerated rates of large-scale mutations in the presence of copper and nickel. *Genome research*, *29*(1), 64-73.

Chopra, I., & Roberts, M. (2001). Tetracycline antibiotics: mode of action, applications, molecular biology, and epidemiology of bacterial resistance. *Microbiol. Mol. Biol. Rev.*, *65*(2), 232-260.

Cox, G., & Wright, G. D. (2013). Intrinsic antibiotic resistance: mechanisms, origins, challenges and solutions. *International Journal of Medical Microbiology*, *303*(6-7), 287-292.

de Carvalho, C. C., & Caramujo, M. J. (2014). Bacterial diversity assessed by cultivation-based techniques shows predominance of Staphylococccus species on coins collected in Lisbon and Casablanca. *FEMS microbiology ecology*, *88*(1), 26-37.

Dollwet, H. H. (1985). Historic uses of copper compounds in medicine. *Trace Elem. Med.*, *2*, 80-87.

Durante-Mangoni, E., Grammatikos, A., Utili, R., & Falagas, M. E. (2009). Do we still need the aminoglycosides?. *International journal of antimicrobial agents*, *33*(3), 201-205.

Elander, R. P. (2003). Industrial production of β-lactam antibiotics. *Applied microbiology and biotechnology*, *61*(5-6), 385-392.

Elguindi, J., Wagner, J., & Rensing, C. (2009). Genes involved in copper resistance influence survival of Pseudomonas aeruginosa on copper surfaces. *Journal of applied*

microbiology, *106*(5), 1448-1455.

Farouk, F., Azzazy, H. M., & Niessen, W. M. (2015). Challenges in the determination of aminoglycoside antibiotics, a review. *Analytica chimica acta*, *890*, 21-43.

Fisher, J. F., Meroueh, S. O., & Mobashery, S. (2005). Bacterial resistance to β-lactam antibiotics: compelling opportunism, compelling opportunity. *Chemical reviews*, *105*(2), 395-424.

Fridman, O., Goldberg, A., Ronin, I., Shoresh, N., & Balaban, N. Q. (2014). Optimization of lag time underlies antibiotic tolerance in evolved bacterial populations. *Nature*, *513*(7518), 418-421.

Gant, V. A., Wren, M. W., Rollins, M. S., Jeanes, A., Hickok, S. S., & Hall, T. J. (2007). Three novel highly charged copper-based biocides: safety and efficacy against healthcare-associated organisms. *Journal of Antimicrobial Chemotherapy*, *60*(2), 294-299.

Gillet-Markowska, A., Louvel, G., & Fischer, G. (2015). bz-rates: A web tool to estimate mutation rates from fluctuation analysis. *G3: Genes, Genomes, Genetics*, *5*(11), 2323-2327.

Glupczynski, Y., Labbe, M., Hansen, W., Crokaert, F., & Yourassowsky, E. (1991). Evaluation of the E test for quantitative antimicrobial susceptibility testing of Helicobacter pylori. Journal of Clinical Microbiology, 29(9), 2072-2075.

Graves, N., Nicholls, T. M., & Morris, A. J. (2003). Modeling the costs of hospital-acquired infections in New Zealand. *Infection Control & Hospital Epidemiology*, *24*(3), 214-223.

Haddad, J., Kotra, L. P., Llano-Sotelo, B., Kim, C., Azucena, E. F., Liu, M., ... & Mobashery, S. (2002). Design of novel antibiotics that bind to the ribosomal acyltransfer site. *Journal of the American Chemical Society*, *124*(13), 3229-3237.

Hannauer, M., Schäfer, M., Hoegy, F., Gizzi, P., Wehrung, P., Mislin, G. L., ... & Schalk, I. J. (2012). Biosynthesis of the pyoverdine siderophore of Pseudomonas aeruginosa involves precursors with a myristic or a myristoleic acid chain. *FEBS letters*, *586*(1), 96-101.

Hao, Z., Lou, H., Zhu, R., Zhu, J., Zhang, D., Zhao, B. S., ... & Chen, P. R. (2014). The multiple antibiotic resistance regulator MarR is a copper sensor in Escherichia coli. *Nature chemical biology*, *10*(1), 21.

Kleanthous, C., & Armitage, J. P. (2015). The bacterial cell envelope.

Lenski, R. E., Rose, M. R., Simpson, S. C., & Tadler, S. C. (1991). Long-term experimental evolution in Escherichia coli. I. Adaptation and divergence during 2,000 generations. The American Naturalist, 138(6), 1315-1341.

Li, B., Qiu, Y., Shi, H., & Yin, H. (2016). The importance of lag time extension in determining

bacterial resistance to antibiotics. *Analyst*, *141*(10), 3059-3067.

Liu, Yunhao, Rainey, Paul B, & Zhang, Xue-Xian. (2015). Molecular mechanisms of xylose utilization by Pseudomonas fluorescens: overlapping genetic responses to xylose, xylulose, ribose and mannitol. Molecular microbiology, 98(3), 553-570.

Luria, S. E., & Delbrück, M. (1943). Mutations of bacteria from virus sensitivity to virus resistance. *Genetics*, *28*(6), 491.

Jacobs, M. A., Alwood, A., Thaipisuttikul, I., Spencer, D., Haugen, E., Ernst, S., ... & Chun-Rong, L. (2003). Comprehensive transposon mutant library of Pseudomonas aeruginosa. *Proceedings of the National Academy of Sciences*, *100*(24), 14339-14344.

Jin, Z., Li, J., Ni, L., Zhang, R., Xia, A., & Jin, F. (2018). Conditional privatization of a public siderophore enables Pseudomonas aeruginosa to resist cheater invasion. *Nature communications*, *9*(1), 1383.

Jun, H., Kurenbach, B., Aitken, J., Wasa, A., Remus-Emsermann, M. N., Godsoe, W., & Heinemann, J. A. (2019). Effects of sub-lethal concentrations of copper ammonium acetate, pyrethrins and atrazine on the response of Escherichia coli to antibiotics. *F1000Research*, *8*.

Macomber, L., & Imlay, J. A. (2009). The iron-sulfur clusters of dehydratases are primary intracellular targets of copper toxicity. *Proceedings of the National Academy of Sciences*, *106*(20), 8344-8349.

Martens, E., & Demain, A. L. (2017). The antibiotic resistance crisis, with a focus on the United States. *The Journal of antibiotics*, *70*(5), 520.

Mathews, S., Hans, M., Mücklich, F., & Solioz, M. (2013). Contact killing of bacteria on copper is suppressed if bacterial-metal contact is prevented and is induced on iron by copper ions. *Appl. Environ. Microbiol.*, *79*(8), 2605-2611.

Mhondoro, M., Ndlovu, N., Bangure, D., Juru, T., Gombe, N. T., Shambira, G., ... & Tshimanga, M. (2019). Trends in antimicrobial resistance of bacterial pathogens in Harare, Zimbabwe, 2012–2017: a secondary dataset analysis. *BMC infectious diseases*, *19*(1), 1-9.

Mittelman, M. W., & Geesey, G. G. (1985). Copper-binding characteristics of exopolymers from a freshwater-sediment bacterium. *Appl. Environ. Microbiol.*, *49*(4), 846-851.

Nguyen, C. C., Hugie, C. N., Kile, M. L., & Navab-Daneshmand, T. (2019). Association between heavy metals and antibiotic-resistant human pathogens in environmental reservoirs: A review. *Frontiers of Environmental Science & Engineering*, *13*(3), 46.

Nies, D. H., & Herzberg, M. (2013). A fresh view of the cell biology of copper in enterobacteria. *Molecular microbiology*, *87*(3), 447-454.

Nord, C. E., Wadström, T., & Wretlind, B. (1975). Antibiotic sensitivity of twoAeromonas and ninePseudomonas species. *Medical microbiology and immunology*, *161*(2), 89-97.

O'gorman, J., & Humphreys, H. (2012). Application of copper to prevent and control infection. Where are we now?. *Journal of Hospital Infection*, *81*(4), 217-223.

O'Neill, J., Davies, S., Rex, J., White, L. J., & Murray, R. (2016). Review on antimicrobial resistance, tackling drug-resistant infections globally: final report and recommendations. *London: Wellcome Trust and UK Government*.

Ordax, M., Marco-Noales, E., López, M. M., & Biosca, E. G. (2006). Survival strategy of Erwinia amylovora against copper: induction of the viable-but-nonculturable state. *Appl. Environ. Microbiol.*, *72*(5), 3482-3488.

Pineda, I., Hubbard, R., & Rodríguez, F. (2017). The role of copper surfaces in reducing the incidence of healthcare-associated infections: A systematic review and meta-analysis. *Canadian Journal of Infection Control*, *32*(1).

Pittet, D., Hugonnet, S., Harbarth, S., Mourouga, P., Sauvan, V., Touveneau, S., & Perneger, T. V. (2000). Effectiveness of a hospital-wide programme to improve compliance with hand hygiene. The Lancet, 356(9238), 1307-1312.

Quintana, J., Novoa-Aponte, L., & Argüello, J. M. (2017). Copper homeostasis networks in the bacterium Pseudomonas aeruginosa. *Journal of Biological Chemistry*, *292*(38), 15691-15704.

Rainey, P. B., & Travisano, M. (1998). Adaptive radiation in a heterogeneous environment. *Nature*, *394*(6688), 69.

Rossolini, G. M., Arena, F., Pecile, P., & Pollini, S. (2014). Update on the antibiotic resistance crisis. *Current opinion in pharmacology*, *18*, 56-60.

Sambrook, J., E. F. Fritsch and T. Maniatis, 1989 *Molecular Cloning: A Laboratory Manual*. Cold Spring Harbor Laboratory Press, Cold Spring Harbor, NY.

Santo, C. E., Taudte, N., Nies, D. H., & Grass, G. (2008). Contribution of copper ion resistance to survival of Escherichia coli on metallic copper surfaces. *Appl. Environ. Microbiol.*, *74*(4), 977-986.

Salgado, C. D., Sepkowitz, K. A., John, J. F., Cantey, J. R., Attaway, H. H., Freeman, K. D., ... & Schmidt, M. G. (2013). Copper surfaces reduce the rate of healthcare-acquired infections in the intensive care unit. *Infection Control & Hospital Epidemiology*, *34*(5), 479-486.

Schmidt, M. G., Attaway, H. H., Sharpe, P. A., John, J., Sepkowitz, K. A., Morgan, A., ... & Freeman, K. D. (2012). Sustained reduction of microbial burden on common hospital

surfaces through introduction of copper. *Journal of clinical microbiology*, *50*(7), 2217-2223.

Singh, N. P., McCoy, M. T., Tice, R. R., & Schneider, E. L. (1988). A simple technique for quantitation of low levels of DNA damage in individual cells. Experimental cell research, 175(1), 184-191.

Speer, B. S., Shoemaker, N. B., & Salyers, A. A. (1992). Bacterial resistance to tetracycline: mechanisms, transfer, and clinical significance. *Clinical microbiology reviews*, *5*(4), 387-399.

Seiler, C., & Berendonk, T. U. (2012). Heavy metal driven co-selection of antibiotic resistance in soil and water bodies impacted by agriculture and aquaculture. *Frontiers in microbiology*, *3*, 399.

Septimus, E., Weinstein, R. A., Perl, T. M., Goldmann, D. A., & Yokoe, D. S. (2014). Approaches for preventing healthcare-associated infections: go long or go wide?. *Infection Control & Hospital Epidemiology*, *35*(7), 797-801.

Sharpe, P. A., & Schmidt, M. G. (2011). Control and mitigation of healthcare-acquired infections: designing clinical trials to evaluate new materials and technologies. *HERD: Health Environments Research & Design Journal*, *5*(1), 94-115.

Sniegowski, P. D., Gerrish, P. J., & Lenski, R. E. (1997). Evolution of high mutation rates in experimental populations of E. coli. *Nature*, *387*(6634), 703.

Tegos, G., Tegos, G., & Mylonakis, E. (2012). *Antimicrobial drug discovery: emerging strategies*. Cabi.

Trippe, K., McPhail, K., Armstrong, D., Azevedo, M., & Banowetz, G. (2013). Pseudomonas fluorescens SBW25 produces furanomycin, a non-proteinogenic amino acid with selective antimicrobial properties. *BMC microbiology*, *13*(1), 111.

Ventola, C. L. (2015). The antibiotic resistance crisis: part 1: causes and threats. Pharmacy and therapeutics, 40(4), 277.

Vriesekoop, F., Chen, J., Oldaker, J., Besnard, F., Smith, R., Leversha, W., ... & Liang, H. (2016). Dirty money: a matter of bacterial survival, adherence, and toxicity. *Microorganisms*, *4*(4), 42.

Wiegand, I., Hilpert, K., & Hancock, R. E. (2008). Agar and broth dilution methods to determine the minimal inhibitory concentration (MIC) of antimicrobial substances. *Nature protocols*, *3*(2), 163.

Vincent, M., Duval, R. E., Hartemann, P., & Engels‐Deutsch, M. (2018). Contact killing and antimicrobial properties of copper. *Journal of applied microbiology*, *124*(5), 1032-1046.

World Health Organization. (2011). Report on the burden of endemic health care-associated infection worldwide.

Warnes, S. L., Green, S. M., Michels, H. T., & Keevil, C. W. (2010). Biocidal efficacy of copper alloys against pathogenic enterococci involves degradation of genomic and plasmid DNAs. *Appl. Environ. Microbiol.*, *76*(16), 5390-5401.

Warnes, S. L., & Keevil, C. W. (2011). Mechanism of copper surface toxicity in vancomycin-resistant enterococci following wet or dry surface contact. *Appl. Environ. Microbiol.*, *77*(17), 6049-6059.

Warnes, S. L., Caves, V., & Keevil, C. W. (2012). Mechanism of copper surface toxicity in Escherichia coli O157: H7 and Salmonella involves immediate membrane depolarization followed by slower rate of DNA destruction which differs from that observed for Gram‐positive bacteria. *Environmental microbiology*, *14*(7), 1730-1743.

Wright, B. W., Kamath, K. S., Krisp, C., & Molloy, M. P. (2019). Proteome profiling of Pseudomonas aeruginosa PAO1 identifies novel responders to copper stress. BMC microbiology, 19(1), 69.